BILLIARDS AND STATISTICAL MECHANICS

A Thesis
Presented to
The Academic Faculty

by

Alexander Grigo

In Partial Fulfillment
of the Requirements for the Degree
Doctor of Philosophy in the
School of Mathematics

Georgia Institute of Technology
August 2009

BILLIARDS AND STATISTICAL MECHANICS

Approved by:

Professor L. Bunimovich, Advisor
School of Mathematics
Georgia Institute of Technology

Professor S-N. Chow
School of Mathematics
Georgia Institute of Technology

Professor P. Cvitanović
School of Physics
Georgia Institute of Technology

Professor F. Bonetto
School of Mathematics
Georgia Institute of Technology

Professor H. Weiss
School of Mathematics
Georgia Institute of Technology

Date Approved: 28 April 2009

ACKNOWLEDGEMENTS

I want to express my sincere gratitude to my advisor, Professor Leonid Bunimovich, for his constant support, encouragement and friendship that made my stay at GeorgiaTech so enjoyable. I am very thankful to Professors Leonid Bunimovich, Shui-Nee Chow and Predrag Cvitanović not only for invaluable lessons and discussions on dynamical systems, but especially for providing such a stimulating environment.

Many thanks goes to my friends and fellow graduate students, in particular, Michael Burkhart, Ken Chen, David Jimenez, Hwa Kil Kim, Yongfeng Li, Domenico Lippolis, Trevis Litherland, Kianoush Naeli, Ian Palmer, Ramazan Tinaztepe, Jorge Viveros Rogel, Benjamin Webb, Hua Xu, Kun Zhao.

Last, but not least, I want to thank my parents, Silke Wichert, and my former Professors Gerd Röpke, Krzysztof Rybakowski, and Peter Takač from the University of Rostock, Germany.

TABLE OF CONTENTS

LIST OF FIGURES

SUMMARY

In this thesis we consider mathematical problems related to different aspects of hard sphere systems.

In the first part we study planar billiards, which arise in the context of hard sphere systems when only one or two spheres are present. We show that the standard design principle of planar hyperbolic billiards with focusing boundary components fails as soon as non-absolutely focusing components are present. This result thus provides a characterization of which focusing boundary components can be used to construct hyperbolic billiards.

A more detailed analysis of this phenomenon is provided for C^2 stadium-like billiards. Here the problem is that unlike in the previous setting we are given a specific billiard table. We show that for a large class of such tables elliptic periodic orbits exists, which is in sharp contrast to the ergodicity of the classical stadium billiard.

In the second part of this thesis we consider hard sphere systems with a large number of particles, which we model by the Boltzmann equation. We develop a new approach to derive hydrodynamic limits, which is based on classical methods of geometric singular perturbation theory of ordinary differential equations. This approach provides new geometric and dynamical aspects of hydrodynamic limits, and we were able to apply these methods also to the dissipative Boltzmann equation. In particular the problem of higher order (Burnett order) corrections is addressed.

CHAPTER I

INTRODUCTION

One of the fundamental models of many particle systems is the hard sphere system. It consists of a number of perfect spheres, which move freely inside a container. Upon collision with the boundary of the container or with other spheres they undergo a specular reflection. Thus it represents a Hamiltonian dynamical system, and can be viewed as a geodesic flow with specular reflection as boundary conditions.

There are several reasons why the study of dynamical properties of such systems is generally very complicated. In a certain sense, the simplest possible setup is to have only one sphere (disk) in a planar container. By choosing center of mass coordinates the case of two disks on a flat torus can be reduced to the case of one disk in a planar domain with boundary, which is called a planar billiard.

Planar billiards are one of the best rigorously studied dynamical systems, which can display stable and hyperbolic motion. The mathematical theory of these systems was pioneered by Birkhoff and later Sinai and many others. In view of applications to models of statistical mechanics proving statistical (ergodic) properties of the billiard dynamics are of significant importance.

At the heart of the appearance of statistical limit laws in (deterministic!) dynamical systems is generally hyperbolicity. In billiards scattering boundary components naturally generate hyperbolic dynamics, which lead Sinai to proof in [62] ergodicity and hyperbolicity of such billiards. Later the more general mechanism of defocusing was discovered by Bunimovich, who proved in [14] (see also [15]) ergodicity and hyperbolicty of certain planar billiards with focusing circular boundary components.

In the first part of this thesis we investigate the class of focusing boundary components, which are admissible in the standard procedure of constructing hyperbolic billiards with focusing boundary components, as proposed by Wojtkowski in [66].

The main result in this direction will be that as soon as non-absolutely focusing boundary components are present, the construction of hyperbolic billiards becomes more difficult. In fact, we show that for a large class of such planar billiards have elliptic periodic orbits.

To make the importance of the impact of non-absolutely focusing boundary components on the billiard dynamics more clear, we also investigate smooth stadium-like billiards. In this situation the billiard tables are essentially given, so that the freedom of designing tables with elliptic is not available anymore.

Yet, we show that there is a large class of smooth stadia which have elliptic periodic orbits. This, of course, is in sharp contrast to the usual stadium billiard, which is ergodic and hyperbolic. It will be made clear, that the appearance of the elliptic orbits is due to the non-absolutely focusing property of the smoothed out boundary component.

Planar billiards provide a model with applications to statistical mechanics, for which a large class of rigorous results are available. In fact, planar billiards are essentially the only Hamiltonian systems where detailed statistical properties are rigorously proven. On the other hand, in applications it is also important to study collective aspects of motion of a large number of particles. In particular transport phenomena are of great interest.

The study of hard sphere systems (or any other related Hamiltonian system for that matter) for a large number of degrees of freedom seems currently out of reach. Despite some partial results on the limit of Hamiltonian dynamics as the number of degrees of freedom tends to infinity, e.g. [50, 49, 48, 47], not much is rigorously known.

But it is generally believed that in the Grad limit the resulting infinite dimensional system is the Boltzmann equation. This model of high dimensional Hamiltonian systems was originally introduced by Boltzmann, and is a standard model in engineering and physics.

In the second part of this thesis the Boltzmann equation is taken as the starting point. In fact, we will even allow for non-Hamiltonian interactions, which dissipate energy due to inelastic collisions. This is of great interest in the modeling of driven granular systems, which were the main motivation of our work.

One major success of the Boltzmann equation is the derivation of a hydrodynamic description of the underlying (infinite) particle system. Furthermore, the transport terms can be directly computed, based on the properties of binary collisions only.

However, derivations of such hydrodynamic limits have not been considered from a dynamical systems point of view. In this thesis we will develop a novel approach to this problem, and show how methods from geometric singular perturbation theory can be applied.

It will be shown how these ideas provide a new, geometric, interpretation of the classical Chapman-Enskog method of kinetic theory. Furthermore, our derivation of the hydrodynamic limit shows that it is possible to treat the convective and dissipative transport on the same footing, without the introduction of multiple time scales or the like. The Chapman-Enskog method provides these to transport terms separately, where the dissipative one is obtained as a higher order correction to the convective one.

Finally, since we allow also for non-Hamiltonian interactions we can apply our methods to the much less investigated hydrodynamic limits of the dissipative Boltzmann equation. In this setting the difference between our method and the usual Chapman-Enskog method becomes much more pronounced.

In fact, it is argued in the literature that for dissipative systems one has to go

beyond the Navier-Stokes order. We show that with our expansion method, this argument can be addressed already at the Navier-Stokes order.

Therefore, this new expansion method not only provides new interpretations of the hydrodynamic limits of the classical (non-dissipative) Boltzmann equation, but it seems to provide a new result and simpler expressions in the dissipative setting.

The organisation of the thesis is as follows. Basic facts about billiards are reviewed in Chapter 2. In Chapter 3 we show that the absolute focusing property is essentially necessary in the construction of hyperbolic billiards with focusing components. The construction of elliptic periodic orbits for C^2-stadia is the main result of Chapter 4. The singular perturbation analysis of hydrodynamic limits of the dissipative Boltzmann equation is presented in Chapter 5. For convenience every chapter includes a separate introduction, which provides more details on the problem studied. Also, summaries of the results are provided at the end of each chapter in form of a conclusions section.

CHAPTER II

BASIC PROPERTIES OF BILLIARDS

2.1 Basic Facts about Billiards

In this section the basic properties of billiards we will need are described. The notation used is close to the one used in [25], which contains most of the results listed below.

Let $Q \subset \mathbb{R}^2$ denote an open bounded domain with piecewise C^3 boundary ∂Q. The dynamics generated by a point-like particle moving along straight lines inside Q and having specular reflections off the boundary ∂Q is called billiard flow Φ^t on the billiard table Q. The induced first return map $\mathcal{F}$ to the boundary ∂Q, where only the state right after the reflection is considered, is called the associated billiard map. These constructions yield

$$\Phi^t \colon Q \times S^1 \to Q \times S^1 \quad \text{and} \quad \mathcal{F} \colon \partial Q \times [-\pi/2, \pi/2] \to \partial Q \times [-\pi/2, \pi/2]$$

which are defined almost everywhere with respect to the Lebesgue measure.

The natural coordinates for the billiard map are the arc length parameter s along the boundary, which we will assume to be oriented in counterclockwise direction, and the angle of reflection φ relative to the normal direction. For the billiard flow the natural coordinates are the angle ω giving the direction of the velocity vector relative to the horizontal direction, and (x, y) denoting the position inside of Q. It is well known that the billiard map preserves the measure $d\mu = \cos\varphi \, d\varphi \, ds$ and that $d\nu = d\omega \, dx \, dy$ is preserved by the billiard flow. (Indeed, even the volume forms are preserved.) In particular, the billiard map is symplectic in the coordinates $(s, \sin\varphi)$.

When working with the billiard flow it is often more convenient to use the so called Jacobi coordinates (η, ξ, ω), which in infinitesimal form read

$$d\eta = \cos\omega \, dx + \sin\omega \, dy \quad \text{and} \quad d\xi = -\sin\omega \, dx + \cos\omega \, dy \, .$$

The derivative of Φ^t then becomes

$$D\Phi^t = \begin{pmatrix} 1 & 0 \\ 0 & U_t \end{pmatrix} \quad \text{with} \quad U_t = \frac{\partial(\xi^t, \omega^t)}{\partial(\xi, \omega)} \quad \text{and} \quad \det U_t = 1$$

since η measures the distance in direction of the flow. We will refer to U_t as the reduced Jacobian of Φ^t.

Throughout we denote by $\mathcal{K} = \mathcal{K}(s)$ the (signed) curvature of the boundary at the point corresponding to the arc length parameter s. The sign of $\mathcal{K}$ is chosen such that it is negative for convex shaped boundary components, as in the case of a billiard inside a circle. Correspondingly, we shall call boundary components for which $\mathcal{K} < 0$, $\mathcal{K} = 0$, $\mathcal{K} > 0$ focusing, neutral, dispersing, respectively.

The derivative of the billiard map is given by

$$D\mathcal{F}(s, \varphi) = -\frac{1}{\cos\varphi_1} \begin{pmatrix} \tau\,\mathcal{K} + \cos\varphi & \tau \\ \tau\,\mathcal{K}\,\mathcal{K}_1 + \mathcal{K}\,\cos\varphi_1 + \mathcal{K}_1\,\cos\varphi & \tau\,\mathcal{K}_1 + \cos\varphi_1 \end{pmatrix}$$

where we set $(s_1, \varphi_1) = \mathcal{F}(s, \varphi)$ and τ the distance (free path) between the two points along the straight line connecting them. In particular, the billiard map is of class C^{k-1} if the boundary components are of class C^k.

Another well known fact is that the (local) generating function of the billiard dynamics is (locally) given by the Euclidean distance along the straight line segments connecting the points of reflection. More precisely, consider a point (s_0, φ_0) such that $(s_k, \varphi_k) := \mathcal{F}^k(s_0, \varphi_0)$ is well defined for $0 \le k \le n$. Denote by Γ_i the boundary component on which the i-th reflection occurs (i.e. on which (s_i, φ_i) lies), so that $\Gamma_i(s_i)$ is the point of the i-th reflection in the plane. Then

$$L(s_0, \ldots, s_n) := \sum_{i=1}^{n} \| \Gamma_i(s_i) - \Gamma_{i-1}(s_{i-1}) \|$$

is the Euclidean length of the corresponding trajectory of the billiard flow, and

$$\partial_{s_0} L = -\sin\varphi_0\,, \qquad \partial_{s_i} L = 0 \quad \text{for} \quad 1 \le i \le n-1\,, \qquad \partial_{s_n} L = \sin\varphi_n$$

hold, which is why L is the generating function (cf. Sections 47 and 48 in [1] for details on generating functions).

2.2 Some Important Formulas

For a quantitative study of the billiard dynamics one needs the derivative of the billiard flow, or the billiard map. The expression for the billiard map was already given. For the billiard flow it is, however, much easier to compute its derivative. As long as there is no reflection off the boundary we have $d\xi_t = d\xi + t\, d\omega$, $d\omega_t = d\omega$. Therefore, the reduced derivative of the billiard flow reads

$$D\Phi^t\Big|_{\text{reduced}} \equiv U_t = \begin{pmatrix} 1 & t \\ 0 & 1 \end{pmatrix} .$$

The change of the Jacobi coordinates from right before the moment of a reflection to right after is given by $d\xi^+ = -d\xi^-$, $d\omega^+ = -\mathcal{R}\, d\xi^- - d\omega^-$. Hence

$$D\Phi^{0+}\Big|_{\text{reduced}} \equiv L_{\mathcal{R}} = -\begin{pmatrix} 1 & 0 \\ \mathcal{R} & 1 \end{pmatrix} \quad \text{with} \quad \mathcal{R} = \frac{2\,\mathcal{K}}{\cos\varphi}$$

for the reduced derivative of the billiard flow at the moment of reflection.

Combining these two parts of the derivative one can compute the Jacobian of the billiard flow along an arbitrary trajectory segment. By using the multiplicative property of the Jacobian we obtain

$$D\Phi^t = U_{t_{n+1}} L_{\mathcal{R}}^{(n)} \cdot \ldots \cdot U_{t_1} L_{\mathcal{R}}^{(1)}\, U_{t_0}$$

along a sequence of n consecutive reflections.

An important quantity to describe the derivative of the billiard flow is the wave-front curvature $\mathcal{B}{:=}d\omega/d\xi$. The geometric meaning of $\mathcal{B}$ is the slope of a curves in Q equipped with normal framing, where the normal vectors are the corresponding velocities. The corresponding slope $\mathcal{V} = \frac{d\varphi}{ds}$ for the projection onto the state space of the map is given by

$$\mathcal{V} = \mathcal{B}^+ \cos\varphi - \mathcal{K} = \mathcal{B}^- \cos\varphi + \mathcal{K} .$$

The above expressions for the derivative of the billiard flow show

$$\mathcal{B}_t = \frac{1}{\dfrac{1}{\mathcal{B}_0} + t} \quad \text{for a free flight of length } t$$

$$\mathcal{B}^+ = \mathcal{B}^- + \mathcal{R} \quad \text{with} \quad \mathcal{R}{:=}\frac{2\,\mathcal{K}}{\cos\varphi} \quad \text{at a point of reflection.}$$

for the evolution of the wave front curvature. In geometric optics the second relation is called mirror formula.

The fact that the double fraction appears for a free flight can be used to compute the wavefront curvature along a sequence of consecutive reflections as a continued fraction. Another way of computing this expression is to use the Jacobian of the flow, which thus shows

$$\mathcal{B}_t = \frac{c_t + d_t\,\mathcal{B}_0}{a_t + b_t\,\mathcal{B}_0} \quad \text{for} \quad U_t = \begin{pmatrix} a_t & b_t \\ c_t & d_t \end{pmatrix}$$

as the relation between the wavefront curvature and the derivative of the flow.

For a segment of a billiard trajectory γ we denote the wavefront curvature of an initially parallel beam of rays sent along γ by $\mathcal{B}_{\text{out}}(\gamma)$. From the above we conclude that

$$\mathcal{B}_{\text{out}}(\gamma){:=}\frac{c}{a} \quad \text{with} \quad U(\gamma) = \begin{pmatrix} a & b \\ c & d \end{pmatrix} \tag{1}$$

where $U(\gamma)$ is the reduced Jacobian of the billiard flow along γ.

Another important observation is that the billiard flow is the suspension flow over the billiard map, where τ is the return time. This implies

$$d\mu = \frac{1}{2\,|\partial Q|}\,\cos\varphi\,d\varphi\,ds \quad \text{and} \quad d\nu = \frac{1}{\bar{\tau}}\,dt\,d\mu \quad \text{with} \quad \bar{\tau} = \int_{\mathcal{M}} \tau(r,\varphi)\,\mu(ds, d\varphi)$$

for the relation of the invariant measure for the map and the flow, respectively. In particular, we obtain

$$2\pi\,|Q| = 2\,|\partial Q|\,\bar{\tau}$$

for the mean free path $\bar{\tau}$.

2.3 Dispersing Billiards

Dispersing (or Sinai) billiards are billiard tables with scattering boundary components without cusps. The free path could be bounded or unbounded. The ambient space could be either $\mathbb{R}^2$ or $\mathbb{T}^2$, where only in the latter case the free path can be unbounded. Typical examples are shown in Fig. 1.

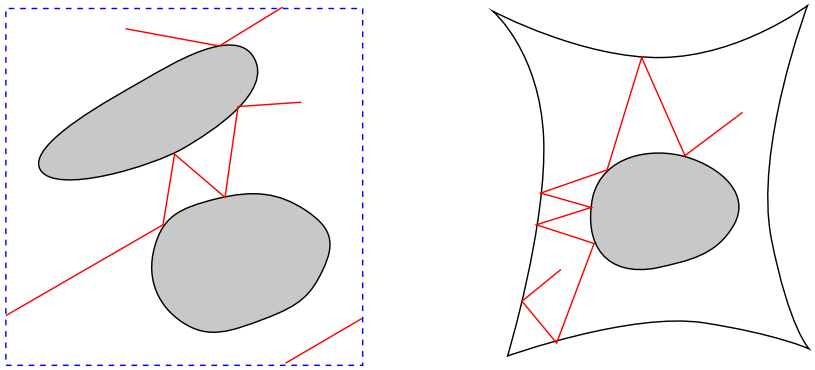

Figure 1: Typical dispersing billiards. On the left the ambient space is $\mathbb{T}^2$; this table is also known as periodic Lorentz gas. The table on the right is part of $\mathbb{R}^2$.

These billiards where the first class of billiards for which hyperbolicity and ergodicity was established, see [62]. The reason for the hyperbolicity is that nearby trajectories will diverge upon a reflection off a scatterer. A sketch of this is shown in Fig. 2.

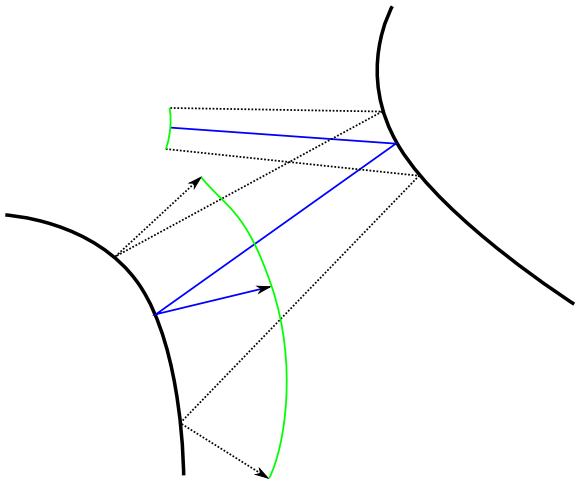

Figure 2: An illustration of the source of hyperbolicity in dispersing billiards.

Consider two disk-like particles on a flat torus (alternatively one could think of this as an infinite periodic configuration with infinitely many particles), which undergo an elastic reflection upon collision. By changing to center of mass coordinates, one can reduce this system to the billiard (of a point particle) on the flat torus with a spared out disk. This configuration is a special case of the periodic Lorentz gas, as shown on the left in Fig. 1. Due to this interpretation dispersing billiards are important models in rigorous statistical mechanics, for which strong statistical properties like exponential decay of correlations or the central limit theorem can be proven.

2.4 The Mechanism of Defocusing

By looking at Fig. 2 it is easy to see that after a reflection off a focusing boundary component (opposed to the shown dispersing one) two nearby trajectories will converge, and not diverge. Thus establishing hyperbolicity in billiards with focusing boundary components is much more delicate. In fact, while dispersing billiards are always hyperbolic, billiards with focusing boundary components can have elliptic periodic orbits, a mixed phase space, or they can be completely integrable (e.g. the billiard in an ellipse).

In [14], see also [15], Bunimovich constructed a class of hyperbolic and ergodic billiards with focusing boundary components. The mechanism behind the hyperbolicity is a generalization of the dispersing scattering (see Fig. 2), and is called the mechanism of defocusing.

The key is that even though right after a reflection off a focusing boundary component nearby trajectories will converge, they will eventually pass through a conjugate point. Once they pass through the conjugate point the trajectories will move apart. If the free path after the conjugate point is sufficiently large, then this expansion can compensate for the initial contraction. Thus, after a long enough free path the evolution of the wave front curvature is just as in the case of dispersing billiards. This

is illustrated in Fig. 3. A typical billiard table where the hyperbolicity of the billiard

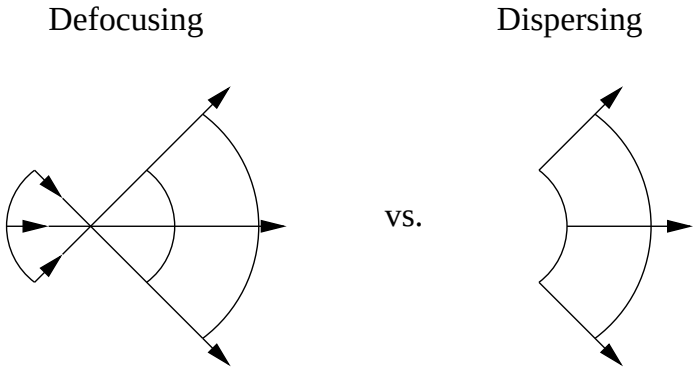

Figure 3: A comparison of the evolution of the wave front curvature within the mechanism of defocusing (left) and dispersing scattering (right).

dynamics is generated by the mechanism of defocusing is the stadium billiard. This billiard table was first constructed in [14, 15]. It consists of two semi-circles, which are connected by straight lines, as shown in Fig. 4.

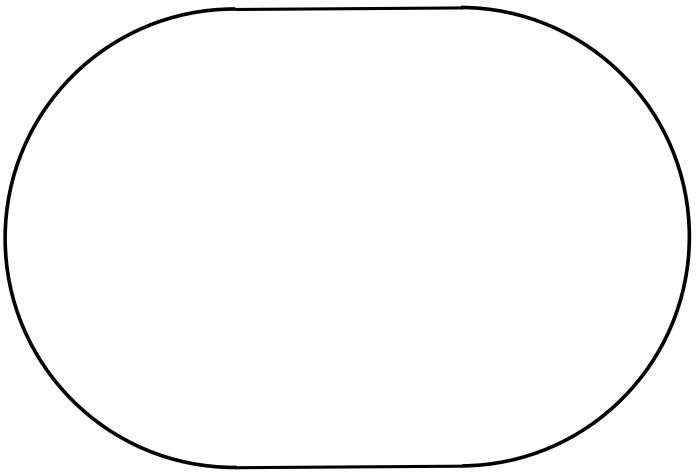

Figure 4: The stadium billiard.

CHAPTER III

ABSOLUTELY FOCUSING BOUNDARY COMPONENTS

3.1 Introduction and Statement of the Main Results

The foundation of the theory of hyperbolic systems with singularities was laid in Sinai's seminal paper [62] where hyperbolicity and ergodicity for billiards with smooth dispersing boundary was proven.

The situation changes drastically if a billiard table has at least one focusing component. Billiards with focusing boundaries demonstrate behaviors from completely regular to strongly chaotic. In fact, Lazutkin proved in [51, 52] that for any strictly convex billiard table with smooth enough boundary there exist caustics near the boundary, which prevent global ergodicity and hyperbolicity. However, certain classes of hyperbolic and ergodic billiards with focusing boundary components were found in [14, 15].

The mechanism behind this is called the mechanism of defocusing. It relies on the fact that a focusing beam will eventually go through a conjugate point, and will be dispersing afterwards. Therefore, if the free path to the next reflection is sufficiently large an essentially analogous situation to the case of dispersing billiard tables arises. This method of placing focusing boundary components sufficiently far away from other boundary components is the only known general procedure of constructing hyperbolic billiard tables [66].

Therefore, after the discovery of the mechanism of defocusing the question of which focusing components could be components of the boundary of a chaotic (hyperbolic) billiard was raised. Two dual classes of such focusing components were introduced in [66] and [56]. Then a much more general class of focusing components, admissible

for chaotic billiard tables, was introduced in [16, 17, 18] and [32]. (Formally the class of focusing components introduced in [32] seems to be more restrictive than the one in [17]. However, these two classes coincide [18].) These focusing components are called absolutely focusing, and were shown in [19, 29] to allow for hyperbolicity and ergodicity. It was conjectured in [17] that in hyperbolic billiards each focusing component of the boundary must be absolutely focusing, and it was outlined there how one can construct a stable periodic orbit if at least one focusing component is not absolutely focusing.

In this part of this thesis we show along the lines described in [17, 19] that as soon as the absolutely focusing property of focusing boundary components fails to hold the general procedure of designing chaotic billiard tables generally fails. Even if one makes the free path after a reflection from a non-absolutely focusing component arbitrarily large, such billiards can still have elliptic periodic points. Thus these billiards have islands of stability and are not completely hyperbolic. These results, once again, indicate that the mechanism of defocusing plays a key role in generic Hamiltonian systems which exhibit coexistence of islands of stability (KAM-islands) and chaotic hyperbolic components. The main result is the following:

Theorem 3.1.1. *Let Γ be a C^5 non-absolutely focusing curve of minimal length which encloses an angle of no more than π, or a small enough extension of such a curve. Then for every $L > 0$ there exist an open set (in the sense of C^5) of billiard tables $Q(L, \Gamma)$, $\Gamma \subset \partial Q(L, \Gamma)$, which all have a nonlinearly stable periodic orbit with free path of length at least L before and after a sequence of consecutive reflections off of Γ.*

The C^5 (C^k) closeness of two billiard tables simply means that there are parametrizations of their respective boundaries, which are piecewise C^5 (C^k) and are piecewise close in the C^5 (C^k) sense as functions from $[0, 1] \to \mathbb{R}^2$.

Remark 3.1.2. *We would like to mention at this point that the corresponding result*

for a linearly *stable, non-resonant periodic orbit can be proved when assuming only* C^3*–smoothness, cf. Theorem 3.2.6 below. This is the usual assumption in the theory of hyperbolic billiards, which deals with the first derivative of the billiard map (or flow) only. To deduce nonlinear stability, however, we need, for technical reasons, to assume* C^5 *smoothness in order to be able to apply KAM theory (Moser's twist theorem [59]), because it takes higher order derivatives of the billiard map into account.*

Dynamics on KAM islands is characterized by a balance between focusing (convergence of nearby orbits) and defocusing (their divergence) while on chaotic components defocusing dominates focusing. Recall that dispersing is just a special case of defocusing (when the focusing time is negative) and neutral components of the boundary cannot generate by themselves a chaotic behavior [9]. Therefore, our results show that there are no other mechanisms of hyperbolicity in billiards besides dispersing and defocusing. If both dispersing and focusing components are present, then they should be arranged in such a way that any initially parallel (infinitesimal) beam of rays in the course of its dynamics arrives at any curved (dispersing or focusing) component of the boundary as a dispersing beam. Then dispersing either takes over focusing, which occurs in the part of phase space where hyperbolicity emerges, or these two are balanced, [20, 22]. This happens on the part with regular dynamics (KAM-island). Thus defocusing is a fundamental mechanism of hyperbolicity (at least in billiards) and its violation leads to the creation of KAM-islands.

The structure of this chapter of the thesis is the following. In Section 3.2 we describe the construction of a linearly stable periodic orbit with a series of consecutive reflections off a non-absolutely focusing components. The nonlinear stability is first established for a very general setting in section Section 3.3 and then applied in Section 3.4 to the linearly stable orbit constructed before, which will prove our main result Theorem 3.1.1.

3.2 Construction of Linearly Stable Periodic Orbits

In this section let Γ be a (focusing) C^3 curve of length $l > 0$, parametrized by its arc length.

Definition 3.2.1 (Absolutely Focusing; see [16, 17])**.** *A closed, focusing component Γ is called absolutely focusing if every incoming infinitesimal beam of parallel rays leaves Γ, after a complete sequence of consecutive reflections, as a focusing beam.*

It was shown in [18, 19, 29, 32] that the defocusing mechanism applies to focusing boundary components which are absolutely focusing. Furthermore, it was also shown in [32] that every short enough piece of a focusing curve is absolutely focusing. This, in particular, motivates the following notion to characterize the transition between absolutely and non-absolutely focusing curves.

Definition 3.2.2 (Non-Absolutely Focusing of Minimal Length)**.** *A focusing curve Γ is called non-absolutely focusing of minimal length, if every of its closed sub-arcs is absolutely focusing, but the curve itself is not absolutely focusing.*

Our approach is based on the one outlined in [17]. The first step is to show that for a non-absolutely focusing curve there exists an infinitesimal beam of parallel rays falling onto Γ which leaves Γ after its last reflection as arbitrary weakly focusing. In the second step such a beam is used to construct a stable periodic orbit.

It is well known that the billiard map satisfies the twist property $ds_1/d\phi < 0$, no matter which type of boundary components are considered. It is also well known, that compositions of twist maps, and iterates of a twist map are in general no longer twist maps. However, it was observed in [32] (Proposition 3.6) that when restricting the billiard map to absolutely focusing boundary components, then its iterates will still be twist maps. This property is the main technical step in the following key lemma, whose result is illustrated in Fig. 5.

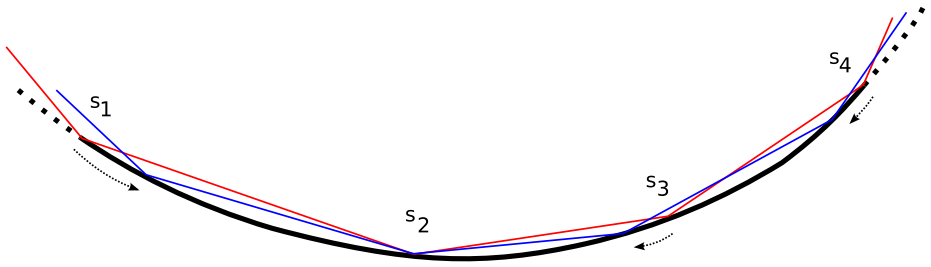

Figure 5: Illustration of the family of trajectories constructed in Lemma 3.2.3.

Lemma 3.2.3. *Let Γ be a C^k ($k \geq 3$) non-absolutely focusing curve of minimal length enclosing an angle of no more than π, and let γ be a part of a billiard trajectory with N consecutive reflections off of Γ (possibly off its endpoints). Then there exists a family of trajectories $(\gamma_\epsilon)_{\epsilon \geq 0}$ with a C^{k-1} dependence on ϵ, such that $\gamma_0 = \gamma$, and for all $\epsilon > 0$ the trajectory γ_ϵ has a sequence of N consecutive reflections off of Γ with no reflections off its endpoints.*

Proof. If all reflections of γ off of Γ are already in the interior of Γ, just set $\gamma_\epsilon \equiv \gamma$, so that we only consider such a γ with at least one reflection off of an endpoint of Γ in the following.

If $N = 1$, then denote by γ_ϵ the trajectory obtained by moving the point of reflection of γ by ϵ into the interior of Γ, while, say, keeping the angle of reflection constant. For $N = 2$, denote by γ_ϵ the trajectory obtained by moving both points of reflection of γ by ϵ into the interior. The corresponding angles of reflection are then determined by the location of the new points of reflection.

It remains to consider the case $N \geq 3$. Since Γ does not enclose an angle of more than π, there are no back reflections possible. Hence the second point of reflection must be in the interior of Γ. Furthermore, by assumption on Γ, the sub-arc on which the 2-nd up to the N-th reflection take place is absolutely focusing.

To construct γ_ϵ proceed as shown in Fig. 5. Increase the (absolute value of the) angle of reflection ϕ_2 by ϵ. Then Proposition 3.6 in [32] shows that the i-th reflection points, $3 \leq i \leq N$, all move closer to the second one. And since the billiard map is of

class C^{k-1}, the implicit function theorem asserts in this case that the dependence of new points of reflection on ϵ is C^{k-1}. Since the location of the second reflection does not change, the general twist property applied to the first reflection point shows that it also moves towards the second reflection point.

Therefore the family of rays γ_ϵ depends C^{k-1}–smooth on ϵ, and γ_ϵ for $\epsilon > 0$ has reflections only off the interior of Γ, as desired. □

Remark 3.2.4. *Although the result of Lemma 3.2.3 seems entirely obvious, especially when looking at Fig. 5, this is not so. In fact, this is the only point where the restriction to curves enclosing an angle of no more than π comes in.*

The reason is that, in general, changing the angle of incidence (at some point of reflection) in either direction may not move all points of reflection into the interior of Γ, as stated in Lemma 3.2.3, because of possibly existing back-reflections. This makes the argument in the construction of the family of orbits of Lemma 3.2.3 fail in general when applying it to curves enclosing an angle of more than π.

However, there are certainly situations where the result of Lemma 3.2.3 is true for such curves as well, e.g. for extensions to a curve enclosing an angle of more than π which do not destroy the constructed family of orbits.

It was conjectured in [17] that for any non-absolutely focusing curve Γ there exists an infinitesimal beam of parallel rays falling onto Γ and leaving it as parallel beam. The next statement proves this claim in a slightly more restricted setting.

Proposition 3.2.5. *Let the C^k ($k \geq 3$) curve Γ be a small enough extension of a non-absolutely focusing curve of minimal length, which encloses an angle of no more than π. Then there exists a family of rays $(\gamma_\epsilon)_{\epsilon \geq 0}$, depending C^{k-1}–smoothly on ϵ, such that they all have the same number of reflections off of Γ, and a parallel beam sent along γ_ϵ leaves Γ as a focusing one (parallel one) if $\epsilon > 0$ ($\epsilon = 0$).*

Proof. Consider first the case where Γ is non-absolutely focusing of minimal length,

enclosing an angle of no more than π. Then, by definition, there exists an incoming infinitesimal beam of parallel rays, say γ_0, which leaves Γ after a sequence of consecutive reflections as either a parallel or dispersing beam.

By Lemma 3.2.3 there is a C^{k-1}–smooth family $(\gamma_\epsilon)_{\epsilon\geq 0}$ such that for any $\epsilon > 0$ the ray γ_ϵ has reflections off the interior of Γ only. Since any sub-arc of Γ is absolutely focusing, a parallel incoming beam sent along γ_ϵ must leave as a focusing one. Hence the continuous dependence on ϵ shows that the parallel incoming beam along γ_0 must leave as a parallel one, and the family (γ_ϵ) is as desired.

Clearly, the constructed family $(\gamma_\epsilon)_{\epsilon\geq 0}$ is not destroyed if we allow for small enough extension of Γ, hence the above construction carries over to this more general case. □

In order to construct a linearly stable periodic orbit it is more convenient to work with the billiard flow, rather than the billiard map. Later on we will see that this changes when we want to establish nonlinear stability.

The next statement shows that if a curve Γ is non-absolutely focusing, then, regardless of how large the free paths before and after a series of consecutive reflections off of Γ are, a linearly stable periodic orbit can exist. To establish later nonlinear stability we need this (linearly stable) periodic orbit to be non-resonant, that means that the eigenvalues $\lambda = e^{\pm i\,\alpha}$ of the corresponding monodromy matrix satisfy $\lambda^2, \lambda^3, \lambda^4 \neq 1$.

Theorem 3.2.6. *Let Γ be a C^3 non-absolutely focusing curve of minimal length which encloses an angle of no more than π, or a small enough extension of such a curve. Then for every $L > 0$ there exists a billiard table $Q(L, \Gamma)$ with Γ as a focusing boundary component which has a linearly stable, non-resonant periodic orbit γ with free path of length at least L before and after a sequence of consecutive reflections off of Γ.*

Proof. Let $(\gamma_\epsilon)_{\epsilon\geq 0}$ be as in Proposition 3.2.5. From (1) we conclude that the reduced

Jacobian U_ϵ along γ_ϵ must read

$$U_\epsilon = \begin{pmatrix} U_{11} + a_\epsilon & U_{12} + b_\epsilon \\ c_\epsilon & \frac{1}{U_{11}} + d_\epsilon \end{pmatrix} \quad \text{with} \quad a_\epsilon, b_\epsilon, c_\epsilon, d_\epsilon = o(1) \quad \text{as} \quad \epsilon \searrow 0 \, .$$

The values of U_{11} and U_{12} satisfy

$$U_{12}\, c_\epsilon + b_\epsilon\, c_\epsilon = U_{11}\, d_\epsilon + \frac{a_\epsilon}{U_{11}} + a_\epsilon\, d_\epsilon$$

because $\det U_\epsilon = 1$. Since $\mathcal{B}_{\text{out}}(\gamma_\epsilon) < 0$ for all $\epsilon > 0$ holds, we must have

$$\frac{c_\epsilon}{U_{11} + a_\epsilon} < 0 \quad \text{hence} \quad c_\epsilon \, \operatorname{sgn} U_{11} < 0$$

for all ϵ small enough.

Let $L > 0$ be arbitrary, and consider τ with

$$\tau > 6\,(L + |\Gamma|)$$

whose value will be chosen in the following. For every $\epsilon > 0$ we can close up γ_ϵ to a periodic orbit $\tilde{\gamma}_\epsilon$ using three plane mirrors such that the length of the free path before and after the sequence of reflections off of Γ is at least L, and the total length of the orbit away from Γ is τ. This is illustrated in Fig. 6. The monodromy matrix

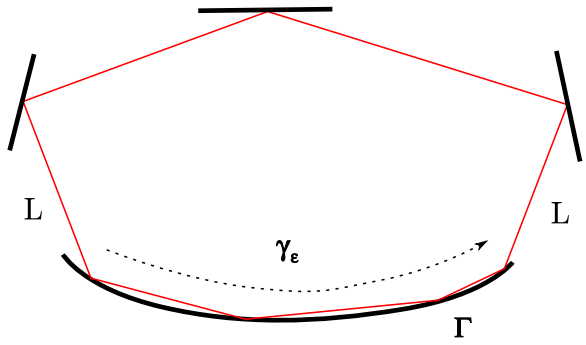

Figure 6: Construction of the periodic orbit using plane mirrors such that the resulting orbit has free paths before and after hitting Γ of length at least L.

M_ϵ along $\tilde{\gamma}_\epsilon$ then reads

$$M_\epsilon = -U_\epsilon \begin{pmatrix} 1 & \tau \\ 0 & 1 \end{pmatrix} = - \begin{pmatrix} U_{11} + a_\epsilon & U_{12} + b_\epsilon + \tau\, U_{11} + \tau\, a_\epsilon \\ c_\epsilon & \frac{1}{U_{11}} + d_\epsilon + \tau\, c_\epsilon \end{pmatrix}$$

where the minus sign is due to the three reflections at the plane mirrors.

In particular, the trace of M_ϵ is

$$-\operatorname{tr} M_\epsilon = U_{11} + a_\epsilon + \frac{1}{U_{11}} + d_\epsilon + \tau\, c_\epsilon$$

so that

$$-\operatorname{sgn} U_{11}\ \operatorname{tr} M_\epsilon = |U_{11}| + \frac{1}{|U_{11}|} - \tau\,|c_\epsilon| + (a_\epsilon + d_\epsilon)\operatorname{sgn} U_{11}$$

holds for all $\epsilon > 0$, where we used $c_\epsilon \operatorname{sgn} U_{11} < 0$. Now let ϵ_* be so small that the relations

$$\frac{2}{3}\,(|U_{11}| + \frac{1}{|U_{11}|}) \le |U_{11}| + \frac{1}{|U_{11}|} + (a_{\epsilon_*} + d_{\epsilon_*})\operatorname{sgn} U_{11} \le \frac{3}{2}\,(|U_{11}| + \frac{1}{|U_{11}|})$$

and

$$|c_{\epsilon_*}|\,6\,(L + |\Gamma|) < \frac{3}{2}\,(|U_{11}| + \frac{1}{|U_{11}|}) - 2$$

hold. By choosing τ_* now such that

$$\frac{3}{2}\,(|U_{11}| + \frac{1}{|U_{11}|}) - 2 < \tau_*\,|c_{\epsilon_*}| < \frac{2}{3}\,(|U_{11}| + \frac{1}{|U_{11}|}) - 1$$

we have

$$1 < -\operatorname{sgn} U_{11}\ \operatorname{tr} M_{\epsilon_*} < 2$$

and $\tau_* > 6\,(L + |\Gamma|)$. And by varying τ_* slightly we can ensure that the two complex eigenvalues $\lambda = e^{\pm i\alpha}$ of M_{ϵ_*} satisfy the non-resonance condition $\lambda^2, \lambda^3, \lambda^4 \neq 1$.

Therefore closing the orbit γ_{ϵ_*} up to form a periodic orbit using three plane mirrors as shown in Fig. 6 with a total length away from Γ equal to τ_* yields a linearly stable orbit with free path of length at least L before and after reflections off of Γ.

Making the three plane mirrors now slightly dispersing C^3 curves, without changing the position of and tangent at the reflection points, preserves the periodic orbit, its linear stability, and its non-resonant property. Completing the billiard table in any way by not destroying the constructed periodic orbit finishes the proof. □

3.3 An Auxiliary Stability Result

To study the nonlinear stability of a linearly stable fixed point of a planar area-preserving mapping T one can use the so-called Birkhoff normal form. This approach was developed by Kolmogorov, Arnold and Moser and is usually referred to as KAM theory. The first step in this approach is finding the explicit form of the normal form, which is given in the following lemma.

Lemma 3.3.1 ([31, 44])**.** *Let $T(s,y)$ be an area-preserving C^4 mapping with an elliptic fixed point at the origin*

$$T(s,y) = \begin{pmatrix} a_{10}\,s + a_{01}\,y + a_{20}\,s^2 + a_{11}\,s\,y + \ldots + a_{03}\,y^3 \\ b_{10}\,s + b_{01}\,y + b_{20}\,s^2 + b_{11}\,s\,y + \ldots + b_{03}\,y^3 \end{pmatrix} + \mathcal{O}_4(s,y)$$

and let $\lambda = e^{\pm i\alpha}$ denote the complex eigenvalues of $DT(0,0)$. If $\lambda^2, \lambda^3, \lambda^4 \neq 1$, then there exists a real-analytic canonical change of coordinates taking T into its Birkhoff normal form $z \mapsto \lambda\, z\, e^{i\,A\,|z|^2} + \mathcal{O}(|z|^4)$. The first Birkhoff coefficient A reads

$$A = \operatorname{Im} c_{21} + \frac{\sin\alpha}{\cos\alpha - 1}\left(3\,|c_{20}|^2 + \frac{2\,\cos\alpha - 1}{2\,\cos\alpha + 1}\,|c_{02}|^2\right)$$

where

$$\begin{aligned}
\operatorname{Im} c_{21} &= \frac{1}{8}\,a_{10}\left[-a_{21} + 3\,\frac{b_{10}\,a_{03}}{a_{01}} - 3\,\frac{a_{01}\,b_{30}}{b_{10}} + b_{12}\right] \\
&\quad - \frac{1}{8}\,b_{10}\left[a_{12} - 3\,\frac{a_{01}\,a_{30}}{b_{10}} - \frac{a_{01}\,b_{21}}{b_{10}} + 3\,b_{03}\right] \\
|c_{20}|^2 &= \frac{1}{16}\sqrt{-\frac{a_{01}}{b_{10}}}\left[\frac{b_{10}}{a_{01}}\,a_{02} + a_{20} + b_{11}\right]^2 + \frac{1}{16}\sqrt{-\frac{b_{10}}{a_{01}}}\left[\frac{a_{01}}{b_{10}}\,b_{20} + b_{02} + a_{11}\right]^2 \\
|c_{02}|^2 &= \frac{1}{16}\sqrt{-\frac{a_{01}}{b_{10}}}\left[\frac{b_{10}}{a_{01}}\,a_{02} + a_{20} - b_{11}\right]^2 + \frac{1}{16}\sqrt{-\frac{b_{10}}{a_{01}}}\left[\frac{a_{01}}{b_{10}}\,b_{20} + b_{02} - a_{11}\right]^2
\end{aligned}$$

are given in terms of the a_{ij} and b_{ij}.

Theorem 2.13 in [59] shows that a nonzero Birkhoff coefficient A implies nonlinear (Lyapunov) stability. However, since we will be considering maps without knowing too many of theirs details, we cannot immediately make use of Lemma 3.3.1 to compute

A directly. Therefore we seek a sufficient condition that allows us to conclude that A is nonzero. And since the actual formula for A is quite involved, it is much easier to try to find a map with non-vanishing Birkhoff coefficient among a continuous family of maps.

In the rest of this section we will consider the following setting. Let $s_* \in \mathbb{R}$ be a point and $U \subset \mathbb{R}$ a neighborhood of s_*. For $\epsilon_0 > 0$, consider a family of C^5 functions

$$L_\epsilon \colon U \times U \to \mathbb{R}^2 \quad \text{for } |\epsilon| < \epsilon_0$$

which satisfy

$$\partial_\epsilon\big|_{\epsilon=0} L_\epsilon(s, s_1) = C\,\frac{s^4 + s_1^4}{24} + \mathcal{O}_5(s, s_1) \quad \text{and} \quad \partial_s \partial_{s_1} L_0(0,0) \neq 0 \tag{2}$$

for some $C \neq 0$. Denote the family of area-preserving maps generated by L_ϵ by T_ϵ (see sections 47 and 48 of [1] for details of this construction) which we will write in coordinate form as

$$T_\epsilon(s, y) \equiv (S_\epsilon(s, y), Y_\epsilon(s, y)) \,.$$

Assume further that the map T_0 has an elliptic fixed point (s_*, y_*)

$$T(s_*, y_*) = (s_*, y_*) \quad \text{with} \quad y_* {:=} \partial_{s_1} L_0(s_*, s_*) = -\partial_s L_0(s_*, s_*)$$

and denote the eigenvalues of $DT_0(s_*, y_*)$ by $\lambda = e^{\pm i\alpha}$. We will assume that the non-resonance conditions $\lambda^2, \lambda^3, \lambda^4 \neq 1$ hold for the elliptic fixed point of T_0. Let us set

$$L_{ij} {:=} \partial_s^i \partial_{s_1}^j L_0(s_*, s_*)$$

to simplify the notations.

Proposition 3.3.2. *The derivative of T_0 at the fixed point (s_*, y_*) reads*

$$DT_0(s_*, y_*) = -\frac{1}{L_{11}} \begin{pmatrix} L_{20} & 1 \\ L_{20}\, L_{02} - L_{11}^2 & L_{02} \end{pmatrix}$$

and the family of maps T_ϵ satisfies

$$\partial_\epsilon\big|_{\epsilon=0} T_\epsilon(s+s_*, y+y_*) = -C\,\frac{1}{6}\begin{pmatrix} \frac{1}{L_{11}}\,s^3 \\ \frac{L_{02}}{L_{11}}\,s^3 + (\frac{L_{20}\,s+y}{L_{11}})^3 \end{pmatrix} + \mathcal{O}_4(s,y)$$

for s and y in a neighborhood of zero.

Proof. The definition of the maps $T_\epsilon(s,y) \equiv (S_\epsilon(s,y), Y_\epsilon(s,y))$ in terms of the generating function L_ϵ

$$\partial_s L_\epsilon(s, S_\epsilon(s,y)) = -y \quad \text{and} \quad \partial_{s_1} L_\epsilon(s, S_\epsilon(s,y)) = Y_\epsilon(s,y) \tag{3}$$

immediately shows

$$DT_0(s_*, y_*) = -\frac{1}{L_{11}}\begin{pmatrix} L_{20} & 1 \\ L_{20}\,L_{02} - L_{11}^2 & L_{02} \end{pmatrix} \tag{4}$$

for the derivative of T_0 at the fixed point (s_*, y_*).

Differentiating equations (3) with respect to ϵ, and evaluating at $\epsilon = 0$ yields

$$\begin{aligned} 0 &= C\,\frac{[s-s_*]^3}{6} + \partial_s\partial_{s_1} L_0(s, S_0(s,y))\,\partial_\epsilon\big|_{\epsilon=0} S_\epsilon(s,y) \\ &\quad + \mathcal{O}_4(s-s_*, y-y_*) \\ \partial_\epsilon\big|_{\epsilon=0} Y_\epsilon(s,y) &= C\,\frac{[S_0(s,y)-s_*]^3}{6} + \partial_{s_1}^2 L_0(s, S_0(s,y))\,\partial_\epsilon\big|_{\epsilon=0} S_\epsilon(s,y) \\ &\quad + \mathcal{O}_4(s-s_*, y-y_*) \end{aligned}$$

where we used the special property of the generating functions stated in equation (2). Solving now for the ϵ-derivatives of S_ϵ and Y_ϵ we obtain

$$\begin{aligned} \partial_\epsilon\big|_{\epsilon=0} S_\epsilon(s+s_*, y+y_*) &= -C\,\frac{s^3}{6\,L_{11}} + \mathcal{O}_4(s,y) \\ \partial_\epsilon\big|_{\epsilon=0} Y_\epsilon(s+s_*, y+y_*) &= -C\,\frac{1}{6}\,\big[\frac{L_{20}\,s+y}{L_{11}}\big]^3 - C\,\frac{L_{02}\,s^3}{6\,L_{11}} + \mathcal{O}_4(s,y) \end{aligned}$$

by Taylor expansion and (4). □

The point of the specific form of the generating functions (2) is now clear. By Proposition 3.3.2 the change of the map to first order in ϵ is of third order in (s, y). Comparing this to the general form of the Birkhoff coefficients A_ϵ, as given in Lemma 3.3.1, we see that $\partial_\epsilon|_{\epsilon=0} A_\epsilon$ only involves the third order term $\operatorname{Im} c_{21}$. This we can further exploit to obtain the main result of this section, which is the following:

Theorem 3.3.3. *Let (s_*, y_*) be a non-resonant elliptic fixed point of a family of planar area-preserving maps T_ϵ which are generated in a neighborhood of (s_*, y_*) by L_ϵ satisfying (2), i.e.*

$$\partial_\epsilon\big|_{\epsilon=0} L_\epsilon(s + s_*, s_1 + s_*) = C\,\frac{s^4 + s_1^4}{24} + \mathcal{O}_5(s, s_1) \quad \textit{for some} \quad C \neq 0$$

and $\partial_s \partial_{s_1} L_0(s_*, s_*) \neq 0$. Then there exists an $\epsilon_* > 0$ such that for every $\epsilon \in (-\epsilon_*, \epsilon_*) \setminus \{0\}$ the point (s_*, y_*) is a nonlinearly stable fixed point of T_ϵ with a nonzero first Birkhoff coefficient.

Proof. Without loss of generality assume that $(s_*, y_*) = (0, 0)$, so that we are exactly in the setting discussed so far in this section. Also, by rescaling ϵ by C we may also assume that $C = 1$. Combining the general expression of the Birkhoff coefficient of Lemma 3.3.1 with the specific structure of the considered family of maps as given in Proposition 3.3.2 we obtain

$$\begin{aligned}
\partial_\epsilon\big|_{\epsilon=0} A_\epsilon &= \partial_\epsilon\big|_{\epsilon=0} \operatorname{Im} c_{21} \\
&= \frac{1}{8}\, a_{10} \big[-\partial_\epsilon\big|_{\epsilon=0} a_{21} + 3\,\frac{b_{10}}{a_{01}}\,\partial_\epsilon\big|_{\epsilon=0} a_{03} - 3\,\frac{a_{01}}{b_{10}}\,\partial_\epsilon\big|_{\epsilon=0} b_{30} + \partial_\epsilon\big|_{\epsilon=0} b_{12} \big] \\
&\quad - \frac{1}{8}\, b_{10} \big[\partial_\epsilon\big|_{\epsilon=0} a_{12} - 3\,\frac{a_{01}}{b_{10}}\,\partial_\epsilon\big|_{\epsilon=0} a_{30} - \frac{a_{01}}{b_{10}}\,\partial_\epsilon\big|_{\epsilon=0} b_{21} + 3\,\partial_\epsilon\big|_{\epsilon=0} b_{03} \big]
\end{aligned}$$

because only third order terms appear in $\partial_\epsilon|_{\epsilon=0} T_\epsilon$.

Using Taylor expansion we can express the various coefficients a_{ij} and b_{ij} in terms of L_{ij} as

$$a_{10} = -\frac{L_{20}}{L_{11}}\,, \qquad a_{01} = -\frac{1}{L_{11}}\,, \qquad b_{10} = \frac{a_{10}\, b_{01} - 1}{a_{01}}\,, \qquad b_{01} = -\frac{L_{02}}{L_{11}}$$

and

$$\partial_\epsilon\big|_{\epsilon=0} a_{30} = -\frac{1}{6}\,\frac{1}{L_{11}} = \frac{a_{01}}{6}\;, \qquad \partial_\epsilon\big|_{\epsilon=0} b_{30} = -\frac{1}{6}\,\frac{L_{02}}{L_{11}} - \frac{1}{6}\,\frac{L_{20}^3}{L_{11}^3} = \frac{1}{6}\,[b_{01} + a_{10}^3]$$

$$\partial_\epsilon\big|_{\epsilon=0} a_{21} = 0\;, \qquad \partial_\epsilon\big|_{\epsilon=0} b_{21} = -\frac{1}{2}\,\frac{L_{20}^2}{L_{11}^3} = \frac{1}{2}\,a_{10}^2\,a_{01}$$

$$\partial_\epsilon\big|_{\epsilon=0} a_{12} = 0\;, \qquad \partial_\epsilon\big|_{\epsilon=0} b_{12} = -\frac{1}{2}\,\frac{L_{20}}{L_{11}^3} = \frac{1}{2}\,a_{10}\,a_{01}^2$$

$$\partial_\epsilon\big|_{\epsilon=0} a_{03} = 0\;, \qquad \partial_\epsilon\big|_{\epsilon=0} b_{03} = -\frac{1}{6}\,\frac{1}{L_{11}^3} = \frac{1}{6}\,a_{01}^3$$

again by using the result of Proposition 3.3.2. Therefore we obtain

$$16\,\partial_\epsilon\big|_{\epsilon=0} A_\epsilon = -\frac{a_{01}^2\,(1+a_{10}^4)}{a_{10}\,b_{01}-1} - a_{01}^2\,a_{10}\,b_{01} + a_{01}^2 + 2\,a_{10}^2\,a_{01}^2\;.$$

Since we assume that the fixed point is elliptic, we must have $|\operatorname{tr} DT_0| = |a_{10} + b_{01}| < 2$ and $a_{01} \neq 0$. With

$$t{:=}\frac{a_{10}+b_{01}}{2} \in (-1,1)$$

the above becomes

$$\partial_\epsilon\big|_{\epsilon=0} A_\epsilon = \frac{a_{01}^2}{8}\left[1 + a_{10}^2\,\frac{1+2\,(t-a_{10})^2}{1-t^2+(t-a_{10})^2}\right] \geq \frac{a_{01}^2}{8} > 0\;.$$

Hence there exists an $\epsilon_* > 0$ such that $A_\epsilon \neq 0$ holds true for all $\epsilon \in (-\epsilon_*, \epsilon_*) \setminus \{0\}$. Moser's twist theorem then implies (see theorem 2.13 in [59]) that the fixed point (s_*, y_*) is nonlinearly stable with a nonzero first Birkhoff coefficient for all maps T_ϵ with $\epsilon \in (-\epsilon_*, \epsilon_*) \setminus \{0\}$. □

3.4 Construction of Nonlinearly Stable Periodic Orbits

In this section we consider the nonlinear stability problem for a linearly stable periodic orbit γ on a general billiard table Q. A typical situation is shown in Fig. 7. Let N denote the number of reflections of γ, and let s_i and φ_i, $i = 1, \ldots, N$, denote the arc length parameter and angle of reflection at the i-th reflection point of γ, respectively. As before, let Φ^t and $\mathcal{F}$ denote the billiard flow and billiard map, respectively.

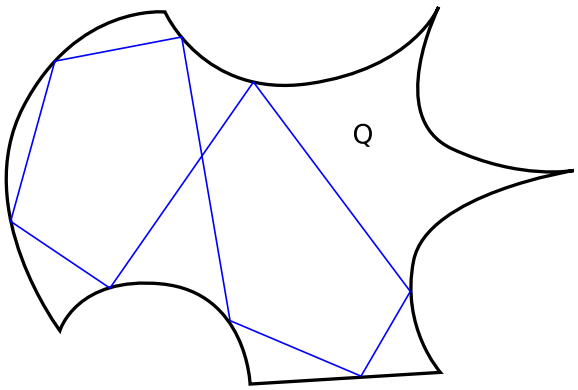

Figure 7: General billiard table Q with an elliptic, non-resonant periodic orbit.

Since we assume that the periodic orbit γ is linearly stable, the eigenvalues of the linearized billiard map are complex conjugate of modulus one, hence

$$\lambda_1 = \overline{\lambda}_2 = e^{i\,\alpha} \equiv \lambda \quad \text{are the eigenvalues of} \quad D\mathcal{F}^N(s_1, \sin\varphi_1)$$

for some angle α. Furthermore we assume that γ is non-resonant, i.e. $\lambda^2, \lambda^3, \lambda^4 \neq 1$ holds.

In the non-resonant case a result due to Moser (see theorems 2.12 and 2.13 in [59]) guarantees that there exists a real-analytic canonical change of coordinates $(s, \sin\varphi) \mapsto z \in \mathbb{C}$ in a neighborhood of any of the $(s_i, \sin\varphi_i)$ such that it conjugates $\mathcal{F}^N$ to its Birkhoff normal form

$$z \mapsto \lambda\, z\, e^{i\,A\,|z|^2} + \mathcal{O}(|z|^4)$$

with $A \in \mathbb{R}$ the first Birkhoff coefficient. A sufficient condition for nonlinear stability of γ then is a nonzero value for A, cf. Theorem 2.13 in [59].

Applying this strategy to our general setup seems intractable because we would need a way to decide whether or not A vanishes. Therefore we will not consider the nonlinear stability problem of γ on the given table Q. Instead we will introduce a family of tables Q_ϵ, which are almost identical to Q and have γ as a periodic orbit. We then want to know whether γ is nonlinearly stable for at least some tables in that family.

A construction of such a family, which allows us to analyze A as a function of the table was given in [31, 44] in the context of two-periodic orbits. It consists of a local perturbation of the boundary curve in normal direction, maintaining a third order contact, as shown in Fig. 8.

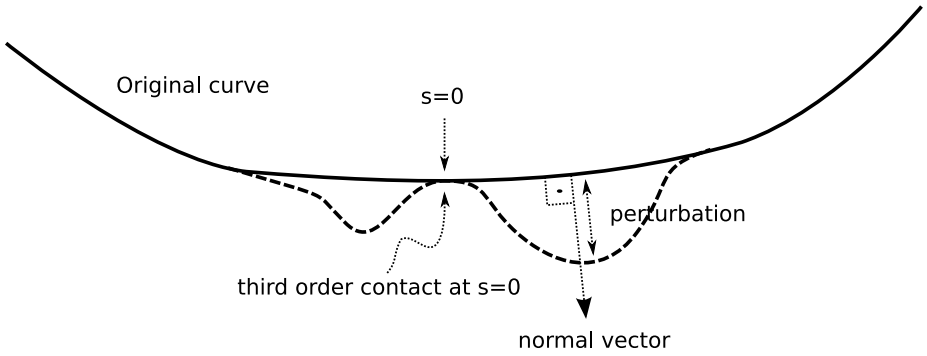

Figure 8: Construction of the curves Γ_ϵ.

Lemma 3.4.1 (Local perturbation in normal direction)**.** *Let Γ be a C^5 curve, parametrized by its arc length s, for s in some interval I containing a neighborhood of $s = 0$. Let $\phi\colon I \to \mathbb{R}$ be a C^5 function with $\phi(0) = \phi'(0) = \phi''(0) = \phi'''(0) = 0$. Then the parametrization of the curve $\Gamma_\phi(\xi) := \Gamma(\xi) + \phi(\xi)\, n(\xi)$ by its arc length reads*

$$\Gamma_\phi(s) = \Gamma(s) + \phi''''(0)\, n_0\, \frac{s^4}{24} + \mathcal{O}(s^5)$$

in a neighborhood of $s = 0$.

Proof. Denote by $t(s) = \Gamma'(s)$ and $n(s) = t(s)^\perp$ the tangent and normal vector of $\Gamma(s)$, respectively. The definition of the curvature $\mathcal{K}(s)$ of $\Gamma(s)$ yields

$$n'(s) = \mathcal{K}(s)\, t(s)$$

hence

$$\Gamma'_\phi(\xi) = [1 + \mathcal{K}(\xi)\, \phi(\xi)]\, t(\xi) + \phi'(\xi)\, n(\xi)\ .$$

In particular we obtain

$$\left\| \Gamma'_\phi(\xi) \right\| = \sqrt{[1 + \mathcal{K}(\xi)\, \phi(\xi)]^2 + \phi'(\xi)^2} = 1 + \mathcal{O}(\xi^4)$$

for the length of the tangent vector of Γ_ϕ. Therefore

$$S_\epsilon(\xi) = \int_0^\xi \parallel \Gamma'_\phi(\zeta) \parallel \, d\zeta = \xi + \mathcal{O}(\xi^5)$$

for the arc length of Γ_ϕ. The claim that Γ_ϕ and Γ have a third order contact (in terms of their arc length parametrizations) at the reference point $\Gamma(0)$ follows now immediately from the definition of Γ_ϕ and Taylor expansion of ϕ and n. □

This perturbation of the boundary was used in [31, 44] to study the stability of two-periodic orbits on strictly convex billiard tables. More precisely, it was shown that the first Birkhoff coefficient can be made nonzero using an arbitrary small local boundary perturbation of the above type. The following theorem generalizes this construction to arbitrary linearly stable, non-resonant periodic orbits on arbitrary billiard tables.

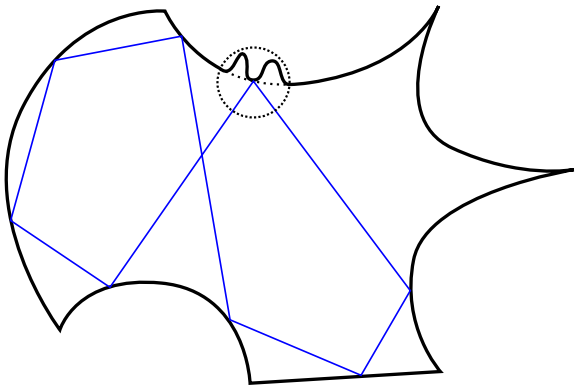

Figure 9: An arbitrarily small local perturbation of the boundary (in the sense of the C^4 topology) of the billiard table that preserves the elliptic periodic orbit and renders it nonlinearly stable.

Theorem 3.4.2. *Consider a billiard table Q with a linearly stable, non-resonant N-periodic orbit γ, which has reflections off of C^5 boundary components. Let $s_1, \ldots, s_N$ denote the arc length parameters corresponding to the N points of reflection. Pick any of the s_i, say s_{i_*}. Then for all small enough $\delta > 0$ there exists a billiard table Q_{δ,i_*}, which is C^5 close to Q and coincides with Q outside the δ-neighborhood $B_\delta(\Gamma(s_{i_*}))$*

of $\Gamma(s_{i_*})$*, and such that* γ *is a nonlinearly stable periodic orbit on* Q_{δ,i_*} *with nonzero Birkhoff coefficient.*

Proof. After possibly relabeling the points we may assume that $i_* = 1$, and without loss of generality we may choose the arc length parametrization of ∂Q such that $s_1 = 0$.

Denote the boundary components of the i-th point of reflection by Γ_i. Let $\delta > 0$ be arbitrary, but so small that $B_\delta(\Gamma(s_1))$ contains no other points of reflection, and has intersection only with the boundary component Γ_1 (see Fig. 9 for an illustration).

Choose a C^∞ function $\phi\colon \mathbb{R} \to \mathbb{R}$ with support in $[-\delta/2, \delta/2]$ such that $\phi(0) = \phi'(0) = \phi''(0) = \phi'''(0) = 0$, $\phi''''(0) = 1$, $|\phi(s)| \leq 1$. Let $n(s)$ denote the unit normal vector at the point $\Gamma_1(s)$. Define

$$\Gamma_1^\epsilon(t) := \Gamma_1(t) + \epsilon\, \phi(t)\, n(t)$$

for all $\epsilon \in [-\delta/2, \delta/2]$.

Clearly the graphs of Γ_1^ϵ and Γ_1 coincide outside $B_\delta(\Gamma(0))$. Moreover, for ϵ small enough Γ_1^ϵ has no self-intersections and thus defines a new billiard table Q_ϵ by replacing Γ_1 by Γ_1^ϵ.

By Lemma 3.4.1

$$\Gamma_1^\epsilon(s) = \Gamma_1(s) + \epsilon\, \frac{s^4}{24} + \mathcal{O}(s^5)$$

in a neighborhood of $s = 0$. In particular, the tangent line at $s = 0$ is preserved, and hence the orbit γ remains N-periodic for all Q_ϵ.

In fact, since the generating function of the N-th iterate of the billiard map in a small enough neighborhood of the periodic orbit γ reads

$$\begin{aligned} L_\epsilon(s_1, \ldots, s_N, s_{N+1}) = \| \Gamma_2(s_2) - \Gamma_1^\epsilon(s_1) \| + \ldots + \| \Gamma_N(s_N) - \Gamma_{N-1}(s_{N-1}) \| \\ + \| \Gamma_1^\epsilon(s_{N+1}) - \Gamma_N(s_N) \| \end{aligned}$$

the above expansion of Γ_1^ϵ immediately implies

$$\begin{aligned}\partial_\epsilon\big|_{\epsilon=0} L_\epsilon(s_1,\dots,s_N,s_{N+1}) &= -\frac{\Gamma_2(s_2)-\Gamma_1(s_1)}{\|\,\Gamma_2(s_2)-\Gamma_1(s_1)\,\|}\cdot\partial_\epsilon\big|_{\epsilon=0}\Gamma_1^\epsilon(s_1)\\ &\quad+\frac{\Gamma_1(s_{N+1})-\Gamma_N(s_N)}{\|\,\Gamma_1(s_{N+1})-\Gamma_N(s_N)\,\|}\cdot\partial_\epsilon\big|_{\epsilon=0}\Gamma_1^\epsilon(s_{N+1})\\ &= -\cos\varphi_1\,\frac{s_1^4+s_{N+1}^4}{24}+\mathcal{O}_5(s_1,s_{N+1})\end{aligned}$$

because only two terms in L_ϵ depend on ϵ.

The boundary curves are of class C^5 in a neighborhood of the reflection points, hence the associated (N-fold iteration of the) billiard map is of class C^4. Since $\cos\varphi_1 > 0$ we can apply Theorem 3.3.3 to conclude that for all small enough nonzero values of ϵ, the N-periodic periodic orbit γ is nonlinearly stable on Q_ϵ. Let $Q_*(\Gamma, L)$ denote one such table on which the periodic orbit γ is nonlinearly stable with nonzero first Birkhoff coefficient. □

Now we are in the position to prove our main result, Theorem 3.1.1.

Proof of Theorem 3.1.1. Let $L > 0$ be arbitrary, and Γ as in the statement of Theorem 3.1.1. By Theorem 3.2.6 there exists a billiard table $Q(L,\Gamma)$ with $\Gamma \subset \partial Q$ which has a linearly stable, non-resonant periodic orbit γ with free path of length at least L before and after a sequence of consecutive reflections off of Γ.

Applying now the result of Theorem 3.4.2 we may assume that this orbit is actually non-linearly stable with nonzero Birkhoff coefficient, otherwise we slightly modify the original table $Q(L,\Gamma)$ as stated in Theorem 3.4.2, which does not change the length of the free path γ before and after Γ to a value less than L.

Notice that by the implicit function theorem the periodic orbit γ persists under any (not just the ones of the type as in Lemma 3.4.1, cf. the proof of Theorem 3.4.2) sufficiently small C^5 perturbation of the boundary of the constructed billiard table. The perturbed periodic orbits will have the same period and are elliptic with a free

path before and after Γ of length at least L. By Lemma 3.3.1 the first Birkhoff coefficient depends C^3-continuously on the map, hence C^4-continuously on the boundary. Thus all the perturbed periodic orbits will have a nonzero Birkhoff coefficient, and hence are non-linearly stable, provided that the perturbation of the boundary is small enough. □

3.5 Conclusion

It is well known that if at least one focusing component is present, then in order to ensure hyperbolicity the boundary should be arranged in such a way that all beams of rays focus after any sequence of consecutive reflection off the focusing part of the boundary, and defocus (i.e. pass through a conjugate point) before the next reflection from a curved part of the boundary of the billiard table.

So far, there are only two examples [20, 22] of hyperbolic billiards where this condition of defocusing between any reflection from a focusing component and the next reflection off the curved part of the boundary is violated. However, both of these classes of billiards are very special. In fact, the absence of defocusing between some reflections from a focusing part of the boundary and the next reflection (off the curved part of the boundary) is allowed in [20] only in those parts of the phase space where the billiard dynamics is integrable. Therefore focusing does not dominate dispersing in this part of the phase space while on the complementary part of the phase space the defocusing mechanism ensures hyperbolicity in the usual way. Likewise, in [22] the billiard table has a very specially designed part where one can control that focusing is dominated by dispersing, although the beams do not defocus after reflections off the focusing component, while on the complement of this part of phase space, yet again, the defocusing mechanism generates hyperbolicity.

Therefore, one may conclude that in all hyperbolic billiards with focusing boundary components constructed so far, it is the mechanism of defocusing which is responsible for hyperbolicity. Hence, the standard strategy to construct ergodic chaotic billiards is to choose all focusing components to be absolutely focusing, and to move them sufficiently far away from all other regular (smooth) components of the boundary, e.g. [66].

In this chapter of this thesis we have shown that for this strategy it is very essential that all focusing components are absolutely focusing, and conjecture that in two-dimensional billiards with at least one focusing, but non-absolutely focusing boundary component typically there are stable periodic orbits.

CHAPTER IV

C^2-STADIA

4.1 Introduction

In 1973 Lazutkin [52] showed that for strictly convex billiard tables Q with a boundary ∂Q of class C^{553} there exists an uncountable family of caustics near the boundary. The presence of these caustics prevents the billiard dynamics from being ergodic and gives rise to nearly integrable motion close to the boundary.

Shortly after, in 1974 it was shown in [13, 14] (see also [15]) that there are convex billiard tables on which the billiard dynamics is hyperbolic and ergodic. In billiards with focusing boundary components the mechanism that creates the hyperbolicity is the mechanism of defocusing. The most famous and best studied convex billiard in this class is the stadium [14, 15], see Fig. 4, whose boundary consists of two semi-circles connected by two straight line segments. For any (nonzero) length of the line segments the resulting billiard is ergodic and hyperbolic. Note that the boundary of the stadium is (globally) C^1.

These two results are in sharp contrast to each other. The difference is due to the smoothness of the boundary of the billiard table. If the boundary of a convex table is smooth enough then the presence of caustics prevents ergodicity. If the boundary is C^1, then there are (continuous families of) convex billiard tables with ergodic and hyperbolic motion. Therefore, the natural question is: which class of smoothness of the boundary of the billiard table separates convex billiards with completely chaotic dynamics and from non-ergodic dynamics with elliptic islands. This question was raised immediately after the appearance of the stadium billiard in 1974 by Anosov, Katok, Arnold, Moser and others. Later Douady [33] lowered the smoothness requirement

for Lazutkin's results to C^6 boundaries.

In this part of the thesis we provide an answer to this long-standing question by showing that critical smoothness of the boundary is C^2. More precisely, we show that if the boundary of the stadium is made C^2 smooth, then elliptic periodic orbits appear, so these billiards are non-ergodic.

In Chapter 3 we showed that as soon as non-absolutely focusing boundary components are present the mechanism of defocusing can fail, and hence stable motion can appear. In particular, focusing boundary components with vanishing curvature, which appear when making the boundary of the stadium C^2 smooth, are never absolutely focusing. Therefore it seems natural to attack the above question from this point of view, especially because the hyperbolicity in the stadium billiard is generated solely by the defocusing mechanism.

However, the problem addressed in here is more challenging than the one of Chapter 3. This is because there one was allowed to design the boundary of the billiard table. Here the problem is that we only allow for small perturbation of a given boundary.

4.2 Setup and Statement of the Main Results

The billiard tables we consider are obtained by the following construction. Take a semi-circle and smooth out some part of the curve near the end points such that the resulting focusing curve Γ has zero curvature at its endpoints, and so that Γ is symmetric just as the semi-circle was. Consider two identical copies of the boundary component Γ. By connecting their endpoints using straight line segments of length L we obtain a continuous family (parametrized by L) of C^2-smooth stadium-like billiard tables, or simply C^2-stadia. See Fig. 10 for the illustration of this construction.

The length L of the straight line segments will be referred to as the separation distance between the curved boundary components. The part of the resulting billiard

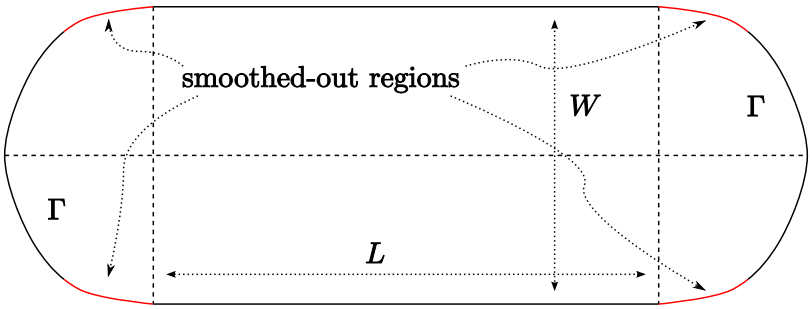

Figure 10: Illustration of the smooth stadium like billiard tables we consider.

table, which is obtained by completing the two parallel line segments to a rectangle will be referred to as the rectangular channel.

We will prove the following main result about the dynamics of the billiard in C^2-stadia.

Theorem 4.2.1 (Large Separations)**.** *For any short enough (in terms of arc length) symmetric smoothed-out regions (near the endpoints) of the curved boundary components there exists constants $\delta, a, b > 0$ and $N \in \mathbb{N}$ such that for any separation distance L with*

$$L \in \bigcup_{n \geq N} [a + n\, b, a + (n+1)\, b + \delta]$$

the resulting C^2-smooth stadium-like billiard table possesses elliptic periodic orbits.

The elliptic periodic orbits of Theorem 4.2.1 are in no sense obtained by a perturbation of the parabolic two-periodic orbit for $L = 0$. In fact, even at a heuristic level there seems to be no obvious reason why elliptic periodic orbits as claimed in Theorem 4.2.1 should exist.

The key observation behind the construction of these orbits is the fact that the curved boundary component Γ is non-absolutely focusing. The elliptic periodic orbits of Theorem 4.2.1 naturally correspond to those constructed in [21]. It means that the violation of the absolutely focusing cannot by compensated for by making the free path arbitrarily large.

4.3 Elliptic Periodic Orbits for Large Separations

In order to find stable periodic orbits for large separations of the two curved boundary components we exploit the fact that the curved components are not absolutely focusing. In particular, the first step will be to find parabolic periodic orbits. This will be accomplished by constructing billiard trajectories such that an initially infinitesimal parallel beam will leave the curved boundary component again as a parallel beam.

4.3.1 General Results

Let $(s_1, \varphi_1), \dots (s_N, \varphi_N)$ denote a complete sequence of reflections off the curved boundary component Γ. Denote by $\tau_{k,k+1}$ the free path between the k-th and $(k+1)$-st reflection, and set $\mathcal{R}_k = \frac{2\,\mathcal{K}(s_k)}{\cos\varphi_k}$.

Suppose that this sequence of reflections is symmetric along Γ. This assumption means, in particular, that $\tau_{k,k+1} = \tau_{N-k,N-k+1}$ and $\mathcal{R}_k = \mathcal{R}_{N-k}$ hold. Therefore, the Jacobian of the billiard flow computed along the sequence of N reflection reads

$$J = (-1)^N \begin{pmatrix} 1 & 0 \\ \mathcal{R}_N & 1 \end{pmatrix} \begin{pmatrix} 1 & \tau_{N-1,N} \\ 0 & 1 \end{pmatrix} \dots \begin{pmatrix} 1 & \tau_{1,2} \\ 0 & 1 \end{pmatrix} \begin{pmatrix} 1 & 0 \\ \mathcal{R}_1 & 1 \end{pmatrix} = \begin{pmatrix} a & b \\ c & a \end{pmatrix}$$

for some real numbers a, b, c satisfying $a^2 - b\,c = 1$.

By simultaneously changing s_1 and s_N to $s_1 + \alpha$ and $s_N - \alpha$ we obtain a one-parametric continuous family of complete sequences of reflections off Γ, provided that $|\alpha|$ is sufficiently small. Denote by $(s_1^{(\alpha)}, \varphi_1^{(\alpha)}), \dots, (s_N^{(\alpha)}, \varphi_N^{(\alpha)})$ the corresponding reflection points and angles, cf Fig. 11.

Since the curved boundary component Γ is symmetric and the modification of the initially symmetric sequence of reflections respects that symmetry the resulting complete sequences of reflections will be symmetric too. Let

$$J_\alpha = \begin{pmatrix} a_\alpha & b_\alpha \\ c_\alpha & a_\alpha \end{pmatrix} \qquad \text{with} \quad a_\alpha^2 - b_\alpha\, c_\alpha = 1$$

denote the Jacobian of the billiard flow corresponding to the sequence of reflections for the parameter value α.

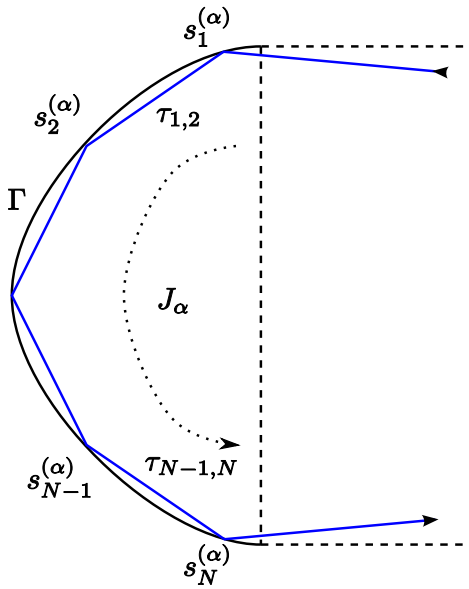

Figure 11: A symmetric, complete sequence of reflections off the curved boundary component Γ. Shown is the case of an odd number of reflections.

Due to the imposed symmetry of the sequence of reflections we consider and the symmetry of the boundary component Γ the angles of the billiard flow (relative to the horizontal direction, cf Fig. 12) at the point of entering and at the point of leaving the parallel segment of the billiard table are the same. Denote this angle by ω_α.

Similarly, the points at which the incoming and outgoing trajectories cross the vertical (cf Fig. 12) are also symmetric. Let s_α denote the distance of that point from the straight boundary segment.

Lemma 4.3.1. *Any of the sequences of reflections closes up to a (symmetric) periodic orbit if and only if*

$$L \equiv L(\alpha, n) = \frac{n\,W - 2\,s_\alpha}{\tan\omega_\alpha}\,, \qquad \tau \equiv \tau(\alpha, n) = \frac{L(\alpha, n)}{\cos\omega_\alpha} + 2\,T_\alpha$$

hold for the separation distance L and the (corresponding) free path between the curved boundary components τ, respectively. The distance T_α is the distance after the last

reflection off of Γ *to the point where the trajectory enters the rectangular channel, cf Fig. 12.*

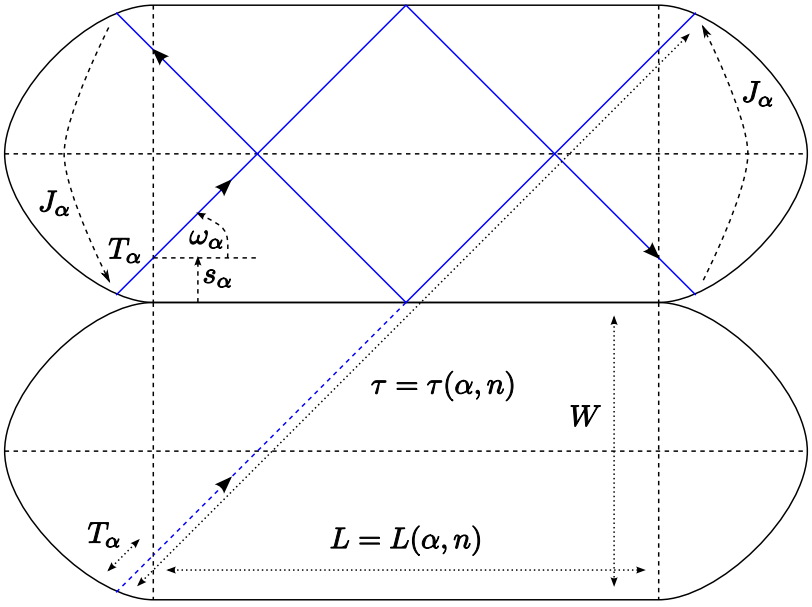

Figure 12: Illustration of the construction of a periodic orbit by closing up a symmetric, complete sequence of reflections off the curved boundary component Γ.

Let $L = L_\alpha$ (and thus τ_α) be chosen such that (at least) the complete sequence of reflections corresponding to the parameter value α becomes a periodic orbit. Linearizing the billiard flow along this periodic orbit yields the monodromy matrix M_α, which is given by

$$M_\alpha = \left[\begin{pmatrix} 1 & \tau_\alpha \\ 0 & 1 \end{pmatrix} J_\alpha \right]^2$$

because of the symmetry and the fact that inside the rectangular channel the linearization of the billiard flow is like the one of a free flight. In particular,

$$\operatorname{tr} M_\alpha = (2\, a_\alpha + \tau_\alpha\, c_\alpha)^2 - 2 \tag{5}$$

follows for its trace.

From this relation it follows that in order to have elliptic orbits for large separation distances L_α, and hence large values of τ_α, the value of c_α must be close to zero. Thus,

from now on we will assume that

$$\text{for} \quad \alpha = 0 \ : \qquad c_0 = 0 \quad \text{hence} \quad J_0 = \begin{pmatrix} a_0 & b_0 \\ 0 & a_0 \end{pmatrix} \qquad \text{with} \quad a_0^2 = 1 \qquad (6)$$

holds.

Lemma 4.3.2. *Since $c_0 = 0$ all periodic orbits corresponding to $\alpha = 0$ are parabolic.*[1]

An immediate consequence of Lemma 4.3.1 and Lemma 4.3.2 is the following

Proposition 4.3.3. *For all separation distances L of the form $L = L(0, n)$, where $n = 1, 2, \ldots$, there exists a parabolic periodic orbit.*

In order to obtain elliptic periodic orbits [2] the values of α and L must be chosen such that the resulting periodic orbit has a monodromy matrix M_α with a trace satisfying $|\operatorname{tr} M_\alpha| < 2$. From (5) and Lemma 4.3.1 we obtain the following

Lemma 4.3.4. *For the periodic orbit $\gamma_{\alpha,n}$ corresponding to α and n the following equivalences*

$$\begin{aligned} \gamma_{\alpha,n} \text{ is elliptic} &\iff a_\alpha + \frac{1}{2}\, c_\alpha\, \tau(\alpha, n) \in (-1, 1) \setminus \{0\} \\ &\iff a_\alpha \left[1 + \frac{1}{2}\, \mathcal{B}_\alpha\, \tau(\alpha, n)\right] \in (-1, 1) \setminus \{0\} \end{aligned}$$

hold.

Proof. By Lemma 4.3.1 we know that the periodic orbit corresponding to α and n exists if and only if the free path inside the rectangular channel is $\tau(\alpha, n)$. From (5) the trace of the corresponding monodromy matrix reads

$$\operatorname{tr} M_\alpha = [2\, a_\alpha + c_\alpha\, \tau(\alpha, n)]^2 - 2$$

[1] *A periodic orbit is called parabolic if its monodromy matrix M satisfies $\operatorname{tr} M = 2$, and thus has eigenvalues $\lambda_{1,2} = 1$.*

[2] A periodic orbit is called elliptic, if its monodromy matrix M satisfies $|\operatorname{tr} M| < 2$, and thus has a pair of (strictly) complex (conjugate) eigenvalues of modulus one.

which always satisfies $\operatorname{tr} M_\alpha \geq -2$.

Therefore, ellipticity of the periodic orbit is equivalent to

$$\begin{aligned}\text{elliptic} &\iff -2 < [2\,a_\alpha + c_\alpha\,\tau(\alpha,n)]^2 - 2 < 2 \iff 0 < \left[a_\alpha + \frac{1}{2}\,c_\alpha\,\tau(\alpha,n)\right]^2 < 1 \\ &\iff a_\alpha + \frac{1}{2}\,c_\alpha\,\tau(\alpha,n) \in (-1,1)\setminus\{0\}\end{aligned}$$

which is the first of the two claimed conditions. The second condition then follows immediately from the definition of $\mathcal{B}_\alpha \equiv \frac{c_\alpha}{a_\alpha}$. □

A slightly different, but more insightful way of rewriting the ellipticity condition is provided by the following result.

Lemma 4.3.5. *The periodic orbit $\gamma_{\alpha,n}$ corresponding to α and n is elliptic if and only if*

$$c_\alpha \neq 0\,, \quad \frac{1}{2}\,\tau(\alpha,n) \neq -\frac{a_\alpha}{c_\alpha} \quad \textit{and} \quad \begin{cases} \frac{1}{2}\,\tau(\alpha,n) < |b_\alpha| & a_\alpha = 0 \\ \frac{1}{2}\,\tau(\alpha,n) < -\frac{b_\alpha\,\operatorname{sgn}(a_\alpha)}{1+|a_\alpha|} & \mathcal{B}_\alpha > 0 \\ -\frac{b_\alpha\,\operatorname{sgn}(a_\alpha)}{1+|a_\alpha|} < \frac{1}{2}\,\tau(\alpha,n) < \frac{1+|a_\alpha|}{|c_\alpha|} & \mathcal{B}_\alpha < 0 \end{cases}$$

hold.

Proof. Another way of writing the condition $|\operatorname{tr} M_\alpha| < 2$ is

$$\begin{aligned}|\operatorname{tr} M_\alpha| < 2 &\iff -2 < [2\,a_\alpha + c_\alpha\,\tau(\alpha,n)]^2 - 2 < 2 \\ &\iff 0 < \left[a_\alpha + \frac{1}{2}\,c_\alpha\,\tau(\alpha,n)\right]^2 < 1 \\ &\iff 0 < |a_\alpha|^2\left[1 + \frac{1}{2}\,\mathcal{B}_\alpha\,\tau(\alpha,n)\right]^2 < 1\end{aligned}$$

provided that $a_\alpha \neq 0$. Assuming for now that

$$a_\alpha \neq 0 \qquad \text{and} \qquad 1 + \frac{1}{2}\,\mathcal{B}_\alpha\,\tau(\alpha,n) \neq 0$$

we obtain

$$\begin{aligned}
\text{elliptic} &\iff -\frac{1}{|a_\alpha|} < 1 + \frac{1}{2}\,\mathcal{B}_\alpha\,\tau(\alpha,n) < \frac{1}{|a_\alpha|} \\
&\iff -\frac{1}{|a_\alpha|} < 1 + \frac{1}{2}\,\mathcal{B}_\alpha\,\tau(\alpha,n) \quad \text{and} \quad 1 + \frac{1}{2}\,\mathcal{B}_\alpha\,\tau(\alpha,n) < \frac{1}{|a_\alpha|} \\
&\iff -\frac{1+|a_\alpha|}{|a_\alpha|} < \frac{1}{2}\,\mathcal{B}_\alpha\,\tau(\alpha,n) \quad \text{and} \quad \frac{1}{2}\,\mathcal{B}_\alpha\,\tau(\alpha,n) < \frac{1-|a_\alpha|}{|a_\alpha|}
\end{aligned}$$

which can be further simplified by observing that

$$\frac{1-|a_\alpha|}{|a_\alpha|} = \frac{1-a_\alpha^2}{|a_\alpha|\,(1+|a_\alpha|)} = \frac{-b_\alpha\,c_\alpha}{|a_\alpha|\,(1+|a_\alpha|)} = -\mathcal{B}_\alpha\,\frac{a_\alpha\,b_\alpha}{|a_\alpha|\,(1+|a_\alpha|)}$$

follows from $a_\alpha^2 - b_\alpha\,c_\alpha = 1$. Therefore

$$\text{elliptic} \iff -\frac{1+|a_\alpha|}{|a_\alpha|} < \frac{1}{2}\,\mathcal{B}_\alpha\,\tau(\alpha,n) \quad \text{and} \quad 0 < -\mathcal{B}_\alpha\left[\frac{a_\alpha\,b_\alpha}{|a_\alpha|\,(1+|a_\alpha|)} + \frac{1}{2}\,\tau(\alpha,n)\right]$$

follows. Since $\tau > 0$ in any case we obtain the claimed third condition after a straightforward case-by-case analysis, including the so far excluded cases $a_\alpha = 0$ and $1 + \frac{1}{2}\,\mathcal{B}_\alpha\,\tau(\alpha,n) = 0$. □

The interpretation of the result of Lemma 4.3.5 is the following. For small enough values of $|\alpha|$ all considered sequences of complete reflections have the same (and hence uniformly in α bounded) number of reflections off the compact boundary component Γ. From the continuity of the Jacobian J_α it follows that the entries a_α, b_α, c_α of J_α are uniformly bounded.

Thus, Lemma 4.3.5 shows that arbitrarily long elliptic periodic orbits can only be constructed for $\mathcal{B}_\alpha < 0$ in the limit as $\mathcal{B}_\alpha \to 0^-$.

Therefore, the strategy to construct elliptic periodic orbits for large separation distances is the following. Start with $\alpha = 0$ and some $n \geq 1$ (sufficiently large), and set the separation distance equal to $L(0,n)$. The resulting billiard table then has a parabolic periodic orbit γ, as was shown in Lemma 4.3.2.

Then start increasing or decreasing the separation distance L in a way that the continuation of the periodic orbit γ becomes an elliptic periodic orbit on the new table.

The main problem then is the following. By how much can one change the separation distance (starting from $L(0,n)$) such that the billiard table admits an elliptic periodic orbit? We will actually consider the following more modest question. By how much can one change the separation distance (starting from $L(0,n)$) such that the continuation of the parabolic orbit is an elliptic periodic orbit?

The answer to the latter problem is weaker, because it could very well be that at the point when the continuation of one of the parabolic orbits stops being elliptic, other elliptic periodic orbits are present.

Theorem 4.3.6. *Suppose that $c_0 = 0$ and that there exists some constant $C > 0$ such that $|s_0 - s_\alpha| \leq C\,|\omega_0 - \omega_\alpha|$ for all $|\alpha|$ sufficiently small. Set*

$$\Delta_{\max} = \frac{2\,a_0}{\sin\omega_0}\,\frac{d\omega_\alpha}{dc_\alpha}\Big|_{\alpha=0}$$

which could be positive, or negative. Then for all sufficiently large $n \geq 1$ and all separation distances L taken from the equally spaced sequence of intervals

$$L \in \left\{ L(0,n) + \xi\,\Delta_{\max} : \frac{1}{4} \leq \xi \leq \frac{3}{4} \right\}$$

the resulting billiard table has at least one elliptic periodic orbit.

Proof. From Lemma 4.3.1 and Lemma 4.3.4 we know that the periodic orbit $\gamma_{\alpha,n}$ corresponding to the separation distance $L(\alpha,n)$ is elliptic if and only if

$$a_\alpha + \frac{1}{2}\,c_\alpha\left[\frac{L(\alpha,n)}{\cos\omega_\alpha} + 2\,T_\alpha\right] \in (-1,1)\setminus\{0\} \quad \text{with} \quad L(\alpha,n) = \frac{n\,W - 2\,s_\alpha}{\tan\omega_\alpha}$$

holds. And since we are interested in the amount by which we can change L we set

$$\Delta(\alpha,n) := L(\alpha,n) - L(0,n)$$

so that

$$a_\alpha + c_\alpha\,T_\alpha + \frac{1}{2}\,\frac{c_\alpha\,L(\alpha,n)}{\cos\omega_\alpha} = a_\alpha + c_\alpha\,T_\alpha + \frac{\Delta(\alpha,n)}{2\,\cos\omega_\alpha}\,\frac{c_\alpha\,L(\alpha,n)}{\Delta(\alpha,n)} \in (-1,1)\setminus\{0\}$$

follows for the ellipticity condition.

Notice that the definition of $L(\alpha,n)$ and $\Delta(\alpha,n)$ imply

$$\begin{aligned}\frac{L(\alpha,n)\,c_\alpha}{\Delta(\alpha,n)} &= \frac{L(\alpha,n)\,c_\alpha}{L(\alpha,n)-L(0,n)} = \frac{c_\alpha}{1-\frac{L(0,n)}{L(\alpha,n)}} = \frac{c_\alpha}{1-\frac{n\,W-2\,s_0}{n\,W-2\,s_\alpha}\,\frac{\tan\omega_\alpha}{\tan\omega_0}} \\ &= \frac{c_\alpha}{1-[1-2\,\frac{s_0-s_\alpha}{n\,W-2\,s_\alpha}]\,\frac{\tan\omega_\alpha}{\tan\omega_0}} = \frac{c_\alpha\,\tan\omega_0}{\tan\omega_0-\tan\omega_\alpha+2\,\frac{s_0-s_\alpha}{n\,W-2\,s_\alpha}\,\tan\omega_\alpha} \\ &= \frac{c_\alpha}{\omega_0-\omega_\alpha}\,\frac{\tan\omega_0}{\frac{\tan\omega_0-\tan\omega_\alpha}{\omega_0-\omega_\alpha}+2\,\frac{s_0-s_\alpha}{\omega_0-\omega_\alpha}\,\frac{\tan\omega_\alpha}{n\,W-2\,s_\alpha}}\end{aligned}$$

By assumption the term $\frac{s_0-s_\alpha}{\omega_0-\omega_\alpha}$ is uniformly bounded for all $|\alpha|$ small enough. Therefore,

$$\begin{aligned}\frac{L(\alpha,n)\,c_\alpha}{\Delta(\alpha,n)} &= \frac{c_\alpha}{\omega_0-\omega_\alpha}\,\frac{\tan\omega_0}{\frac{\tan\omega_0-\tan\omega_\alpha}{\omega_0-\omega_\alpha}+\mathcal{O}(n^{-1})} \\ &= \frac{c_\alpha}{\omega_0-\omega_\alpha}\,\frac{\tan\omega_0}{\frac{1}{\omega_0-\omega_\alpha}\int_{\omega_\alpha}^{\omega_a}\frac{1}{\cos^2 x}\,dx+\mathcal{O}(n^{-1})} \\ &= \frac{c_\alpha}{\omega_0-\omega_\alpha}\,\frac{\tan\omega_0}{\frac{1}{2\,\cos^2\omega_\alpha}+\frac{1}{2\,\cos^2\omega_0}+\mathcal{O}[(\omega_0-\omega_\alpha)^2,n^{-1}]}\end{aligned}$$

where the error term is uniform for $(n^{-1},\alpha)\to(0,0)$.

Therefore the condition for $\gamma_{\alpha,n}$ to be elliptic becomes

$$a_\alpha+c_\alpha\,T_\alpha-\frac{c_\alpha-c_0}{\omega_\alpha-\omega_0}\,\frac{\Delta(\alpha,n)\,\sin\omega_0}{\frac{\cos\omega_0}{\cos\omega_\alpha}+\frac{\cos\omega_\alpha}{\cos\omega_0}+\mathcal{O}[(\omega_0-\omega_\alpha)^2,n^{-1}]}\in(-1,1)\setminus\{0\}\,.$$

where we used the assumption $c_0=0$. By Lemma 4.3.5 the orbit $\gamma_{\alpha,n}$ can only be elliptic for large values of n if c_α is close to zero, i.e. α is close to zero.

Because

$$\frac{c_\alpha-c_0}{\omega_0-\omega_\alpha}=-\frac{dc_\alpha}{d\omega_\alpha}\Big|_{\alpha=0}\,[1+\mathrm{o}(1)]\quad\text{as}\quad\alpha\to0$$

and, furthermore, as $\alpha\to0$ we have that $c_\alpha\to0$, T_α is bounded, and $a_\alpha\to a_0=\pm1$, the ellipticity condition becomes

$$a_0-\frac{1}{2}\,\Delta(\alpha,n)\,\sin\omega_0\,\frac{dc_\alpha}{d\omega_\alpha}\Big|_{\alpha=0}\,[1+\mathrm{o}(1)]\,[1+\mathcal{O}(n^{-1})]+o(1)\in(-1,1)\setminus\{0\}$$

as $\alpha\to0$ and $n\to\infty$, where the error terms are uniformly small.

Therefore, setting $\Delta_{\max}$ equal to

$$\Delta_{\max} = \frac{2\,a_0}{\sin\omega_0}\,\frac{d\omega_\alpha}{dc_\alpha}\Big|_{\alpha=0}$$

a sufficient condition for the ellipticity of the continuation of the orbit $\gamma_{\alpha,n}$ is (recall that $a_0 = \pm 1$)

$$1 - \frac{1}{2\,a_0}\,\Delta(\alpha,n)\,\sin\omega_0\,\frac{dc_\alpha}{d\omega_\alpha}\Big|_{\alpha=0} = 1 - \frac{\Delta(\alpha,n)}{\Delta_{\max}} \in \Big[\frac{1}{4},\frac{3}{4}\Big]$$

for all sufficiently large n. This yields precisely the condition claimed in the statement of the theorem, And the continuation of $\gamma_{\alpha,n}$ provides one elliptic periodic, as was to be shown. □

4.3.2 Existence

As long a periodic orbit has only reflections off the part of the curved boundary component which is the original circle (i.e. no reflection off the smoothed-out part of Γ), it will be hyperbolic. Therefore, the simplest possible elliptic periodic orbit is symmetric and has only three reflections off the curved boundary component, as shown in Fig. 13.

Lemma 4.3.7. *For a symmetric billiard trajectory with three reflections such that $\tau\,\mathcal{R}_2$ and $\tau\,\mathcal{R}$ are both finite (i.e. not $\pm\infty$), the condition*

$$1 + \tau\,\mathcal{R} = 0 \quad \textit{or} \quad (1+\tau\,\mathcal{R})\left(1 + \tau\,\frac{\mathcal{R}_2}{2}\right) = 1$$

is equivalent to having $\mathcal{B}_1^- = \mathcal{B}_3^+ = 0$.

Proof. In general the continued fraction expansion yields

$$\mathcal{B}_3^+ = \mathcal{R}_3 + \cfrac{1}{\tau_{23} + \cfrac{1}{\mathcal{R}_2 + \cfrac{1}{\tau_{12} + \cfrac{1}{\mathcal{R}_2 + \mathcal{B}_1^-}}}} \equiv \mathcal{R} + \cfrac{1}{\tau + \cfrac{1}{\mathcal{R}_2 + \cfrac{1}{\tau + \cfrac{1}{\mathcal{R} + \mathcal{B}_1^-}}}}$$

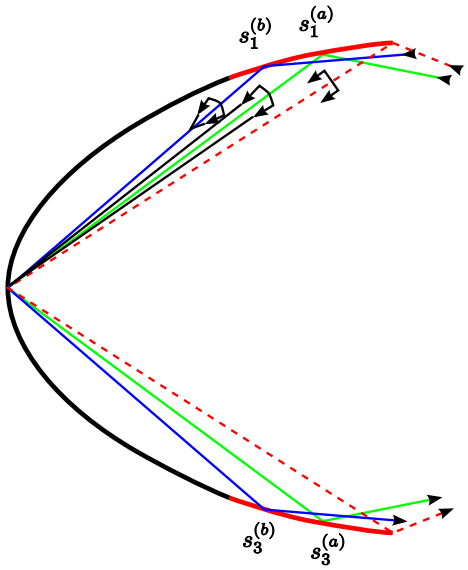

Figure 13: Illustration of the construction of the family of symmetric billiard trajectories as shown in the proof of Proposition 4.3.8.

where we dropped the subscripts at the quantities, which are equal by the assumed symmetry of the trajectory.

In the particular case $\mathcal{B}_1^- = 0$, the above general relation becomes

$$\mathcal{B}_3^+ = \frac{1+\tau\,\mathcal{R}}{\tau}\,\frac{\tau\,\mathcal{R}_2 + 2\,\tau\,\mathcal{R} + \tau^2\,\mathcal{R}\,\mathcal{R}_2}{1+\tau\,\mathcal{R}_2 + 2\,\tau\,\mathcal{R} + \tau^2\,\mathcal{R}\,\mathcal{R}_2}$$

so that $\mathcal{B}_3^+ = 0$ holds if and only if the claimed condition is satisfied (provided that $\tau\,\mathcal{R}$ and $\tau\,\mathcal{R}_2$ are assumed to be finite). □

Proposition 4.3.8. *For any sufficiently short (in terms of arc length) symmetric smoothed-out regions (near the endpoints) of the curved boundary components there exist two continuous families $(\gamma_\alpha^{(a)})_\alpha$, $(\gamma_\alpha^{(b)})_\alpha$ of symmetric billiard trajectories with three reflections off the curved component, such that*

1. *An initially parallel beam will leave as a parallel beam when sent along the trajectory $\gamma_0^{(a)}$ or $\gamma_0^{(b)}$;*

2. *An initially parallel beam will leave as a focusing or dispersing beam when sent along the trajectory $\gamma_\alpha^{(a)}$ or $\gamma_\alpha^{(b)}$ for $\alpha \neq 0$.*

Proof. By assumption the curved boundary component Γ is symmetric. Therefore, any family of symmetric billiard trajectories with only three reflections off the curved boundary component must be such that the second point of reflection must always be at the midpoint of the curved boundary component.

Notice that if the first (and hence the third) point of reflection is close enough to the second one, then all three reflections are off an absolutely focusing subsegment of Γ. In this case the existence of conjugate points between the first and second, and second and third point of reflection implies

$$1 + \tau\,\mathcal{R} < 0 \quad \text{and} \quad (1 + \tau\,\mathcal{R})\left(1 + \tau\,\frac{\mathcal{R}_2}{2}\right) > 1$$

However, if the first (and hence third) point of reflection is off the endpoint of $\mathcal{K}$, then

$$1 + \tau\,\mathcal{R} = 1 \quad \text{and} \quad (1 + \tau\,\mathcal{R})\left(1 + \tau\,\frac{\mathcal{R}_2}{2}\right) = 1 + \tau\,\frac{\mathcal{R}_2}{2} < 1$$

hold.

By continuity there must exist two distinct arc length parameters $s_1^{(a)}$ and $s_1^{(b)}$ such that

$$(a): \quad 1 + \tau\,\mathcal{R} = 1 \qquad \text{and} \qquad (b): \quad (1 + \tau\,\mathcal{R})\left(1 + \tau\,\frac{\mathcal{R}_2}{2}\right) = 1$$

hold for the first point of reflection at $s_1^{(a)}$ and $s_1^{(b)}$, respectively.

By Lemma 4.3.7 the corresponding trajectories $\gamma^{(a)}$ and $\gamma^{(b)}$ are such that an incoming parallel beam leaves Γ also as a parallel beam. □

Proposition 4.3.9. *For the family* $(\gamma_\alpha^{(b)})_\alpha$ *it follows that*

$$\left.\frac{dc_\alpha}{d\omega_\alpha}\right|_{\alpha=0} = \frac{2\,\mathcal{R}\,\tan\varphi_2}{1 + \tau\,\mathcal{R}} + \left(1 - \frac{1}{2}\,\tau\,\mathcal{R}\right)\frac{2\,\mathcal{R}}{(1 + \tau\,\mathcal{R})^2}\,\tan\varphi + \frac{2\,\tau\,\mathcal{R}}{(1 + \tau\,\mathcal{R})^2}\,\frac{\mathcal{K}'}{\mathcal{K}}\,\frac{1}{\cos\varphi}$$

$$\left.\frac{ds_\alpha}{d\omega_\alpha}\right|_{\alpha=0} = \frac{1}{\cos\omega_0}\left[T_0 + \frac{\tau}{1 + \tau\,\mathcal{R}}\right]$$

hold.

Proof. In general, the relation between the billiard map coordinates (s,φ) and the billiard flow coordinates right after the moment of reflection (ξ,ω) is given by

$$\begin{pmatrix} d\xi \\ d\omega \end{pmatrix} = -\begin{pmatrix} \cos\varphi & 0 \\ \mathcal{K}(s) & 1 \end{pmatrix}\begin{pmatrix} ds \\ d\varphi \end{pmatrix} \quad \text{and} \quad \begin{pmatrix} ds \\ d\varphi \end{pmatrix} = -\frac{1}{\cos\varphi}\begin{pmatrix} 1 & 0 \\ -\mathcal{K}(s) & \cos\varphi \end{pmatrix}\begin{pmatrix} d\xi \\ d\omega \end{pmatrix}$$

in infinitesimal form. However, in the case of the point of crossing the vertical line defining the rectangular channel we have that $\omega_\alpha = \varphi_\alpha$, just by notation. Therefore

$$\frac{ds_\alpha}{d\omega_\alpha} \equiv \frac{ds_\alpha}{d\varphi_\alpha}$$

in terms of the billiard map inside the "virtual" table formed by the curved boundary component and the vertical line defining the rectangular channel.

Notice that the curve $(s_\alpha,\varphi_\alpha)$ is the image of the curve $(s_2,\varphi_2(\alpha))$ under the "virtual" billiard map. Thus the pre-image is a curve of infinite slope in phase space, which means that

$$\frac{ds_\alpha}{d\omega_\alpha} \equiv \frac{ds_\alpha}{d\varphi_\alpha} = \frac{1}{\cos\omega_\alpha}\frac{1}{\mathcal{B}^*_\alpha} = \frac{1}{\cos\omega_\alpha}\left[T_\alpha + \cfrac{1}{\mathcal{R} + \cfrac{1}{\tau + \cfrac{1}{\infty}}}\right] = \frac{1}{\cos\omega_\alpha}\left[T_\alpha + \frac{\tau}{1+\tau\,\mathcal{R}}\right]$$

follows.

The linearization J_α of the billiard flow along the three refections reads

$$\begin{aligned} J_\alpha = \begin{pmatrix} a_\alpha & b_\alpha \\ c_\alpha & a_\alpha \end{pmatrix} &= -\begin{pmatrix} 1 & 0 \\ \mathcal{R} & 1 \end{pmatrix}\begin{pmatrix} 1 & \tau \\ 0 & 1 \end{pmatrix}\begin{pmatrix} 1 & 0 \\ \mathcal{R}_2 & 1 \end{pmatrix}\begin{pmatrix} 1 & \tau \\ 0 & 1 \end{pmatrix}\begin{pmatrix} 1 & 0 \\ \mathcal{R} & 1 \end{pmatrix} \\ &= -\begin{pmatrix} 1+\tau\,\mathcal{R}_2+2\,\tau\,\mathcal{R}+\tau^2\,\mathcal{R}\,\mathcal{R}_2 & \tau\,(2+\tau\,\mathcal{R}_2) \\ (1+\tau\,\mathcal{R})\,(\mathcal{R}_2+2\,\mathcal{R}+\tau\,\mathcal{R}\,\mathcal{R}_2) & 1+\tau\,\mathcal{R}_2+2\,\tau\,\mathcal{R}+\tau^2\,\mathcal{R}\,\mathcal{R}_2 \end{pmatrix} \end{aligned}$$

where we suppressed the subscript α for notational simplicity.

Recall that the case (b) is when $\mathcal{R}_2 + 2\,\mathcal{R} + \tau\,\mathcal{R}\,\mathcal{R}_2 = 0$ at $\alpha = 0$, hence

$$-dc_\alpha\big|_{\alpha=0} = (1+\tau\,\mathcal{R})\,d\big[\mathcal{R}_2+2\,\mathcal{R}+\tau\,\mathcal{R}\,\mathcal{R}_2\big]_{\alpha=0}\,.$$

Since $ds_2(\alpha) = 0$ we have that

$$d\mathcal{R} = \mathcal{R}\,\big[\frac{\mathcal{K}'}{\mathcal{K}}\,ds + \tan\varphi\,d\varphi\big]\,, \quad d\mathcal{R}_2 = \mathcal{R}_2\,\tan\varphi_2\,d\varphi_2\,, \quad d\tau = \sin\varphi\,ds$$

and therefore

$$\begin{aligned} d\big[\mathcal{R}_2 + 2\,\mathcal{R} + \tau\,\mathcal{R}\,\mathcal{R}_2\big] &= (1+\tau\,\mathcal{R})\,d\mathcal{R}_2 + \mathcal{R}\,\mathcal{R}_2\,d\tau + (2+\tau\,\mathcal{R}_2)\,d\mathcal{R} \\ &= (1+\tau\,\mathcal{R})\,\mathcal{R}_2\,\tan\varphi_2\,d\varphi_2 + \mathcal{R}\,\mathcal{R}_2\,\sin\varphi\,ds + (2+\tau\,\mathcal{R}_2)\,\mathcal{R}\,\big[\frac{\mathcal{K}'}{\mathcal{K}}\,ds + \tan\varphi\,d\varphi\big] \\ &= (1+\tau\,\mathcal{R})\,\mathcal{R}_2\,\tan\varphi_2\,d\varphi_2 - \mathcal{R}\,\mathcal{R}_2\,\sin\varphi\,\frac{\tau}{\cos\varphi}\,d\varphi_2 \\ &\quad - (2+\tau\,\mathcal{R}_2)\,\mathcal{R}\,\big[\frac{\mathcal{K}'}{\mathcal{K}}\,\frac{\tau}{\cos\varphi} + \tan\varphi\,(1+\frac{1}{2}\,\tau\,\mathcal{R})\big]\,d\varphi_2 \end{aligned}$$

follows by using the explicit formula of the derivative of the billiard map, which shows $ds = -\frac{\tau}{\cos\varphi}\,d\varphi_2$ and $d\varphi = -(1+\frac{1}{2}\,\tau\,\mathcal{R})\,d\varphi_2$.

At $\alpha = 0$ the family (b) satisfies

$$\mathcal{R}_2 + 2\,\mathcal{R} + \tau\,\mathcal{R}\,\mathcal{R}_2 = 0 \quad \text{i.e.} \quad \mathcal{R}_2 = -\frac{2\,\mathcal{R}}{1+\tau\,\mathcal{R}}$$

hence

$$\frac{dc_\alpha}{d\varphi_2}\Big|_{\alpha=0} = 2\,\mathcal{R}\,\tan\varphi_2 + \big(1-\frac{1}{2}\,\tau\,\mathcal{R}\big)\,\frac{2\,\mathcal{R}}{1+\tau\,\mathcal{R}}\,\tan\varphi + \frac{2\,\tau\,\mathcal{R}}{1+\tau\,\mathcal{R}}\,\frac{\mathcal{K}'}{\mathcal{K}}\,\frac{1}{\cos\varphi}\,.$$

Finally, notice that

$$\frac{d\varphi_2}{d\omega_\alpha} = \frac{d\varphi_2}{d\varphi_\alpha} = -\frac{d\varphi_2}{\mathcal{K}\,ds + d\varphi} = \frac{d\varphi_2}{\mathcal{K}\,\frac{\tau}{\cos\varphi}\,d\varphi_2 + (1+\frac{1}{2}\,\tau\,\mathcal{R})\,d\varphi_2} = \frac{1}{1+\tau\,\mathcal{R}}$$

implies

$$\begin{aligned} \frac{dc_\alpha}{d\omega_\alpha}\Big|_{\alpha=0} &= \frac{dc_\alpha}{d\varphi_2}\Big|_{\alpha=0}\frac{d\varphi_2}{d\omega_\alpha}\Big|_{\alpha=0} \\ &= \frac{2\,\mathcal{R}\,\tan\varphi_2}{1+\tau\,\mathcal{R}} + \big(1-\frac{1}{2}\,\tau\,\mathcal{R}\big)\,\frac{2\,\mathcal{R}}{(1+\tau\,\mathcal{R})^2}\,\tan\varphi + \frac{2\,\tau\,\mathcal{R}}{(1+\tau\,\mathcal{R})^2}\,\frac{\mathcal{K}'}{\mathcal{K}}\,\frac{1}{\cos\varphi} \end{aligned}$$

which finishes the proof. □

As an immediate consequence of the general Theorem 4.3.6 and the existence of certain family of periodic orbits Proposition 4.3.8 and Proposition 4.3.9 we obtain Theorem 4.2.1.

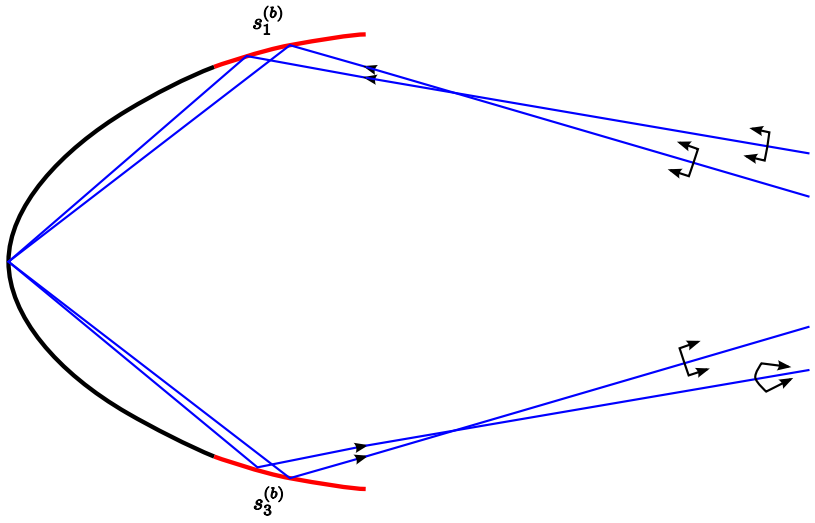

Figure 14: Illustration of the result of Proposition 4.3.9.

4.4 Conclusions

Since the appearance of [52] and [14, 15] it is known that the dynamics of the billiard map depends on the smoothness of the boundary in an essential way.

More precisely, as long as the boundary of a (strictly) convex billiard table is of class C^6 it was shown in [33] that a positive measure family of caustics is present near the boundary of the billiard table. In particular, such billiards are never completely ergodic.

The results of [14, 15] show that the if the boundary of convex billiards is allowed to be only C^1, then the resulting billiards may be hyperbolic and ergodic. In fact, the C^1 smoothness is only imposed at a few isolated points, and off these points the boundary can be C^∞.

A typical example of billiards considered in [14, 15] is the stadium billiard. Our result of Theorem 4.2.1 shows that if the (four) points of the boundary of the stadium, where the curvature is discontinuous, is smoothed out, then elliptic periodic orbits are present for a large class of such C^2 stadium like billiards.

Due to the assumption that the boundary is piecewise smooth (C^3), the global smoothness either C^2 (or better), or C^1, C^0. No fractional intermediate global

smoothness like $C^{1+\alpha}$ for some $0 < \alpha < 1$ is possible. For global C^1 or C^0 smoothness [14, 15] provides large classes of completely ergodic and hyperbolic billiards. Therefore, our results seem to indicate that for piecewise smooth (C^3 is enough) convex billiards elliptic periodic orbits are generally present if global C^2 smoothness is imposed, and hence global C^2 smoothness seems to represent the critical smoothness where elliptic structures in convex billiards are generally present. However, a more rigorous formulation of these ideas is currently not available and needs to be further investigated.

CHAPTER V

HYDRODYNAMIC LIMITS

5.1 Introduction

Gases and fluids are at the microscopic level made of many (of the order of 10^{23}) interacting particles. A mechanical model would thus require a very large number of coupled ordinary differential equations to describe the dynamics of all the particles. However, the macroscopic properties of a fluid are very well described by the (compressible) Navier-Stokes equations (or Euler equation, if dissipation can be neglected). Such partial differential equations relating temperature, density and mean velocity of the fluid are referred to as hydrodynamic equations.

The derivation of macroscopic equations from microscopic interaction models thus is of great importance, and has a long history in statistical physics. A typical approximation is the Boltzmann equation, which takes only binary collisions of particles into account, and assumes rapid decay of correlations in-between successive collisions.

In order to derive the hydrodynamic equations one identifies a small parameter in the Boltzmann equation, and performs a perturbation analysis. So far scaling limits, Grad's moment method, and expansion methods like Chapman-Enskog and Hilbert methods were proposed to obtain the Navier-Stokes equations from the Boltzmann equation. Cercignani's monograph [23] provides a comprehensive overview of these methods.

Experiments on pattern formation in fluidized sand beds, and the availability of fast numerical algorithms for direct simulations of granular media (see [5, 6] by Bizon, de Bruyn, McCormick, Shattuck, Swift, Swinney) opened new approaches to studies of interacting systems.

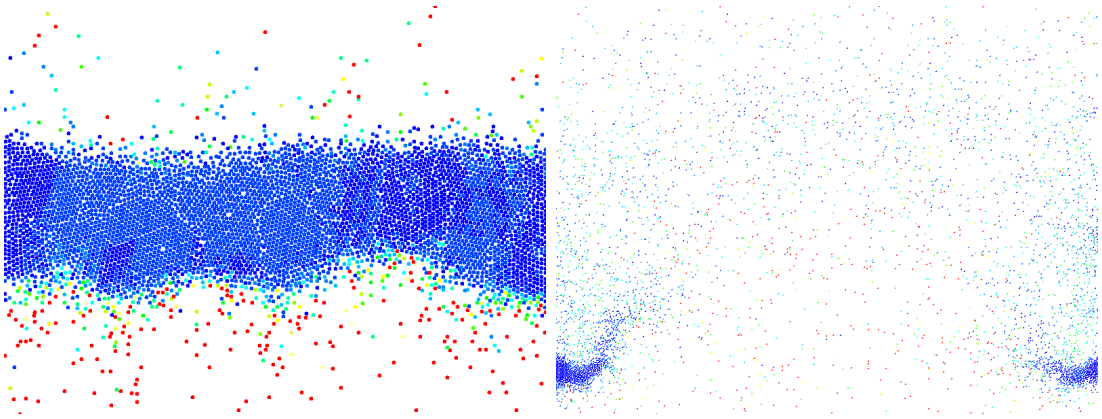

Figure 15: Snapshots of computer simulations of the high (on the left) and low (on the right) density regime of granular media.

In granular media typically two different regimes are considered. If the mean free path between two consecutive collision is of the order of the size of the particles, the motion of each particle is dominated by collisions. In this dense packing regime phenomena, to the finite size of the particles, like jamming can occur, which are not of fluid dynamical nature.

If the mean free path between two consecutive collisions is much larger than the size of the particles, then their individual motion is dominated by free motion. Only rarely particles will collide with each other. This is the low density gas-like regime, to which kinetic methods apply.

Snapshots of a computer simulation of high and low density regimes are shown in Fig. 15. A priori, kinetic models only apply to the gas-like (low density) regime. It was demonstrated by Du, Li and Kadanoff [34] that in certain dissipative systems a hydrodynamic description breaks down. However, direct simulations of fluidized sand beds by Bizon et al. [61] have shown good agreement with kinetic models, even at rather high densities.

Even though direct numerical simulations provide important insight, they are limited to rather small particle numbers. The first macroscopic equations for granular systems based on a phenomenological approach using balance equations were proposed

by Haff [41]. A more direct link to microscopic models using the kinetic theory was given by Jenkins and Richman in [43].

Another aspect of dissipative systems is that due to the dissipation the usual Maxwell distribution no longer constitutes an equilibrium for the spatially homogeneous system. Rather special self-similar distributions (the so called homogeneous cooling states) appear, and as studied by Bobylev et al. [7, 8, 38].

In the non-dissipative case, rigorous results on the hydrodynamic limits of the Boltzmann equation are based on a variety of methods. Scaling limits result in the Euler equations when using a hyperbolic scaling, or the incompressible Navier-Stokes equations in the parabolic scaling. Good references for this line of approach are the papers by Esposito et al. [36, 28]. Toscani [63] provides a good overview of the current mathematical state of the art for the much less studied case of the dissipative Boltzmann equation.

Whether the interactions are dissipative or not, the compressible Navier-Stokes equations are obtained by using a series expansion in terms of a small parameter, the ratio of microscopic to macroscopic length scales. At the leading order one obtains the Euler equations, and including the next order correction yields the compressible Navier-Stokes equations.

The reason why in all these methods the Euler equation appears at leading order (in the hyperbolic scaling) and the compressible Navier-Stokes arises as a formal higher order correction is usually explained by the presence of two different time scales; diffusive phenomena are typically much slower than convective ones.

The aim of this part of the thesis is to present a novel derivation of the compressible Navier-Stokes equations for a weakly dissipative collision model (and hence is also applicable to the non-dissipative setting), by starting from the Boltzmann equation. In contrast to usual methods based on series expansions we apply dynamical systems methods, and construct a reduced dynamics on an invariant manifold for all times

and all small enough dissipations. The compressible Navier-Stokes equations are then the first order approximation when expanding the resulting manifold in terms of the small parameter, but not the dynamical equations.

In this approach the Navier-Stokes equations are not a higher order correction to the Euler equations. Rather, they appear as the first order correction to a stationary Maxwellian distribution. Thus our approach is able to capture both the convective and diffusive transport terms simultaneously.

Furthermore, in contrast to previous works, our method also generates spatial gradient in the cooling term at the Navier-Stokes order. This shortcoming is in fact argued (e.g. see Brey et al. [11]) to be the reason why even higher order corrections (Burnett order) of the usual series expansion should be taken into account.

In Section 5.2 we describe the kinetic model we study. In Section 5.4 we describe the dynamical systems methods that we use to analyze the dynamics of the dissipative Boltzmann equation. Based on this dynamical systems approach we introduce special coordinates for the dissipative Boltzmann equation in Section 5.5. The main results are summarized in Section 5.6. The corresponding proofs are presented in Section 5.7 and Section 5.8. Finally, in Section 5.9 we test the derived macroscopic equations by direct numerical simulations, and present the results on the cooling rate.

5.2 The Kinetic Model

5.2.1 The Boltzmann Equation

The system we will consider consists of a large number N of identical particles, confined to a domain $\Omega \subset \mathbb{R}^d$. Physically relevant values of the dimension d are 1, 2 and 3. Other values of d are interesting, for example, for numerical simulations.

At each instant of time the state of the i-th particle

$$z_i \equiv (x_i, v_i)$$

is determined by its position $x_i \in \Omega$ and its velocity $v_i \in \mathbb{R}^d$. [1] The motion of the N interacting particles is, usually, determined by a Hamiltonian of the form

$$H(z_1, \ldots, z_N) = \sum_{i=1}^{N} \frac{m}{2} \parallel v_i \parallel^2 + \sum_{i<j=1}^{N} U(\parallel x_i - x_j \parallel) \ ,$$

with U the interaction potential, and m the mass of the particles. For simplicity we did not include external forces, as they will not play any role in our considerations.

Thus the dynamics is usually given by a (smooth) flow on the state space

$$\Gamma_N = (\Omega \times \mathbb{R}^d)^N \ ,$$

with the micro-canonical invariant measure

$$d\Gamma_N := dx_1 \, dv_1 \ldots dx_N \, dv_N \ .$$

For physically interesting values of N, e.g. several thousand up to 10^{23}, this microscopic approach of describing the system is not appropriate. Instead we will take a probabilistic point of view. For this let $\rho = \rho(x_1, v_1, \ldots, x_N, v_N, t)$ be a probability density on the state space. Then

$$f(x, v, t) := \int_{\Gamma_N} \sum_{i=1}^{N} \delta(x_i - x) \, \delta(v_i - v) \, \rho(x_1, v_1, \ldots, x_N, v_N, t) \, d\Gamma_N$$

is the associated single particle or occupation number density. It satisfies the normalization condition

$$N = \int_{\Omega} \int_{\mathbb{R}^d} f(x, v, t) \, dx \, dv$$

and gives, up to this normalization, the probability density of finding some particle at (x, v) at time t.

Taking only binary interactions into account and assuming loss of correlation in-between successive interactions, the interaction part of the N-particle dynamics is completely described by the transition rate

$$\mathcal{W}(z_1, z_2, z_3, z_4)$$

[1] Traditionally in (non-relativistic classical) statistical physics velocities rather than momenta are used in this context.

which gives the probability of two particles z_1 and z_2 to interact per unit time such that their final states are z_3 and z_4, respectively. We will always assume the symmetry relation

$$\mathcal{W}(z_1, z_2, z_3, z_4) = \mathcal{W}(z_2, z_1, z_4, z_3) \tag{7}$$

which expresses the invariance of the collision process under relabeling the particles.

Within this approximation the evolution equation of the occupation number density f is given by the Boltzmann equation (without external forces)

$$\partial_t f(x, v, t) + v \cdot \nabla_x f(x, v, t) = Q(f, f)(x, v, t) \tag{8}$$

with the collision operator $Q(f, f)$ defined by

$$\begin{aligned} Q(f,f)(z,t) := & \int\int\int \mathcal{W}(y_3, y_4, z, y_2)\, f(y_3, t)\, f(y_4, t)\, dy_2\, dy_3\, dy_4 \\ & - \int\int\int \mathcal{W}(z, y_2, y_3, y_4)\, f(z, t)\, f(y_2, t)\, dy_2, dy_3\, dy_4 \ . \end{aligned} \tag{9}$$

The two integrals represent the gain and loss of particles at $z = (x, v)$ per unit time, respectively.

An important structural property of the Boltzmann collision operator is given by the following

Proposition 5.2.1. *For any (test) function $\psi(z)$ and any density function $f(z, t)$*

$$\begin{aligned} & \int Q(f,f)(z,t)\, \psi(z)\, dz \\ & \quad = \int\int\int\int \mathcal{W}(z_1, z_2, z_3, z_4)\, f(z_1, t)\, f(z_2, t)\, [\psi(z_3) - \psi(z_1)]\, dz_1\, dz_2\, dz_3\, dz_4 \\ & \quad = \frac{1}{2} \int\int\int\int \mathcal{W}(z_1, z_2, z_3, z_4)\, f(z_1, t)\, f(z_2, t) \cdot \\ & \qquad\qquad \cdot [\psi(z_3) + \psi(z_4) - \psi(z_1) - \psi(z_2)]\, dz_1\, dz_2\, dz_3\, dz_4 \end{aligned}$$

gives the weak formulation of the collision operator.

Proof. Use the symmetry relation (7). □

5.2.2 The Interaction Model

Conservative interactions preserve the total momentum and the total energy, that is the post-collisional velocities v_1' and v_2' and pre-collisional velocities v_1 and v_2 satisfy

$$v_1 + v_2 = v_1' + v_2' \quad \text{and} \quad \| v_1 \|^2 + \| v_2 \|^2 = \| v_1' \|^2 + \| v_2' \|^2 \ .$$

The prototypical example of such an interaction is the elastic collision of two hard spheres, as shown in Fig. 16. The interaction the positions do not change at the

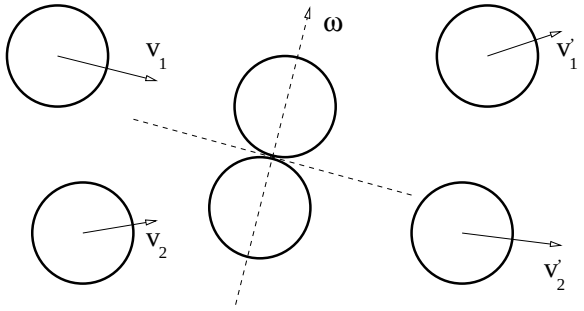

Figure 16: Schematic illustration of the hard sphere interaction.

moment of collision, i.e.

$$x_1 = x_1' \quad \text{and} \quad x_2 = x_2' \ ,$$

while the velocities change by reflecting them about the plane with normal vector ω, see Fig. 16.

For general conservative interactions we will assume that the interaction region is spatially much smaller than the free paths. We idealize this by assuming point-like spatial interaction regions, i.e.

$$\mathcal{W}(z_1, z_2, z_3, z_4) = \mathcal{W}(z_1, z_2, z_3, z_4)\, \delta(x_1 - x_3)\, \delta(x_2 - x_4)$$

for the transition rate. Since the interaction is assumed to be spatially localized we will consider only the asymptotic momenta corresponding to the infinite past and the infinite future, because the free flight does not change the velocities.

For any conservative interaction $(v_1, v_2) \to (v_1', v_2')$ there exists a unique, up to the sign, $\omega = \omega(v_1, v_2) \in S^{d-1}$, such that the post-collisional velocities (v_1', v_2') can be obtained from (v_1, v_2) by

$$v_1' = v_1 + [(v_2 - v_1) \cdot \omega]\, \omega \quad \text{and} \quad v_2' = v_2 - [(v_2 - v_1) \cdot \omega]\, \omega$$

a reflection about the plane with normal vector ω, as shown in Fig. 17. The explicit

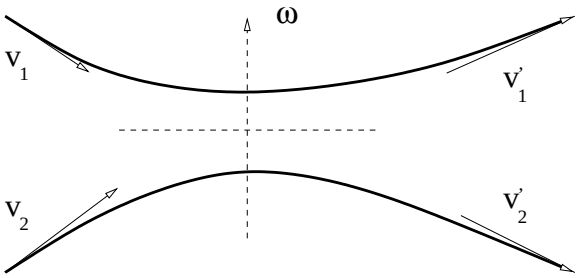

Figure 17: Schematic illustration of the hard sphere like reflection associated to general conservative interactions.

form of ω reads

$$\omega = \pm \frac{(v_2' - v_2) - (v_1' - v_1)}{\| (v_2' - v_2) - (v_1' - v_1) \|} \in S^{d-1} \, .$$

Thus the details of the interaction can be encoded entirely in $\omega(v_1, v_2)$ and essentially looks like a hard sphere collision.

Therefore the transition rate $\mathcal{W}$ will be assumed to be of the form

$$\begin{aligned} \mathcal{W}(z_1, z_2, z_3, z_4)\, dz_1\, dz_2\, dz_3\, dz_4 = \int_{S^{d-1}} B(v_2 - v_1, \omega)\, \delta(v_1' - v_3)\, \delta(v_2' - v_4) \cdot \\ \cdot \delta(x_1 - x_2)\, \delta(x_2 - x_3)\, \delta(x_3 - x_4)\, d\omega\, dz_1\, dz_2\, dz_3\, dz_4 \end{aligned} \tag{10a}$$

for some function B, which describes the details of the interaction. Furthermore, since the reflection plane is invariant under $\omega \mapsto -\omega$, so must be the transition rate. Hence the symmetry

$$B(v_2 - v_1, \omega) = B(v_2 - v_1, -\omega) \tag{10b}$$

must hold.

Furthermore, in the special case where the interaction is rotationally invariant $B(R(v_2 - v_1), R\omega) = B(v_2 - v_1, \omega)$ holds for any rotation matrix R. Averaging over all R then yields

$$\text{rotational invariance} \implies B = B\big(\| v_2 - v_1 \|, \frac{|(v_2 - v_1) \cdot \omega|}{\| v_2 - v_1 \|} \big) \tag{10c}$$

where the absolute value of the dot product is due to the general symmetry (10b).

To include non-conservative interactions, i.e. interaction which do not originate from a Hamiltonian, we proceed phenomenologically. Considering again our prototypical example of hard sphere interactions, the simplest implementation of energy dissipation is to consider inelastic collisions. In this case the total momentum is preserved and the relative momentum is reduced (compared to the conservative case) by a factor $(1 - \eta)$ with η in between 0 and 1. Thus $\eta = 0$ corresponds to the non-dissipative (conservative) case and $\eta = 1$ to the completely sticky (in normal direction) one. We will consider the parameter η to be a constant, i.e. independent of relative momenta and other dynamical quantities. In general we will implement the dissipative interactions in analogy with inelastic collisions, which model dissipation in "normal direction".

Assumption 5.2.2 (Dissipative Interaction Model)**.** *Throughout we assume repulsive interactions with energy dissipation in the "normal direction" for which the post-collisional velocities (v_1', v_2') are obtained from the pre-collisional velocities (v_1, v_2) via*

$$v_1' = v_1 + \big(1 - \frac{\eta}{2}\big) \left[(v_2 - v_1) \cdot \omega\right] \omega \quad \textit{and} \quad v_2' = v_2 - \big(1 - \frac{\eta}{2}\big) \left[(v_2 - v_1) \cdot \omega\right] \omega$$

for some η between 0 and 1, and

$$v_1^* = v_1 + \frac{1}{2} \frac{2 - \eta}{1 - \eta} \left[(v_2 - v_1) \cdot \omega\right] \omega \quad \textit{and} \quad v_2^* = v_2 - \frac{1}{2} \frac{2 - \eta}{1 - \eta} \left[(v_2 - v_1) \cdot \omega\right] \omega$$

is the reverse transformation, which expresses the pre-collisional velocities (v_1^*, v_2^*) in terms of the post-collisional velocities (v_1, v_2). The transition rate $\mathcal{W}$ is assumed to

be given by equation (10a)*, i.e.*

$$\mathcal{W}(z_1, z_2, z_3, z_4)\, dz_1\, dz_2\, dz_3\, dz_4 = \int_{S^{d-1}} B(v_2 - v_1, \omega)\, \delta(v_1' - v_3)\, \delta(v_2' - v_4) \cdot$$
$$\cdot \delta(x_1 - x_2)\, \delta(x_2 - x_3)\, \delta(x_3 - x_4)\, d\omega\, dz_1\, dz_2\, dz_3\, dz_4$$

and the function B is independent of the restitution coefficient η.

This model of dissipative interactions is quite standard in the context of the dissipative Boltzmann equation. See, for example, the review article by Toscani [63].

Remark 5.2.3. *The change of variables $(v_1, v_2) \mapsto (v_1', v_2')$ has*

$$|\det \frac{\partial(v_1', v_2')}{\partial(v_1, v_2)}| = 1 - \eta$$

as its Jacobian.

Proposition 5.2.4. *Let $f(x, v, t)$ be some density function. Assuming the interaction model as in Assumption 5.2.2, for any test function $\psi(x, v)$*

$$\int_\Omega \int_{\mathbb{R}^d} Q(f, f)(x, v, t)\, \psi(x, v)\, dx\, dv =$$
$$= \frac{1}{2} \int_\Omega \int_{\mathbb{R}^d} \int_{\mathbb{R}^d} \int_{S^{d-1}} B(v_2 - v_1, \omega)\, f(x, v_1, t)\, f(x, v_2, t)$$
$$[\psi(x, v_1') + \psi(x, v_2') - \psi(x, v_1) - \psi(x, v_2)]\, d\omega\, dv_1\, dv_2\, dx$$

holds.

Proof. Applying Proposition 5.2.1 with the interaction model as in Assumption 5.2.2 to ψ yields

$$\int Q(f, f)(z, t)\, \psi(z)\, dz$$
$$= \frac{1}{2} \int \int \int \int \mathcal{W}(z_1, z_2, z_3, z_4)\, f(z_1, t)\, f(z_2, t)$$
$$[\psi(z_3) + \psi(z_4) - \psi(z_1) - \psi(z_2)]\, dz_1\, dz_2\, dz_3\, dz_4$$
$$= \frac{1}{2} \int_\Omega \int_{\mathbb{R}^d} \int_{\mathbb{R}^d} \int_{S^{d-1}} B(v_2 - v_1, \omega)\, f(x, v_1, t)\, f(x, v_2, t)$$
$$[\psi(x, v_1') + \psi(x, v_2') - \psi(x, v_1) - \psi(x, v_2)]\, d\omega\, dv_1\, dv_2\, dx$$

as was claimed. □

An immediate consequence of the weak form of the collision operator and the change of variables formula is the following

Corollary 5.2.5. *The explicit form of the collision operator reads*

$$Q(f,f)(x,v_1,t) = \int_{S^{d-1}} \int_{\mathbb{R}^d} \Big[\frac{1}{1-\eta} B(v_2^* - v_1^*, \omega)\, f(x,v_1^*,t)\, f(x,v_2^*,t) \\ - B(v_2 - v_1, \omega)\, f(x,v_1,t)\, f(x,v_2,t) \Big]\, dv_2\, d\omega$$

for any density function f.

5.3 Geometric and Dynamic Aspects of the Navier-Stokes Limit

5.3.1 Introduction to the Main Ideas

In the non-dissipative case the Chapman-Enskog expansion is the standard method to obtain the Navier-Stokes equation as a formal asymptotic expansion of solutions to the Boltzmann equation, see [23] for a detailed exposition. We will present a geometric and dynamical approach to derive the hydrodynamic equations from the Boltzmann equation. In the non-dissipative case we will recover the Chapman-Enskog method, but this new approach will also allow us to shed light on the less well established case of weakly dissipative interaction.

In the presence of dissipation the assumed collision model, see Assumption 5.2.2, the energies before and after a binary collision are related by

$$\| v_1' \|^2 + \| v_2' \|^2 = \| v_1 \|^2 + \| v_2 \|^2 - \alpha\, |(v_2 - v_1)\cdot\omega|^2 \quad \text{with} \quad \alpha := \eta\left(1 - \frac{\eta}{2}\right) \tag{11}$$

so that α is a natural dimensionless parameter.

We are going to consider small dissipations, i.e. $\alpha \ll 1$, only. Furthermore, as in the non-dissipative setting we will assume that the dimensionless parameter, which is called Knudsen number [23],

$$\epsilon := \frac{\text{mean free path}}{\text{spatial length-scale of } f} \tag{12}$$

is also a small parameter. Rescaling space

$$\xi = \epsilon\, x$$

captures spatial variations of f for ξ of order one. The Boltzmann equation (without external forces) then becomes

$$\partial_t f + \epsilon\, v \cdot \nabla_\xi f = Q(f, f) \tag{13}$$

and we are interested in studying solutions to this equation for ϵ and α both very small.

In general, the equations one obtains in the limit $(\epsilon, \alpha) \to (0, 0)$ do depend on the path along which the two small parameters approach the origin simultaneously. This reflects the fact that their relative sizes describe different physical situations. For example, $\alpha \ll \epsilon$ corresponds to systems where the dissipation is small compared to the usual non-dissipative phenomena like diffusion, whereas for $\alpha \gg \epsilon$ dissipation dominates all other effects even at very short time scales.

We shall consider here the setting where $\alpha = O(\epsilon)$, which can be thought of as a perturbation of ordinary fluid mechanics. This also allows for $\alpha \ll \epsilon$, and contains the non-dissipative case $\alpha = 0$ as a special case.

In this regime it is natural to chose the path in the parameter plane as a graph of a function parametrized by ϵ, i.e. $\alpha = \alpha(\epsilon)$ is a function of ϵ which determines the path along which we consider the limit $(\epsilon, \alpha) \to (0, 0)$, as shown in Fig. 18.

Another choice for scaling limit often found in the literature, e.g. [11], is to fix $\alpha > 0$ and let only ϵ tend to zero. The limit $\alpha \to 0$ is taken afterwards. This corresponds to the regime $\epsilon \ll \alpha$ and thus models a spatially homogeneous cooling.

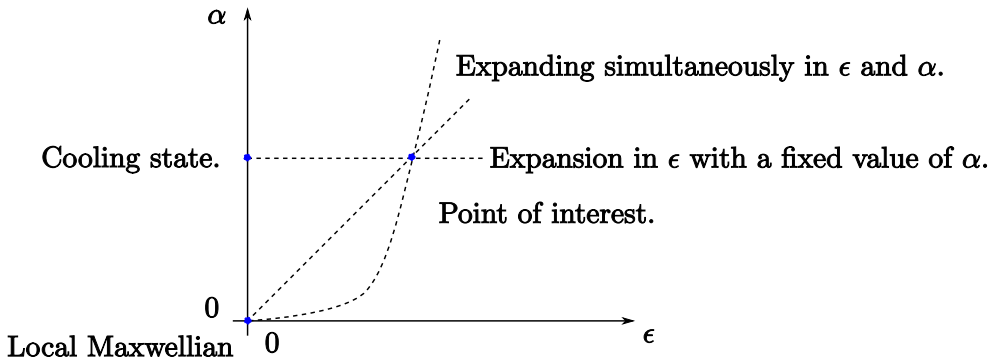

Figure 18: Illustration of the different expansion methods.

5.3.2 Analysis of the Reference System

For $\epsilon = 0$ our choice of the scaling limit implies that also $\alpha = 0$, so that the rescaled Boltzmann equation (13) becomes

$$\partial_t f = Q_0(f, f) \, . \tag{14}$$

Notice that the collision operator in this case is the one with with non-dissipative interactions.

Set

$$g_0(w) := \frac{1}{\sqrt{2\pi}^d} \, e^{-\frac{\| w \|^2}{2}} \tag{15a}$$

and define

$$\mathcal{M}_0 := \Big\{ \frac{n}{\sqrt{T}^d} g_0\big(\frac{v-u}{\sqrt{T}}\big) : n(x) \in \mathbb{R}, u(x) \in \mathbb{R}^d, T(x) \geq 0, x \in \Omega \Big\} \tag{15b}$$

which is the set of all local Maxwellians. The variables n, u and T are the particle density, velocity and temperature, respectively, see Definition 5.5.1 below.

Boltzmann's H-theorem asserts that (we always assume repulsive interactions) for any initial distribution the corresponding solution of the Boltzmann equation with $\epsilon = 0$ will converge to a local Maxwellian. And the local Maxwellians are equilibrium solutions. A dynamical reformulation of this well known fact is given in the following

Theorem 5.3.1 (Normally Hyperbolic Manifold)**.** *At $\epsilon = 0$ the set of all local Maxwellians $\mathcal{M}_0$ is a globally attractive, normally hyperbolic invariant manifold consisting of fixed points of the (rescaled) Boltzmann equation.*

Proof. Since $\mathcal{M}_0$ is globally attractive and invariant, linearizing the equation about a local Maxwellian yields a linear operator. Because the interaction potential is always assumed to be repulsive the linearized collision operator has a spectral gap in a suitable function space. A detailed analysis for hard spheres was given in [60]. The spectral gap implies that the convergence towards the local Maxwellians occurs (eventually) at an exponential rate, i.e. $\mathcal{M}_0$ is normally hyperbolic. □

This basic fact is what will allow us to study the case of small, but finite, values for ϵ. However, there will be a change of coordinates required to successfully analyze this case. To the best of our knowledge this change of coordinates is completely novel. In order to motivate and illustrate the reason why this change of coordinates has to be done we first consider the analogous situation for finite dimensional differential equations in Section 5.4.

5.4 Normally Hyperbolic Invariant Manifolds in Finite Dimensions

5.4.1 Singular Perturbation Setup

Formally, the (rescaled) Boltzmann equation can be written as an ordinary differential equation in an appropriate infinite dimensional function space. The purpose of this section is to outline the methods we are going to apply to the Boltzmann equation in the technically simpler setting of finite dimensional differential equation

$$\frac{dz}{dt} = H(z, \epsilon) \tag{16}$$

where the vector z plays the role of the distribution function f.

Since Theorem 5.3.1 shows that for $\epsilon = 0$ the (rescaled) Boltzmann equation possess a manifold of fixed points, we will consider here vector fields H for which there exists an invariant manifold $\mathcal{M}_0$ of fixed points for $\epsilon = 0$.

If (16) is a singularly perturbed system, then it is very likely that the invariant manifold $\mathcal{M}_0$ will persist for $\epsilon > 0$. The first attempt to study such systems using geometric properties of invariant manifolds was made by Fenichel [37].

5.4.2 Normal Hyperbolicity

In general, to study properties of a dynamical system, one considers how fast infinitesimally nearby trajectories diverge or converge. The average exponential rate of divergence or convergence is given by the Lyapunov exponents. In general, the value of the Lyapunov exponents can only be estimated by constructing invariant cone fields or invariant quadratic forms. However, if the reference orbit is a fixed point, then its Lyapunov exponents are obtained from the eigenvalues of its linearization. If $\mathcal{M}_0$ consists of only fixed points z, then the linearization of the vector field about z has zero eigenvalues (i.e. zero Lyapunov exponents) corresponding to the tangent space of $\mathcal{M}_0$ at z. If these are the only eigenvalues with zero real parts, then the manifold $\mathcal{M}_0$ is called normally hyperbolic.

In this section we assume the normal hyperbolicity of $\mathcal{M}_0$ (or of most of its points).

5.4.3 The van der Pol equation

To illustrate the above results consider the extensively studied van der Pol equation

$$u'' - (1 - u^2)\, u' + \epsilon\, u = 0 \,,$$

which was originally introduced as a model for non-linear circuits [65].

Rewriting it as a first order system by setting $v = u'$, we obtain

$$\frac{d}{dt} \begin{pmatrix} u \\ v \end{pmatrix} = \begin{pmatrix} v \\ (1 - u^2)\, v - \epsilon\, u \end{pmatrix}$$

which generates a flow on $\mathbb{R}^2$. It is easy to see that for $\epsilon = 0$ the set of fixed points of the flow is given by

$$\mathcal{M}_0 = \{(u, v) : v = 0,\ u \in \mathbb{R}\}$$

which are exponentially stable for $|u| > 1$ and exponentially unstable for $|v| < 1$. In particular, the above system is a singular perturbation problem.

Integrating the original second order equation once for $\epsilon = 0$ suggests a different set of coordinates

$$x = u' + \Phi(u) \quad \text{and} \quad y = u \quad \text{with} \quad \Phi(u) = \frac{1}{3}\, u^3 - u\ .$$

In these coordinates the van der Pol equation takes on the form

$$\frac{d}{dt} \begin{pmatrix} x \\ y \end{pmatrix} = \begin{pmatrix} -\epsilon\, y \\ x - \Phi(y) \end{pmatrix}\ , \tag{17}$$

which generates an equivalent flow on $\mathbb{R}^2$, and is of standard form, cf. (19) below. A graph of the function $\Phi(u)$ is is shown in Fig. 19.

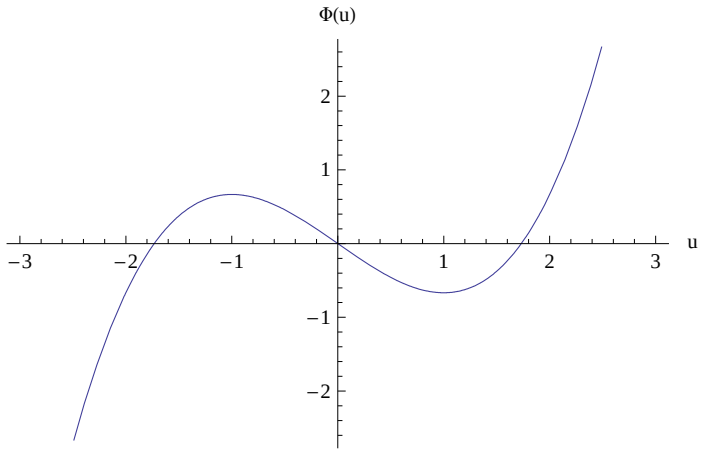

Figure 19: The graph of the function $\Phi(u)$.

For $\epsilon = 0$ the system (17) becomes

$$\frac{d}{dt} \begin{pmatrix} x \\ y \end{pmatrix} = \begin{pmatrix} 0 \\ x - \Phi(y) \end{pmatrix}\ ,$$

with the manifold of fixed points given by

$$\mathcal{M}_0 = \{(x, y) : x = \Phi(y)\}$$

in terms of x and y. This manifold is the graph of Φ, which is shown in Fig. 19. Furthermore, the dynamics for $\epsilon = 0$ is readily read off the system: x stays constant, and the sign of $x - \Phi(y)$ determines whether y increases or decreases. The corresponding phase portrait is shown in Fig. 20. From Fig. 20 we can also see the meaning of

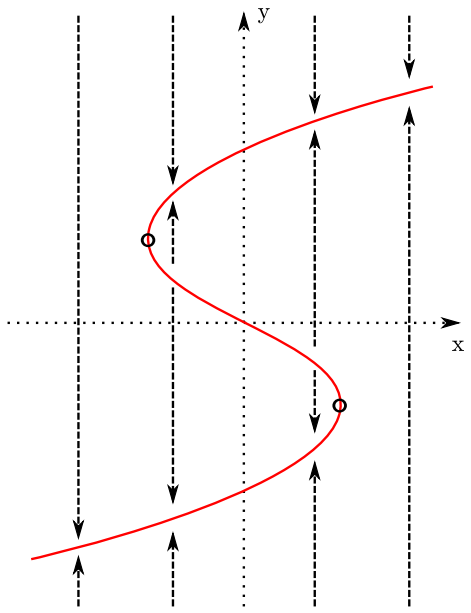

Figure 20: The system for $\epsilon = 0$ on the fast time scale. The dynamics becomes very complicated at the fold points of the invariant manifold, which are indicated by the circles.

normal hyperbolicity. All points on $\mathcal{M}_0$, except for $y = \pm 1$ are normally hyperbolic. The two special points $y = -1$ and $y = 1$ are indicated by a circle in Fig. 20. They correspond to turning (or fold) points, at which normal hyperbolicity breaks down. At these points, in order to "continue" the invariant manifold, one has to increase the dimension, because the center direction has to be included. Rigorous results on the persistence of the extended invariant manifold near $\mathcal{M}_0$ can be found in the recent work of Chow, Liu and Yi [26, 27]. Normal forms around the fold points we derived in Brunovsky, Chow and Mallet-Paret [12]. Generally, the existence of turning points

gives rise to rather complicated features of the global dynamics for $\epsilon > 0$ and is very difficult to study.

The usefulness of the standard form of a singular perturbation problem can also be illustrated with this example. For $\epsilon = 0$ the points on $\mathcal{M}_0$ are fixed. For $\epsilon > 0$, however, they will generically start to move, as fixed points are generically isolated. The vector field at these points will then be of the order of ϵ. In order to describe this slow motion we introduce the slow time

$$\tau = \epsilon\, t$$

which captures the slow motion at timescales of order $\mathcal{O}(1)$ (opposed to $\mathcal{O}(\epsilon^{-1})$ when using t). The system (17) then becomes the associated slow system

$$\frac{d}{d\tau}\begin{pmatrix} x \\ \epsilon\, y \end{pmatrix} = \begin{pmatrix} -y \\ x - \Phi(y) \end{pmatrix} . \tag{18}$$

Due to the choice of the time scale we can now pass to $\epsilon = 0$ and obtain

$$\frac{d}{d\tau}x = -y \quad \text{and} \quad 0 = x - \Phi(y)$$

which yields a flow on the originally invariant manifold of fixed points. Thus, this equation really corresponds to a scaling limit $\epsilon \to 0$ with $\tau = \epsilon\, t$. Differentiating the algebraic constraint yields the equivalent form

$$\frac{d}{d\tau}y = -\frac{y}{\Phi'(y)} \equiv -\frac{y}{y^2 - 1} \quad \text{and} \quad 0 = x - \Phi(y)$$

which has the advantage of being a differential equation in y only. The corresponding phase portrait can now be easily obtained and is shown in Fig. 21 below. We can see that the slow dynamics on $\mathcal{M}_0$ now has an unstable fixed point at the origin, and two stable ones at the turning points.

Of course, the actual dynamics of the van der Pol equation for $\epsilon > 0$ is neither given by the fast nor the slow system (each at $\epsilon = 0$). For small $\epsilon > 0$ the solution of

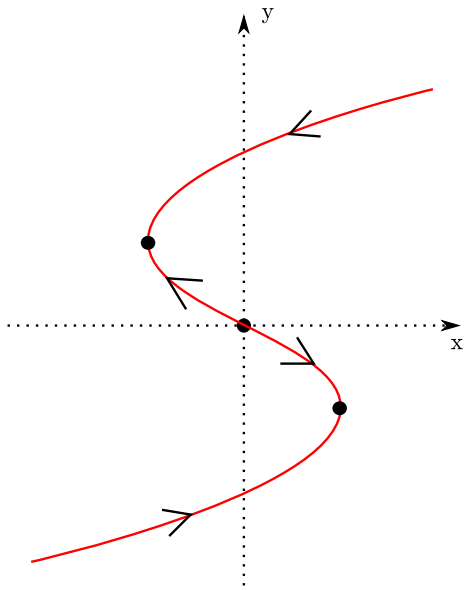

Figure 21: The illustration of the $\epsilon = 0$ system for the slow system. Notice that the invariant manifold of fixed points for the fast system becomes the supporting manifold of the slow system.

the van der Pol equation will rapidly come close to $\mathcal{M}_0$ as in the fast system, but will simultaneously move slowly along $\mathcal{M}_0$ as in the slow system. This can be expressed as a matched asymptotic expansion.

However, as soon as the solution approaches one of the two turning points (and it will do so, as they are attractive in the slow system) the slow system scaling limit will break down. The solution will "fall off" $\mathcal{M}_0$ near the turning point and jump, just as the fast system would do, to another branch of $\mathcal{M}_0$, giving raise to a periodic like cycle. These are not simple limit cycles, due to the complicated behavior, "canards", near the turning points of $\mathcal{M}_0$. So, even in this low dimensional example of the van der Pol equation very complicated dynamics arises, which is not completely understood at a rigorous level.

5.4.4 The Standard Form of Singular Perturbation Problems

The first step towards understanding the dynamical behavior of singular perturbation problems is the introduction of appropriate coordinates which reflect the dynamical

aspects explicitly.

Let $z_0 \in \mathcal{M}_0$ be a normally hyperbolic fixed point. Then there exist [37] local coordinates $z = \phi(x, y)$ in a neighborhood of z_0 such that $z_0 = \phi(0, 0)$, and the differential equation $z' = H(z, \epsilon)$ becomes

$$\frac{dx}{dt} = \epsilon\, F(x, y, \epsilon) \quad \text{and} \quad \frac{dy}{dt} = G(x, y, \epsilon) \tag{19}$$

in terms of these local coordinates. Furthermore, the manifold $\mathcal{M}_0$ near by z_0 corresponds to the set of coordinates $\{(x, y) : G(x, y, 0) = 0\}$. This form of the singular perturbation problem is called the standard form.

The next step is based on the following observation. For $\epsilon = 0$ the points with coordinates $\{(x, y) : G(x, y, 0) = 0\}$ are fixed points, and hence do not move. For $\epsilon > 0$, however, the vector field on these points is of order ϵ, as equation (19) shows.

In order to make this rather slow motion visible at times of order one, we use the slow time scale

$$\tau = \epsilon\, t$$

so that

$$\frac{dx}{d\tau} = F(x, y, \epsilon) \quad \text{and} \quad \epsilon\, \frac{dy}{d\tau} = G(x, y, \epsilon)$$

follows for the evolution equation in terms of local coordinates. This form is called the associated slow system, and satisfies the following key property:

Proposition 5.4.1 (Scaling Limit of the Slow System [37])**.** *On the normally hyperbolic part of $\mathcal{M}_0$ for $\epsilon = 0$ the slow system reduces to*

$$\frac{dx}{d\tau} = F(x, y, 0) \quad \textit{and} \quad 0 = G(x, y, 0) \quad \textit{i.e.} \quad (x, y) \in \mathcal{M}_0\ ,$$

or equivalently to

$$\frac{dz}{d\tau} = P_{\mathcal{M}_0} H(z, 0) \quad \textit{for} \quad z \in \mathcal{M}_0\ ,$$

where $P_{\mathcal{M}_0}$ denotes the projection onto the tangent space of $\mathcal{M}_0$.

5.4.5 Invariant Manifolds for $\epsilon > 0$

In order to include first order corrections for the dynamics on the fast time scale we need to understand what happens to the invariant manifold of fixed points $\mathcal{M}_0$ for $\epsilon > 0$.

Under the assumption of normal hyperbolicity (i.e. no additional center direction due to turning points) it is known that the invariant manifold persists [37, 40, 27, 26, 46, 42]. A particularly easy to handle situation is when $\mathcal{M}_0$ is a graph with respect to the slow variable

$$\mathcal{M}_0 = \{(x, y) : y = \mathcal{Y}_0(x)\}$$

in which case

$$\mathcal{M}_\epsilon = \{(x, y) : y = \mathcal{Y}_\epsilon(x)\}$$

determines the invariant manifold for $\epsilon > 0$ through the function $\mathcal{Y}_\epsilon(x)$. The invariance of $\mathcal{M}_\epsilon$ becomes

$$G(x, \mathcal{Y}_\epsilon(x), \epsilon) = \epsilon\, \partial_x \mathcal{Y}_\epsilon(x)\, F(x, \mathcal{Y}_\epsilon(x), \epsilon) \tag{20a}$$

which is a time independent equation for $\mathcal{Y}_\epsilon(x)$. The dynamics on $\mathcal{M}_\epsilon$ is given by

$$\begin{aligned} \frac{dx}{dt} &= \epsilon\, F(x, y, \epsilon) \\ y &= \mathcal{Y}_\epsilon(x) \end{aligned} \tag{20b}$$

and is valid for all times and all sufficiently small values of $\epsilon > 0$.

Using the normal fibration (parts of stable manifolds of points on $\mathcal{M}_\epsilon$) one can construct to any initial data (sufficiently close to $\mathcal{M}_\epsilon$) a point on $\mathcal{M}_\epsilon$ such that the trajectories starting at these two points converge to each other exponentially fast. This is some times called shadowing property, and it allows one to study the properties of the dynamics off $\mathcal{M}_\epsilon$ using the dynamics on $\mathcal{M}_\epsilon$. Thus we only have to consider the dynamics on $\mathcal{M}_\epsilon$. In Fig. 22 an illustration of the shadowing property is shown.

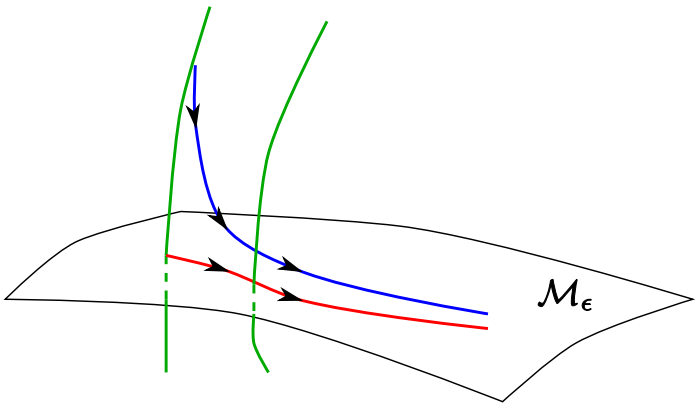

Figure 22: Illustration of the shadowing of any orbit by a trajectory on the normally hyperbolic invariant manifold. The shading point is found by projection along the normal fibers.

Due to the shadowing property there is no restriction on the time interval on which the approximation of some trajectory by its shadow is valid. Therefore, the construction and analysis of the geometric properties (invariant manifold theory) explains why formal series expansion for inner and outer solutions and their matching work. Moreover, the geometric analysis actually tells us which parts of the dynamics correspond to inner and which correspond to outer solutions and how the matching is done by using boundary layer corrections. This is not at all obvious from a formal series expansion point of view, and especially so for the case of infinite dimensional systems.

5.4.6 The Expansion Step

In order to construct an approximate solution to the reduced dynamics (20) we will compute the first order correction of $\mathcal{M}_\epsilon$ in ϵ. More precisely, we will assume that $\mathcal{Y}_\epsilon(x)$ is regular enough in ϵ to have

$$\mathcal{Y}_\epsilon(x) = \mathcal{Y}_0(x) + \epsilon\,\mathcal{Y}_1(x) + \mathcal{O}(\epsilon^2)\ .$$

Substituting this expansion into (20a) yields

$$G(x, \mathcal{Y}_0(x), 0) = 0$$
$$\partial_2 G(x, \mathcal{Y}_0(x), 0)\, \mathcal{Y}_1(x) + \partial_3 G(x, \mathcal{Y}_0(x), 0) = \partial_x \mathcal{Y}_0(x)\, F(x, \mathcal{Y}_0(x), 0)$$

at the first order in ϵ.

An immediate consequence of normal hyperbolicity (in direction of y) at $\epsilon = 0$ is that $\partial_2 G(x, 0, 0)$ is invertible. Thus

$$\begin{aligned} \frac{dx}{dt} &= \epsilon\, F(x, y, \epsilon) \\ y &= \mathcal{Y}_0(x) + \epsilon\, \mathcal{Y}_1(x) + \mathcal{O}(\epsilon^2) \\ \mathcal{Y}_1(x) &= \partial_2 G(x, \mathcal{Y}_0(x), 0)^{-1} \big[\partial_x \mathcal{Y}_0(x)\, F(x, \mathcal{Y}_0(x), 0) - \partial_3 G(x, \mathcal{Y}_0(x), 0)\big] \end{aligned} \tag{21}$$

follows for the invariant manifold $\mathcal{M}_\epsilon$ and the reduced dynamics at first order in ϵ. Of course, due to the expansion of the differential equation we now must restrict the time interval in order to maintain the shadowing property.

5.5 Slow-Fast Coordinates for the Boltzmann Equation

Recall that by Theorem 5.3.1 the set of all local Maxwellians, $\mathcal{M}_0$, is a normally hyperbolic invariant manifold consisting of fixed points for the rescaled Boltzmann equation. And thus the study of the Boltzmann equation for small but finite values of ϵ is a singular perturbation problem.

As was shown in Section 5.4, in order to efficiently study singular perturbation problems we need to introduce coordinates, which parametrize the normally hyperbolic invariant manifold $\mathcal{M}_0$ and its normal direction. As definition (15) already suggests, we will introduce the coordinates on $\mathcal{M}_0$ as follows.

Definition 5.5.1 (Slow-Fast Coordinates)**.** *Any $f(x, v)$, with $f(x, .) \in \mathscr{L}^2(\mathbb{R}^d)$, is in*

one-to-one correspondence with n, u, T and h via

$$
\begin{aligned}
n(x) &:= \int_{\mathbb{R}^d} f(x,v)\,dv && \textit{particle density}\\
u(x) &:= \frac{1}{n(x)} \int_{\mathbb{R}^d} v\, f(x,v)\,dv && \textit{velocity}\\
T(x) &:= \frac{1}{n(x)} \int_{\mathbb{R}^d} \frac{1}{d}\, \| v-u \|^2\, f(x,v)\,dv && \textit{temperature}\\
h(x,w) &:= \frac{T(x)^{d/2}}{n(x)}\, \frac{f\big(x, u(x) + w\, T(x)^{1/2}\big)}{g_0(w)} - 1 && \textit{normal component}
\end{aligned}
$$

where $g_0(w) = \frac{1}{\sqrt{2\pi}^d} \exp(-\| w \|^2/2)$ is the standard normal density.

Notice that an alternative choice for h could have been

$$\frac{T(x)^{d/2}}{n(x)}\, f\big(x, u(x) + w\, T(x)^{1/2}\big)$$

which is more natural in general. However, we know from Theorem 5.3.1 that the Maxwellians are globally attractive for $\epsilon = 0$. Therefore we would like to compare f to a Maxwellian for small ϵ, i.e. h to a standard normal distribution. This is the reason why the ratio in the expression for h was chosen. Subtracting 1 makes the set of all h a linear space, which follows from Lemma 5.5.2 below.

Since x enters in Definition 5.5.1 only as a parameter it is clear that any functions $n(x)$, $u(x)$ and $T(x)$ are admissible. The following Lemma 5.5.2 gives a necessary and sufficient condition for h to be a normal component of some f.

Lemma 5.5.2. *For a given $f(x,v)$ the corresponding normal component $h(x,w)$ satisfies the normalization conditions*

$$
\begin{aligned}
0 &= \int_{\mathbb{R}^d} h(x,w)\, g_0(w)\,dw\\
0 &= \int_{\mathbb{R}^d} w\, h(x,w)\, g_0(w)\,dw\\
0 &= \int_{\mathbb{R}^d} \| w \|^2\, h(x,w)\, g_0(w)\,dw
\end{aligned}
$$

which are also necessary for h to be the normal component to some f.

Instead of f we may as well consider the corresponding quantities n, u, T, h. By Theorem 5.3.1 the normally hyperbolic invariant manifold $\mathcal{M}_0$ is parametrized by n, u and T. Therefore h is the coordinate (of f) along the direction normal to $\mathcal{M}_0$, which is why we call it the normal component (of f).

This motivates the introduction of the following weighted Hilbert spaces

$$g_0(w) = \frac{1}{\sqrt{2\pi}^d}\, e^{-\frac{\| w \|^2}{2}}$$

$$\mathscr{H} := \mathscr{L}^2(\mathbb{R}^d, g_0(w)\, dw) \quad \text{with} \quad \langle h, g \rangle = \int_{\mathbb{R}^d} h(w)\, g(w)\, g_0(w)\, dw \tag{22a}$$

$$\mathscr{H}^\perp := \Big\{ h \in \mathscr{H} : \langle h, 1 \rangle = \langle h, w_i \rangle = \big\langle h, \| w \|^2 \big\rangle = 0 \Big\}$$

with

$$\mathscr{P} \colon \mathscr{H} \to \mathscr{H}^\perp \subset \mathscr{H} \tag{22b}$$

the corresponding orthogonal projector.

Therefore Lemma 5.5.2 shows that the representation of the function f in terms of h has the following geometric interpretation:

Proposition 5.5.3 (Formal State-Space in terms of the Fast-Slow Coordinates)**.** *The function $f(x, v)$ is in one-to-one correspondence*

$$\Big\{ f(x,v) : f(x,.) \in \mathscr{H} \Big\} \leftrightarrow \Big\{ \big(n(x), u(x), T(x), h(x,v)\big) : h(x,.) \in \mathscr{H}^\perp \Big\}$$

with n, u, T, h.

Remark 5.5.4. *The introduction of weighted Hilbert-spaces such as in* (22) *is known in the literature, e.g. [23, 10]. However, there is an important difference between our choice and the usual choice of the weight function g_0 in the scalar product. Common is to make the weight a local Maxwellian, which thus depends on the hydrodynamic fields. Our choice is a standard Gaussian, and hence independent of the hydrodynamic fields.*

Therefore the distances and angles measured by the norm in $\mathscr{H}$ have an independent meaning in our setup, because they do not vary in time. In particular, a true

separation of the hydrodynamic fields and the remaining part of the velocity distribution (i.e. h) is achieved. This allows to define the solutions of the Boltzmann equation as a dynamical system on a proper state space, which acts on the coordinates n, u, T and h.

In view of Theorem 5.3.1 the advantage of introducing the coordinates n, u, T and h is that these coordinates are adapted to the dynamics of the Boltzmann equation in the singular limit $\epsilon \to 0$.

In Section 5.4 we outlined how singularly perturbed problems can be studied in finite dimensions by introducing such specialized coordinates. Therefore, the coordinates n, u and T play the role of the slow state variables, which were denoted by x in Section 5.4. The fast state variable y from that section corresponds here to h, and the function f corresponds to z.

5.6 Hydrodynamic Limits – Main Results

5.6.1 Slow-Fast Decomposition

In Section 5.5 we introduced slow-fast coordinates, which are adapted to the dynamics of the Boltzmann equation in the singular limit $\epsilon \to 0$.

The next step is to rewrite the (rescaled) Boltzmann equation

$$\partial_t f + \epsilon\, v \cdot \nabla_\xi f = Q(f, f)$$

in terms of n, u, T and h, instead of f. This is the content of Theorem 5.6.1, which is the key result to study the dynamics of the Boltzmann equation for small ϵ. The notation used in Theorem 5.6.1 will be explained below.

Theorem 5.6.1 (Slow-Fast-Decomposition)**.** *There exist real-valued functions*

$$\widehat{\Pi}_{ij} = \widehat{\Pi}_{ij}(n, T, h) \qquad \widehat{q}_i = \widehat{q}_i(n, T, h) \qquad \text{for} \quad i, j = 1, \dots, d$$
$$\widehat{\mathcal{S}} = \widehat{\mathcal{S}}(n, T, h) \qquad \widehat{G} = \widehat{G}(n, u, T, h, \epsilon)$$

such that the rescaled Boltzmann equation becomes

$$\begin{aligned} 0 &= (\partial_t + \epsilon\, u \cdot \nabla_\xi) n + \epsilon\, n\, \operatorname{div}_\xi u \\ 0 &= n\,(\partial_t + \epsilon\, u \cdot \nabla_\xi) u_i + \epsilon \sum_{j=1}^{d} \partial_{\xi_j} \widehat{\Pi}_{ji} \\ -\alpha\, \widehat{\mathcal{S}} &= n\, \frac{d}{2}\,(\partial_t + \epsilon\, u \cdot \nabla_\xi) T + \epsilon\, \operatorname{div}_\xi \widehat{q} + \epsilon \sum_{i,j=1}^{d} \widehat{\Pi}_{ij}\, \partial_{\xi_j} u_i \end{aligned} \tag{23a}$$

and

$$\widehat{G} = (\partial_t + \epsilon\, u \cdot \nabla_\xi) h \tag{23b}$$

with

$$\begin{aligned} \widehat{G}(n, u, T, h, 0) &= n\, \mathscr{P}\mathcal{Q}_0(1 + h, 1 + h) \\ \widehat{G}(n, u, T, 0, \epsilon) &= n\, \mathscr{P}\mathcal{Q}(1, 1) - \epsilon \sum_{i=1}^{d} \phi_i\, \partial_{\xi_i} \sqrt{T} - \epsilon \sum_{i,j=1}^{d} \phi_{ij}\, \partial_{\xi_j} u_i \end{aligned} \tag{23c}$$

in terms of the coordinates n, u, T and h.

The form of the Boltzmann equation in the slow-fast coordinates as given in Theorem 5.6.1 corresponds to the standard form (fast-slow-decomposition) of a singular perturbation problem as in equation (19) of Section 5.4. In this form the Boltzmann equation (formally) defines a flow on

$$\text{state space} = \Big\{ \big(n(\xi), u(\xi), T(\xi), h(\xi, w)\big) : h(\xi, .) \in \mathscr{H}^\perp \Big\}$$

which will not be specified further (hence a formal definition).

Equations (23a) are the well known hydrodynamic balance equations. They can be obtained directly from the usual Boltzmann equation $\partial_t f + v \cdot \nabla_x f = Q(f, f)$ by integrating with respect to v after multiplying both sides by 1, v_i, $\| v \|^2$, respectively.

The difference to the usual non-dissipative balance equations is the presence of the source term $-\alpha\, \widehat{\mathcal{S}}$ in the balance equation for the temperature. This is due to Assumption 5.2.2 on the interaction model, which preserves the total momentum and particle number, but dissipates energy in binary collisions.

The main point of Theorem 5.6.1, however, is the equation for h. This set of four equations is equivalent to the Boltzmann equation, but is more suited to study the dynamical properties in singular limit as $\epsilon \to 0$. Thus this choice of adapted coordinates represents the core of our approach. The usefulness of such coordinates is well known in the study of ordinary differential equations, and was outlined in Section 5.4.

To the best of our knowledge this approach to study the limit $\epsilon \to 0$ is new. For the non-dissipative Boltzmann equation a similar approach is the micro-macro decomposition, introduced by Liu and Yu [55]. In [54, 53] this method was used to obtain results on the long time behavior of solutions to the non-dissipative Boltzmann equation. We will compare our method to the micro-macro decomposition in Section 5.10.

5.6.2 Slow-Motion Limit – Compressible Euler Equations

Before giving the proof of Theorem 5.6.1 we want to show how this rewriting of the rescaled Boltzmann equation helps in deriving asymptotic expansions of its solutions.

As was explained in Section 5.4, once the singular perturbation problem is transformed into standard form one can proceed in two different ways. Introducing a slow time $\epsilon\, t$ and then passing to the limit as ϵ tends to zero yields a scaling limit for the slow motion on the invariant manifold $\mathcal{M}_0$. The following Theorem 5.6.2 is the result of Proposition 5.4.1 applied to the rescaled Boltzmann equation.

Theorem 5.6.2 (Scaling Limit of the Slow Dynamics on $\mathcal{M}_0$)**.** *On the slow time scale $\tau = \epsilon\, t$ the rescaled Boltzmann equation becomes the dissipative compressible*

Euler equations

$$
\begin{aligned}
0 &= (\partial_\tau + u \cdot \nabla_\xi) n + n \ \mathrm{div}_\xi \, u \\
0 &= n \, (\partial_\tau + u \cdot \nabla_\xi) u_i + \partial_{\xi_i} [n \, T] \\
-\alpha'(0) \, \widehat{\mathcal{S}} &= n \, \frac{d}{2} \, (\partial_\tau + u \cdot \nabla_\xi) T + n \, T \ \mathrm{div}_\xi \, u \\
h &= 0
\end{aligned}
$$

in the limit as ϵ tends to zero.

Remark 5.6.3. *The dissipative compressible Euler equations of Theorem 5.6.2 define a flow only on the slow manifold $\mathcal{M}_0$ of fixed points of the Boltzmann equation. This is just like the slow motion limit for the van der Pol equation, as illustrated in Fig. 21, except that here there are no fold points.*

5.6.3 Normal Hyperbolicity – Compressible Navier-Stokes Equations

To obtain an asymptotic expansion of the Boltzmann equation, the second approach of Section 5.4 is used. This approach consists of expanding the invariant manifold $\mathcal{M}_\epsilon$, but not the differential equations. Notice that in the case of the rescaled Boltzmann equation the normally hyperbolic invariant manifold becomes

$$\mathcal{M}_0 = \{n(x), u(x), T(x), h \equiv 0\}$$

which can be written as a graph in terms of the slow variables as

$$\mathcal{Y}_0(n, u, T) = 0 \quad \text{for all} \quad n, u, T \, .$$

As was explained in Section 5.4, in order to obtain an asymptotic expansion of a singularly perturbed system one has to study the dependence of the invariant manifold $\mathcal{M}_\epsilon$ on the parameter ϵ, because the flow will be asymptotic to the flow on this manifold (and not $\mathcal{M}_0$).

The key step we used in Section 5.4 to derive an asymptotic expansion for the singularly perturbed system was the persistence and regularity of the invariant manifold $\mathcal{M}_\epsilon$ for all sufficiently small values of ϵ.

Even though the persistence of normally hyperbolic invariant manifolds, as outlined in Section 5.4 for the finite dimensional case, can be generalized to infinite dimensional Banach spaces (e.g. [3, 2, 4]), we did not as of yet prove this in the case of the Boltzmann equation. This is the reason why Theorem 5.6.4 and ultimately our derivation of compressible Navier-Stokes equations Theorem 5.6.6 are currently formal in the sense of an asymptotic expansions.

Theorem 5.6.4. *Formally, for small enough ϵ the normally hyperbolic invariant manifold $\mathcal{M}_0$ persists as $\mathcal{M}_\epsilon$, and shadows the dynamics of the Boltzmann equation for all times.*

Remark 5.6.5. *Formally, this result is "true", because the spectrum of the linearization has a negative real part, which is bounded away from zero. At a rigorous level, one has to precisely define the state space and construct the invariant manifold locally. The rigorous proof of this result is currently under investigation.*

With the result of Theorem 5.6.4 we can apply the first order asymptotic expansion (21) to the rescaled Boltzmann equation and obtain the following Theorem 5.6.6. The details of the proof will be given in Section 5.8.

Theorem 5.6.6 (Asymptotic Expansion on $\mathcal{M}_\epsilon$)**.** *Assume that the binary interactions for $\alpha = 0$ are rotationally symmetric. Then for ϵ small enough, the dissipative*

compressible Navier-Stokes equations (which are the same as (23a) *above)*

$$
\begin{aligned}
0 &= (\partial_t + \epsilon\, u\cdot\nabla_\xi) n + \epsilon\, n\ \mathrm{div}_\xi\, u \\
0 &= n\,(\partial_t + \epsilon\, u\cdot\nabla_\xi) u_i + \epsilon \sum_{j=1}^{d} \partial_{\xi_j} \widehat{\Pi}_{ji} \\
-\alpha\, \widehat{\mathcal{S}} &= n\,\frac{d}{2}\,(\partial_t + \epsilon\, u\cdot\nabla_\xi) T + \epsilon\ \mathrm{div}_\xi\, \widehat{q} + \epsilon \sum_{i,j=1}^{d} \widehat{\Pi}_{ij}\, \partial_{\xi_j} u_i
\end{aligned}
$$

together with

$$
h = -\epsilon\, \partial_\epsilon\big|_{\epsilon=0} \mathcal{L}_\perp^{-1} \mathscr{P}\mathcal{Q}(1,1) + \epsilon \sum_{i=1}^{d} \frac{\partial_{\xi_i}\sqrt{T}}{n}\, \mathcal{L}_\perp^{-1}\phi_i + \epsilon \sum_{i,j=1}^{d} \frac{\partial_{\xi_j} u_i}{n}\ \mathcal{L}_\perp^{-1}\phi_{ij}
$$

and the hydrodynamic quantities

$$
\begin{aligned}
\frac{\widehat{\Pi}_{ij}}{n\,T} - \delta_{ij} &= \frac{\epsilon}{n}\Big[\partial_{\xi_j} u_i + \partial_{\xi_i} u_j - \delta_{ij}\,\frac{2}{d}\ \mathrm{div}_\xi\, u\Big]\,\frac{1}{2}\,\frac{d}{d-1}\big\langle\, \mathcal{L}_\perp^{-1}\phi_{11}, \phi_{11}\,\big\rangle_{\mathscr{H}^\perp} \\
\frac{2\,\widehat{q}_i}{n\,\sqrt{T}^3} &= \epsilon\,\frac{\partial_{\xi_i}\sqrt{T}}{n}\,\big\langle\, \mathcal{L}_\perp^{-1}\phi_1, \phi_1\,\big\rangle_{\mathscr{H}^\perp} \\
\frac{2\,\widehat{\mathcal{S}}}{n^2\,T} &= \overline{\mathcal{C}}(1 - \epsilon\,\partial_\epsilon\big|_{\epsilon=0}\mathcal{L}_\perp^{-1}\mathscr{P}\mathcal{Q}(1,1), 1 - \epsilon\,\partial_\epsilon\big|_{\epsilon=0}\mathcal{L}_\perp^{-1}\mathscr{P}\mathcal{Q}(1,1)) \\
&\quad + \overline{\mathcal{C}}(\mathcal{L}_\perp^{-1}\phi_1, \mathcal{L}_\perp^{-1}\phi_1)\ \Big\|\ \frac{\epsilon}{n}\,\nabla_\xi\sqrt{T}\ \Big\|^2 \\
&\quad + \frac{1}{2}\,\frac{d}{d-1}\,\overline{\mathcal{C}}(\mathcal{L}_\perp^{-1}\phi_{11}, \mathcal{L}_\perp^{-1}\phi_{11}) \sum_{i,j=1}^{d} \frac{\epsilon^2}{n^2}\,\big[\partial_{\xi_j} u_i\,\partial_{\xi_j} u_i + \partial_{\xi_j} u_i\,\partial_{\xi_i} u_j \\
&\qquad\qquad - \frac{2}{d}\,\partial_{\xi_i} u_i\,\partial_{\xi_j} u_j\big]
\end{aligned}
$$

are the first order asymptotic expansion of the rescaled Boltzmann equation, when restricted to the invariant manifold $\mathcal{M}_\epsilon$*. The expression for the linear operator* $\mathcal{L}_\perp^{-1}$ *and the bilinear functional* $\overline{\mathcal{C}}$ *will be given below.*

Note that in our approach the Navier-Stokes equations of Theorem 5.6.6 are obtained without rescaling time (unlike for the Euler equation). Therefore the Navier-Stokes equations are obtained not in a scaling limit, rather are they a consequence of the persistence of the normally hyperbolic invariant manifold $\mathcal{M}_\epsilon$. This is precisely what was illustrated in Fig. 20 and Fig. 22 for the corresponding situation for the van der Pol equation.

The normal fibration of the invariant manifold $\mathcal{M}_\epsilon$ makes the Boltzmann equation look like a skew-product flow over the slow manifold $\mathcal{M}_0$. Therefore, the analysis of the Boltzmann equation for small values of ϵ corresponds to Fenichels analysis [37] of ordinary differential equations. Furthermore, the normal fibers also allow for rigorous matched expansions.

At the level of the Navier-Stokes equations, not only is the scalar pressure not affected by the dissipation, but Theorem 5.6.6 shows that for rotationally invariant interactions (in the non-dissipative setting) also the stress tensor and the heat conductivity are the same expressions as in the non-dissipative case. Thus the effect of the dissipation at the level of the Navier-Stokes equations is the extra source term in the energy balance equation. The transport coefficients are affected by the dissipation only indirectly through their dependence on the temperature.

The fact that the momentum-tensor (i.e. the scalar pressure and the stress tensor) and the heat conductivity are unaffected by the dissipation at the level of the Navier-Stokes equation seems reasonable by the following heuristics. Due to dissipation the temperature decreases, hence the leading order correction must be a function of the temperature, not its gradient. And since the momentum-tensor and the heat conductivity multiply the spatial gradients of u and T, they are not affected by the dissipation at the leading order. Only higher order corrections will involve spatial gradients, and thus contribute to the transport coefficients.

5.6.4 Haff's Cooling Law

A special case of the Navier-Stokes equations is the spatially homogeneous situation. In that case the balance equations in the Navier-Stokes system become trivial except for the source term in the equation for the temperature. The result is summarized in the following

Theorem 5.6.7 (Haff's Law – I)**.** *In the spatially homogeneous situation the general*

Navier-Stokes equations of Theorem 5.6.6 reduce to

$$0 = \partial_t n \ , \qquad 0 = \partial_t u_i \ , \quad \textit{and}$$
$$\partial_t T = -\alpha \, \frac{n\,T}{d} \, \overline{\mathcal{C}}(1 - \epsilon \, \partial_\epsilon \big|_{\epsilon=0} \mathcal{L}_\perp^{-1} \mathscr{P} \mathcal{Q}(1,1), 1 - \epsilon \, \partial_\epsilon \big|_{\epsilon=0} \mathcal{L}_\perp^{-1} \mathscr{P} \mathcal{Q}(1,1)) \ .$$

Actually the equation for the temperature in Theorem 5.6.7 is not the usual Haff law (e.g. [41]). As will be clear from the definition of the bilinear functional $\overline{\mathcal{C}}$, under natural assumptions we have that $\overline{\mathcal{C}} \sim \sqrt{T}$ as $T \to 0$. More precisely we have the following result

Corollary 5.6.8 (Haff's Law – II)**.** *Suppose that the collision kernel $B(v,\omega)$ is continuously differentiable with respect to v at $v = 0$. Then the equation for the temperature of Theorem 5.6.7 becomes asymptotically*

$$\frac{1}{\sqrt{T(t)}} - \frac{1}{\sqrt{T(0)}} = \alpha \, \frac{n}{2\,d} \, \overline{\mathcal{C}}_0(1,1)\, t \qquad \textit{with} \qquad \overline{\mathcal{C}}_0(1,1) := \lim_{T \to 0} \frac{\overline{\mathcal{C}}(1,1)}{\sqrt{T}}$$

as $T \to 0$ and $\epsilon \to 0$.

Proof. The differentiability assumption we impose on B imply that the limit

$$\overline{\mathcal{C}}_0(g,g) := \lim_{T \to 0} \frac{\overline{\mathcal{C}}(g,g)}{\sqrt{T}}$$

is well defined for any function g (independent of T). Therefore by Taylor's theorem we can simplify the equation for the temperature of Theorem 5.6.7 to

$$\begin{aligned} \partial_t T &= -\alpha \, \frac{n \sqrt{T}^3}{d} \, \overline{\mathcal{C}}_0(1 - \epsilon \, \partial_\epsilon \big|_{\epsilon=0} \mathcal{L}_\perp^{-1} \mathscr{P} \mathcal{Q}(1,1), 1 - \epsilon \, \partial_\epsilon \big|_{\epsilon=0} \mathcal{L}_\perp^{-1} \mathscr{P} \mathcal{Q}(1,1)) + \alpha \ \mathrm{o}(\sqrt{T}^3) \\ &= -\alpha \, \frac{n \sqrt{T}^3}{d} \, \overline{\mathcal{C}}_0(1,1) + \alpha \, [\mathrm{o}(\sqrt{T}^3) + \mathcal{O}(\epsilon)] \end{aligned}$$

as $T \to 0$ and $\epsilon \to 0$.

Therefore at leading order we obtain

$$\partial_t T = -\alpha \, \frac{n \sqrt{T}^3}{d} \, \overline{\mathcal{C}}_0(1,1)$$

which can be integrated by separating the variables, because $\overline{\mathcal{C}}_0(1,1)$ does not depend on T. □

Remark 5.6.9. *The equation for the temperature of Corollary 5.6.8, which describes the asymptotic cooling law for spatially homogeneous systems is the usual form of Haff's law. It predicts that eventually (i.e. for small enough temperatures) the cooling is such that* $t \mapsto 1/\sqrt{T(t)}$ *is a straight line, regardless of the details of the inter-particle interaction.*

5.7 Hydrodynamic Limits I – Proof of Theorem 5.6.1

In this section we will prove the results stated in Section 5.6. The first step is to derive the form of the Boltzmann equation in terms of the coordinates n, u, T and h, as introduced in Definition 5.5.1.

Recall the rescaled Boltzmann equation (without external forces)

$$\partial_t f + \epsilon\, v \cdot \nabla_\xi f = Q(f, f)$$

in terms of f, and the associated coordinates n, u, T, h as in Definition 5.5.1. Furthermore, we will keep using

$$g_0(w) = \frac{1}{\sqrt{2\pi}^d} \exp(-\parallel w \parallel^2 /2)$$

to denote the standard normal density.

Definition 5.7.1. *Let* B *denote the kernel of the collision operator* Q *as in Corollary 5.2.5. For any* $g(w)$ [2] *define*

$$\mathcal{Q}(g,g)(w_1) := \int_{S^{d-1}} \int_{\mathbb{R}^d} \Big[\frac{B(\sqrt{T}\,[w_2^* - w_1^*], \omega)}{\sqrt{1-2\,\alpha}}\, g(w_1^*)\, g(w_2^*)\, e^{-\frac{1}{2}\,\alpha\,|(w_2-w_1)\cdot\omega|^2} - B(\sqrt{T}\,(w_2 - w_1), \omega)\, g(w_1)\, g(w_2) \Big]\, g_0(w_2)\, dw_2\, d\omega$$

which generates a symmetric, bilinear operator.

[2] *To simplify the notation we dropped the dependence of* g *on* ξ*, because the operator* $\mathcal{Q}$ *acts on* w *only. We will use this slight abuse of notation without further notice wherever it does not cause confusion.*

The following Lemma 5.7.2 relates the collision operator $Q(f,f)$ in the Boltzmann equation to the corresponding expression $\mathcal{Q}(1+h,1+h)$ in terms of h.

Lemma 5.7.2. *For any $f(\xi,v)$ and its associated coordinates $n(\xi)$, $u(\xi)$, $T(\xi)$, $h(\xi,v)$ the identity*

$$\frac{\sqrt{T}^d}{n^2\, g_0(w)} Q(f,f)(\xi, u + w\sqrt{T}) = \mathcal{Q}(1+h,1+h)(\xi,w)$$

holds.

Proof. Since ξ only enters as a parameter in $Q(f,f)$ we do not indicate the dependence on ξ explicitly to shorten the notation. By Definition 5.5.1 f and h are related via

$$f(u + w\sqrt{T}) = [1 + h(w)]\, \frac{n}{\sqrt{T}^d}\, g_0(w)\ .$$

In Corollary 5.2.5 the explicit form of Q

$$\begin{aligned} Q(f,f)(v_1) = \int_{S^{d-1}} \int_{\mathbb{R}^d} \Big[\frac{1}{\sqrt{1-2\,\alpha}}\, B(v_2^* - v_1^*, \omega)\, f(v_1^*)\, f(v_2^*) \\ - B(v_2 - v_1, \omega)\, f(v_1)\, f(v_2) \Big]\, dv_2\, d\omega \end{aligned}$$

in terms of f was shown.

The change of variables $v_1 = u + w_1\sqrt{T}$, $v_2 = u + w_2\sqrt{T}$ then shows

$$\begin{aligned} &Q(f,f)(u + w_1\sqrt{T}) = \\ &\quad = \sqrt{T}^d \int_{S^{d-1}} \int_{\mathbb{R}^d} \Big[\frac{B(\sqrt{T}\,(w_2^* - w_1^*), \omega)}{\sqrt{1-2\,\alpha}}\, f(u + w_1^*\sqrt{T})\, f(u + w_2^*\sqrt{T}) \\ &\qquad - B(\sqrt{T}\,(w_2 - w_1), \omega)\, f(u + w_1\sqrt{T})\, f(u + w_2\sqrt{T}) \Big]\, dw_2\, d\omega \\ &\quad = \frac{n^2}{\sqrt{T}^d} \int_{S^{d-1}} \int_{\mathbb{R}^d} \Big[\frac{B(\sqrt{T}\,(w_2^* - w_1^*), \omega)}{\sqrt{1-2\,\alpha}}\, [1 + h(w_1^*)]\, [1 + h(w_2^*)]\, g_0(w_1^*)\, g_0(w_2^*) \\ &\qquad - B(\sqrt{T}\,(w_2 - w_1), \omega)\, [1 + h(w_1)]\, [1 + h(w_2)]\, g_0(w_1)\, g_0(w_2) \Big]\, dw_2\, d\omega \end{aligned}$$

where we used the relation between f and h.

Finally, notice that due to (11) and the explicit structure of the standard normal density $g_0(w)$ the identity

$$g_0(w_1^*)\, g_0(w_2^*) = \exp\Big(-\frac{1}{2}\,\alpha\,|(w_2 - w_1)\cdot\omega|^2\Big)\, g_0(w_1)\, g_0(w_2)$$

follows. Therefore the expression for $Q(f,f)(u + w_1\sqrt{T})$ becomes

$$\begin{aligned}\frac{\sqrt{T}^d}{n^2\, g_0(w_1)} Q(f,f)(u + w_1\sqrt{T}) = \\ = \int_{S^{d-1}}\int_{\mathbb{R}^d} \Big[\frac{B(\sqrt{T}\,(w_2^* - w_1^*),\omega)}{\sqrt{1-2\,\alpha}}\,[1+h(w_1^*)]\,[1+h(w_2^*)]\, e^{-\frac{1}{2}\,\alpha\,|(w_2-w_1)\cdot\omega|^2} \\ - B(\sqrt{T}\,(w_2 - w_1),\omega)\,[1+h(w_1)]\,[1+h(w_2)]\Big]\, g_0(w_2)\, dw_2\, d\omega\end{aligned}$$

which proves the claim. □

For applications it is useful to have the weak form of $\mathcal{Q}$. Using the explicit form of $\mathcal{Q}$ we obtain the weak form of $\mathcal{Q}$ by the same symmetry and change of variable argument we used in the proof of Corollary 5.2.5.

Lemma 5.7.3. *For any two functions g, ψ the equation*

$$\begin{aligned}\langle\, \mathcal{Q}(g,g), \psi\,\rangle_{\mathscr{H}} = \int_{\mathbb{R}^d}\int_{\mathbb{R}^d}\int_{S^{d-1}} B(\sqrt{T}\,(w_2 - w_1),\omega)\, g(w_1)\, g(w_2)\cdot \\ \cdot\,\frac{1}{2}\,\big[\psi(w_1') + \psi(w_2') - \psi(w_1) - \psi(w_2)\big]\, d\omega\, g_0(w_1)\, dw_1\, g_0(w_2)\, dw_2\end{aligned}$$

holds, and gives the weak form of $\mathcal{Q}$.

Substituting for f the corresponding h, n, u, T back into the Boltzmann equation yields, after a straightforward but lengthy calculation, the following

Lemma 5.7.4. *The rescaled Boltzmann equation $\partial_t f + \epsilon\, v\cdot\nabla_\xi f = Q(f,f)$ becomes*

$$\begin{aligned}n\,\mathcal{Q}(1+h,1+h) = \partial_t h + \epsilon\,(\sqrt{T}\,w + u)\cdot\nabla_\xi h \\ + \frac{1}{n}\Big[\partial_t n + \epsilon\,(\sqrt{T}\,w+u)\cdot\nabla_\xi n\Big]\,(1+h) \\ - \frac{1}{\sqrt{T}}\Big[\partial_t\sqrt{T} + \epsilon\,(\sqrt{T}\,w+u)\cdot\nabla_\xi\sqrt{T}\Big]\,\frac{\mathrm{div}_w[w\,(1+h)\,g_0]}{g_0} \\ - \sum_{i=1}^{d}\frac{1}{\sqrt{T}}\Big[\partial_t u_i + \epsilon\,(\sqrt{T}\,w+u)\cdot\nabla_\xi u_i\Big]\,\frac{\partial_{w_i}[(1+h)\,g_0]}{g_0}\end{aligned}$$

in terms of n, u, T, h.

The choice of $\mathscr{H}$ allows us to separate h from n, u, T by an orthogonal projection. Observe that for all g the equations

$$\begin{aligned}
0 &= \langle\, \mathcal{Q}(g,g), 1 \,\rangle_{\mathscr{H}} \\
0 &= \langle\, \mathcal{Q}(g,g), w_i \,\rangle_{\mathscr{H}} \\
\overline{\mathcal{C}}(g,g) &:= \frac{1}{2} \int_{\mathbb{R}^d} \int_{\mathbb{R}^d} \int_{S^{d-1}} |(w_2 - w_1)\cdot\omega|^2 \, B(\sqrt{T}\,(w_2 - w_1), \omega) \cdot \\
&\qquad\qquad \cdot\, g(w_1)\, g(w_2)\, g_0(w_1)\, g_0(w_2)\; d\omega\, dw_1\, dw_2 \\
&= -\frac{1}{\alpha} \left\langle\, \mathcal{Q}(g,g), \| w \|^2 \,\right\rangle_{\mathscr{H}}
\end{aligned} \tag{24}$$

hold. They follow immediately by applying Lemma 5.7.3 to the particular choices of 1, w_i, $\| w \|^2$ for ψ. Taking the inner product (in $\mathscr{H}$) on both sides of the Boltzmann equation with 1, w_i, $\| w \|^2$ then yields

$$\begin{aligned}
0 &= \frac{1}{n}\, \partial_t n + \epsilon\, \frac{1}{n}\, u \cdot \nabla_\xi n + \epsilon\, \operatorname{div}_\xi u \\
0 &= \sqrt{T}\, \epsilon \sum_{i=1}^{d} \partial_{\xi_i} \langle\, w_k\, w_i, h \,\rangle_{\mathscr{H}} + \frac{\sqrt{T}}{n}\, \epsilon \sum_{i=1}^{d} \langle\, w_k\, w_i, 1 + h \,\rangle_{\mathscr{H}}\, \partial_{\xi_i} n \\
&\quad + 2\, \epsilon \sum_{i=1}^{d} \langle\, w_k\, w_i, 1 + h \,\rangle_{\mathscr{H}}\, \partial_{\xi_i} \sqrt{T} + \frac{1}{\sqrt{T}} \left[\partial_t u_k + \epsilon\, u \cdot \nabla_\xi u_k \right] \\
-\alpha\, n\, \overline{\mathcal{C}}(1+h, 1+h) &= \epsilon \sqrt{T} \sum_{i=1}^{d} \partial_{\xi_i} \left\langle\, w_i\, \| w \|^2, h \,\right\rangle_{\mathscr{H}} \\
&\quad + \frac{d}{n} \left[\partial_t n + \epsilon\, u \cdot \nabla_\xi n \right] + \epsilon\, \frac{\sqrt{T}}{n} \sum_{i=1}^{d} \left\langle\, w_i\, \| w \|^2, h \,\right\rangle_{\mathscr{H}} \partial_{\xi_i} n \\
&\quad + \frac{2\, d}{\sqrt{T}} \left[\partial_t \sqrt{T} + \epsilon\, u \cdot \nabla_\xi \sqrt{T} \right] + 3\, \epsilon \sum_{i=1}^{d} \left\langle\, w_i\, \| w \|^2, h \,\right\rangle_{\mathscr{H}} \partial_{\xi_i} \sqrt{T} \\
&\quad + d\, \epsilon\, \operatorname{div}_\xi u + 2\, \epsilon \sum_{i,j=1}^{d} \langle\, w_i\, w_j, 1 + h \,\rangle_{\mathscr{H}}\, \partial_{\xi_j} u_i
\end{aligned}$$

respectively, where we used (24) to simplify. Upon further simplifications we obtain

$$\begin{aligned}
0 &= (\partial_t + \epsilon\, u\cdot\nabla_\xi) n + \epsilon\, n\, \operatorname{div}_\xi u \\
0 &= n\,(\partial_t + \epsilon\, u\cdot\nabla_\xi) u_k + \epsilon \sum_{i=1}^{d} \partial_{\xi_i}\left[n\, T\, (\delta_{ik} + \langle\, w_k\, w_i, h\,\rangle_{\mathscr{H}})\right] \\
-\alpha\, \frac{n^2\, T}{2}\overline{\mathcal{C}}(1+h, 1+h) &= \frac{d}{2}\, n\,(\partial_t + \epsilon\, u\cdot\nabla_\xi) T \\
&\quad + \epsilon \sum_{i,j=1}^{d} n\, T\, (\delta_{ij} + \langle\, w_i\, w_j, h\,\rangle_{\mathscr{H}})\, \partial_{\xi_j} u_i \\
&\quad + \epsilon \sum_{i=1}^{d} \partial_{\xi_i}\Big[\frac{1}{2}\, n\, \sqrt{T}^3 \left\langle\, w_i\, \| \, w\, \|^2, h\,\right\rangle_{\mathscr{H}}\Big]
\end{aligned} \tag{25}$$

which are of the form as the claimed equations (23a) of Theorem 5.6.1.

To obtain the actual form of (23a) we introduce some standard notation from hydrodynamics.

Definition 5.7.5. *Let $f(\xi, v)$ be some density function. Then*

$$\begin{aligned}
\widehat{\Pi}_{ij} &:= \int_{\mathbb{R}^d} (v_i - u_i)\,(v_j - u_j)\, f(\xi, v)\, dv && \textit{(reduced) momentum tensor} \\
\widehat{q}_i &:= \int \frac{1}{2}\, \| \, v - u\, \|^2\, (v_i - u_i)\, f(\xi, v)\, dv && \textit{heat current} \\
-\alpha\, \widehat{\mathcal{S}} &:= \int_{\mathbb{R}^d} \frac{\| \, v - u\, \|^2}{2}\, Q(f, f)(\xi, v)\, dv && \textit{energy dissipation}
\end{aligned}$$

are functions of ξ and t.

The hydrodynamic quantities of Definition 5.7.5 are associated to f, as is standard in kinetic theory. Since we rewrite f in terms of n, u, T, h, the next Lemma 5.7.6 will be important when separating the Boltzmann equation.

To shorten the notation, we introduce the functions

$$\begin{aligned}
\phi_{ij} &:= w_i\, w_j - \delta_{ij}\, \frac{1}{d}\, \| \, w\, \|^2 = \mathscr{P}\, w_i\, w_j \in \mathscr{H}^\perp \\
\phi_i &:= w_i \left[\, \| \, w\, \|^2 - (d+2)\right] = \mathscr{P}\, w_i\, \| \, w\, \|^2 \in \mathscr{H}^\perp
\end{aligned} \tag{26}$$

Lemma 5.7.6. *Let $f(\xi, v)$ be some density function, and let $n(\xi)$, $u(\xi)$, $T(\xi)$, $h(\xi, w)$ be the corresponding coordinates. Then*

$$\begin{aligned}
\widehat{\Pi}_{ij} \equiv \widehat{\Pi}_{ij}(n,T,h) &= n\,T\left[\delta_{ij} + \langle\, \phi_{ij}, h\,\rangle_{\mathscr{H}^\perp}\right] \\
\widehat{q}_i \equiv \widehat{q}_i(n,T,h) &= \frac{n}{2}\sqrt{T}^3 \langle\, \phi_i, h\,\rangle_{\mathscr{H}^\perp} \\
\widehat{\mathcal{S}} \equiv \widehat{\mathcal{S}}(n,T,h) &= -\frac{1}{2\,\alpha}\, n^2\, T \big\langle\, \| w \|^2\,, \mathcal{Q}(1+h,1+h)(w)\,\big\rangle_{\mathscr{H}} \\
&\equiv \frac{1}{2}\, n^2\, T\, \overline{\mathcal{C}}(1+h,1+h)
\end{aligned}$$

are the relations between the hydrodynamic quantities and the geometry in $\mathscr{H}^\perp$.

Proof. Suppressing again the dependence on ξ, we have

$$\widehat{\Pi}_{ij} = \int_{\mathbb{R}^d} v_i\, v_j\, f(u+v)\, dv = T \int_{\mathbb{R}^d} w_i\, w_j\, f(u + w\sqrt{T})\, \sqrt{T}^d\, dw\,.$$

From the definition of h as given in Definition 5.5.1

$$f(u + w\sqrt{T}) = [1 + h(w)]\, \frac{n}{\sqrt{T}^d}\, g_0(w)$$

hence

$$\begin{aligned}
\widehat{\Pi}_{ij} &= T \int_{\mathbb{R}^d} w_i\, w_j\, [1+h(w)]\, \frac{n}{\sqrt{T}^d}\, g_0(w)\, \sqrt{T}^d\, dw \\
&= n\,T \int_{\mathbb{R}^d} w_i\, w_j\, [1+h(w)]\, g_0(w)\, dw = n\,T\,\delta_{ij} + n\,T \int_{\mathbb{R}^d} w_i\, w_j\, h(w)\, g_0(w)\, dw \\
&= n\,T\left[\delta_{ij} + \langle\, w_i\, w_j, h(w)\,\rangle_{\mathscr{H}}\right]
\end{aligned}$$

follows. To obtain the claimed expression notice that $h \in \mathscr{H}^\perp$. Therefore

$$\widehat{\Pi}_{ij} = n\,T\left[\delta_{ij} + \langle\, w_i\, w_j, h(w)\,\rangle_{\mathscr{H}}\right] = n\,T\left[\delta_{ij} + \langle\, \phi_{ij}, h\,\rangle_{\mathscr{H}}\right]$$

where both functions ϕ_{ij} and h are elements of $\mathscr{H}^\perp$.

The claimed expression for $\widehat{q}_i$ follows from the line of arguments as for $\widehat{\Pi}_{ij}$

$$\begin{aligned}
\widehat{q}_i &= \frac{1}{2}\sqrt{T}^3 \int \| w \|^2\, w_i\, f(u + w\sqrt{T})\, \sqrt{T}^d\, dw \\
&= \frac{n}{2}\sqrt{T}^3 \int \| w \|^2\, w_i\, [1+h(w)]\, g_0(w)\, dw = \frac{n}{2}\sqrt{T}^3 \langle\, \phi_i, h\,\rangle_{\mathscr{H}}
\end{aligned}$$

where the two functions in the scalar product are again both in $\mathscr{H}^{\perp}$.

The expression for the energy dissipation source $\widehat{\mathcal{S}}$ becomes

$$-\alpha\,\widehat{\mathcal{S}} = T\int_{\mathbb{R}^d} \frac{\|\,w\,\|^2}{2}\,Q(f,f)(u+w\,\sqrt{T})\,\sqrt{T}^d\,dw$$

so that Lemma 5.7.2 yields

$$\begin{aligned}
-\alpha\,\widehat{\mathcal{S}} &= T\int_{\mathbb{R}^d} \frac{\|\,w\,\|^2}{2}\,\frac{n^2\,g_0(w)}{\sqrt{T}^d}\,\mathcal{Q}(1+h,1+h)(w)\,\sqrt{T}^d\,dw \\
&= \frac{1}{2}\,n^2\,T\int_{\mathbb{R}^d} \|\,w\,\|^2\;\mathcal{Q}(1+h,1+h)(w)\,g_0(w)\,dw \\
&= \frac{1}{2}\,n^2\,T\big\langle\,\|\,w\,\|^2\,,\mathcal{Q}(1+h,1+h)(w)\,\big\rangle_{\mathscr{H}} \equiv -\alpha\,\frac{1}{2}\,n^2\,T\,\overline{\mathcal{C}}(1+h,1+h)
\end{aligned}$$

which finishes the proof. □

Now we are in the position to proof Theorem 5.6.1.

Proof of Theorem 5.6.1. With Lemma 5.7.6 equation (25) for n, u and T becomes

$$\begin{aligned}
0 &= (\partial_t + \epsilon\,u\cdot\nabla_\xi)n + \epsilon\,n\;\mathrm{div}_\xi\,u \\
0 &= n\,(\partial_t + \epsilon\,u\cdot\nabla_\xi)u_k + \epsilon\sum_{i=1}^{d}\partial_{\xi_i}\widehat{\Pi}_{ik} \\
-\alpha\,\widehat{\mathcal{S}} &= \frac{d}{2}\,n\,(\partial_t + \epsilon\,u\cdot\nabla_\xi)T + \epsilon\sum_{i,j=1}^{d}\widehat{\Pi}_{ij}\,\partial_{\xi_j}u_i + \epsilon\;\mathrm{div}_\xi\,\widehat{q}
\end{aligned}$$

which are precisely (23a) of Theorem 5.6.1.

It remains to show (23b). The rescaled Boltzmann equation of Lemma 5.7.4 can be rewritten as

$$\begin{aligned}
n\,\mathcal{Q}(1+h,1+h) &= (\partial_t + \epsilon\,u\cdot\nabla_\xi)h + \epsilon\,\sqrt{T}\,w\cdot\nabla_\xi h \\
&\quad + \frac{1}{n}\Big[(\partial_t + \epsilon\,u\cdot\nabla_\xi)n + \epsilon\,\sqrt{T}\,w\cdot\nabla_\xi n\Big]\,(1+h) \\
&\quad - \frac{1}{2\,T}\Big[(\partial_t + \epsilon\,u\cdot\nabla_\xi)T + \epsilon\,\sqrt{T}\,w\cdot\nabla_\xi T\Big]\,\frac{\mathrm{div}_w[w\,(1+h)\,g_0]}{g_0} \\
&\quad - \sum_{i=1}^{d}\frac{1}{\sqrt{T}}\Big[(\partial_t + \epsilon\,u\cdot\nabla_\xi)u_i + \epsilon\,\sqrt{T}\,w\cdot\nabla_\xi u_i\Big]\,\frac{\partial_{w_i}[(1+h)\,g_0]}{g_0}
\end{aligned}$$

Using (23a) we can eliminate the time derivatives of n, u, T, and obtain

$$\begin{aligned}
n\,\mathcal{Q}(1+h,1+h) &= (\partial_t + \epsilon\, u\cdot\nabla_\xi)h + \epsilon\sqrt{T}\, w\cdot\nabla_\xi h \\
&\quad + \frac{1}{n}\Big[-\epsilon\, n\ \mathrm{div}_\xi\, u + \epsilon\sqrt{T}\, w\cdot\nabla_\xi n\Big](1+h) \\
&\quad - \frac{1}{2\,T}\Big[-\frac{2}{n\,d}\left[\alpha\,\widehat{\mathcal{S}} + \epsilon\ \mathrm{div}_\xi\,\widehat{q} + \epsilon\sum_{i,j=1}^{d}\widehat{\Pi}_{ij}\,\partial_{\xi_j}u_i\right] + \epsilon\sqrt{T}\, w\cdot\nabla_\xi T\Big]\cdot \\
&\qquad\qquad \cdot\frac{\mathrm{div}_w[w\,(1+h)\,g_0]}{g_0} \\
&\quad - \sum_{i=1}^{d}\frac{1}{\sqrt{T}}\Big[-\epsilon\,\frac{1}{n}\sum_{j=1}^{d}\partial_{\xi_j}\widehat{\Pi}_{ji} + \epsilon\sqrt{T}\, w\cdot\nabla_\xi u_i\Big]\frac{\partial_{w_i}[(1+h)\,g_0]}{g_0}
\end{aligned}$$

which gives the evolution equation for h.

However, since $h\in\mathscr{H}^\perp$ for all times we also must have that $(\partial_t+\epsilon\,u\cdot\nabla_\xi)h\in\mathscr{H}^\perp$ for all times. In order to make this fact a manifest part of the evolution equation of h, we project the above to $\mathscr{H}^\perp$ using the orthogonal projector $\mathscr{P}\colon\mathscr{H}\to\mathscr{H}^\perp$.

$$\begin{aligned}
n\,\mathscr{P}\mathcal{Q}(1+h,1+h) &= (\partial_t + \epsilon\, u\cdot\nabla_\xi)h + \epsilon\sqrt{T}\ \mathrm{div}_\xi\,\mathscr{P}[w\,h] \\
&\quad - \epsilon\ \mathrm{div}_\xi\, u\,h + \epsilon\,\frac{\sqrt{T}}{n}\,\nabla_\xi n\cdot\mathscr{P}[w\,h] \\
&\quad + \frac{1}{n\,d\,T}\left[\alpha\,\widehat{\mathcal{S}} + \epsilon\ \mathrm{div}_\xi\,\widehat{q} + \epsilon\sum_{i,j=1}^{d}\widehat{\Pi}_{ij}\,\partial_{\xi_j}u_i\right]\mathscr{P}\Big[\frac{\mathrm{div}_w[w\,(1+h)\,g_0]}{g_0}\Big] \\
&\quad - \epsilon\,\nabla_\xi\sqrt{T}\cdot\mathscr{P}\Big[w\,\frac{\mathrm{div}_w[w\,(1+h)\,g_0]}{g_0}\Big] \\
&\quad + \epsilon\,\frac{1}{n\,\sqrt{T}}\sum_{i,j=1}^{d}\partial_{\xi_j}\widehat{\Pi}_{ji}\,\mathscr{P}\Big[\frac{\partial_{w_i}[(1+h)\,g_0]}{g_0}\Big] \\
&\quad - \epsilon\sum_{i=1}^{d}\nabla_\xi u_i\cdot\mathscr{P}\Big[w\,\frac{\partial_{w_i}[(1+h)\,g_0]}{g_0}\Big]
\end{aligned}$$

where we used Lemma 5.7.6.

Furthermore, this explicit form of the equation for h immediately shows

$$\begin{aligned}
\widehat{G}(n,u,T,h,0) &= n\,\mathscr{P}\mathcal{Q}_0(1+h,1+h) \\
\widehat{G}(n,u,T,0,\epsilon) &= n\,\mathscr{P}\mathcal{Q}(1,1) - \epsilon\sum_{i=1}^{d}\phi_i\,\partial_{\xi_i}\sqrt{T} - \epsilon\sum_{i,j=1}^{d}\phi_{ij}\,\partial_{\xi_j}u_i
\end{aligned}$$

where we used the definitions of ϕ_i and ϕ_{ij} as in (26). This completes the proof of Theorem 5.6.1. $\square$

For computations the following Proposition 5.7.7 provides a simplified formula for $\overline{\mathcal{C}}(1,1)$ for rotationally invariant interactions.

Proposition 5.7.7. *If the particle interactions are rotationally invariant, i.e.* $B(v_2 - v_1, \omega) = B(\| v_2 - v_1 \|, |\cos\theta|)$ *with* $\| v_2 - v_1 \| \cos\theta = (v_2 - v_1) \cdot \omega$ *then*

$$\overline{\mathcal{C}}(1,1) = \frac{16\,\sqrt{\pi}^{d-1}}{\Gamma\left(\frac{d}{2}\right)\Gamma\left(\frac{d-1}{2}\right)} \int_0^\infty \int_0^1 B(2\sqrt{T}\,x, z)\, x^{d+1}\, e^{-x^2}\, z^2\, \sqrt{1-z^2}^{d-3}\, dz\, dx\ .$$

Proof. By its definition

$$\overline{\mathcal{C}}(g,g) = \frac{1}{2} \int_{\mathbb{R}^d} \int_{\mathbb{R}^d} \int_{S^{d-1}} |(w_2 - w_1)\cdot\omega|^2\, B(\sqrt{T}\,(w_2 - w_1), \omega) \cdot \\ \cdot\, g(w_1)\, g(w_2)\, g_0(w_1)\, g_0(w_2)\ d\omega\, dw_1\, dw_2$$

for any g, where $g_0(w) = \frac{1}{\sqrt{2\pi}^d}\, e^{-\| w \|^2/2}$. Using the special form of B then yields

$$\begin{aligned}\overline{\mathcal{C}}(g,g) &= \frac{1}{2} \int_{\mathbb{R}^d} \int_{\mathbb{R}^d} \int_{S^{d-1}} \| w_2 - w_1 \|^2\ |\cos\theta|^2\, B(\sqrt{T}\ \| w_2 - w_1 \|, |\cos\theta|) \cdot \\ &\qquad \cdot\, g(w_1)\, g(w_2)\, g_0(w_1)\, g_0(w_2)\ d\omega\, dw_1\, dw_2 \\ &= |S^{d-2}| \int_{\mathbb{R}^d} \int_{\mathbb{R}^d} \int_0^{\pi/2} \| w_2 - w_1 \|^2\ |\cos\theta|^2\, B(\sqrt{T}\ \| w_2 - w_1 \|, |\cos\theta|) \cdot \\ &\qquad \cdot\, g(w_1)\, g(w_2)\, g_0(w_1)\, g_0(w_2)\, |\sin\theta|^{d-2}\, d\theta\, dw_1\, dw_2\end{aligned}$$

after integrating with respect to ω.

With a change of variables we obtain

$$\begin{aligned}
\overline{\mathcal{C}}(1,1) &= |S^{d-2}| \int_{\mathbb{R}^d} \int_{\mathbb{R}^d} \int_0^{\pi/2} \| w \|^2 \, |\cos\theta|^2 \, B(\sqrt{T} \, \| w \| \, , |\cos\theta|) \cdot \\
&\qquad \cdot g_0(w_1) \, g_0(w_1 + w) \, |\sin\theta|^{d-2} \, d\theta \, dw_1 \, dw \\
&\equiv \frac{|S^{d-2}|}{(2\pi)^d} \int_{\mathbb{R}^d} \int_{\mathbb{R}^d} \int_0^{\pi/2} \| w \|^2 \, |\cos\theta|^2 \, B(\sqrt{T} \, \| w \| \, , |\cos\theta|) \cdot \\
&\qquad \cdot e^{-\frac{\| w_1 \|^2 + \| w + w_1 \|^2}{2}} \, |\sin\theta|^{d-2} \, d\theta \, dw_1 \, dw \\
&= \frac{|S^{d-2}|}{(2\pi)^d} \int_{\mathbb{R}^d} \int_{\mathbb{R}^d} \int_0^{\pi/2} \| w \|^2 \, |\cos\theta|^2 \, B(\sqrt{T} \, \| w \| \, , |\cos\theta|) \cdot \\
&\qquad \cdot e^{-\| w_1 + w/2 \|^2} \, e^{-\frac{\| w \|^2}{4}} \, |\sin\theta|^{d-2} \, d\theta \, dw_1 \, dw \\
&= \frac{|S^{d-2}|}{(2\pi)^d} \int_{\mathbb{R}^d} \int_{\mathbb{R}^d} \int_0^{\pi/2} \| w \|^2 \, |\cos\theta|^2 \, B(\sqrt{T} \, \| w \| \, , |\cos\theta|) \cdot \\
&\qquad \cdot e^{-\| v \|^2} \, e^{-\frac{\| w \|^2}{4}} \, |\sin\theta|^{d-2} \, d\theta \, dv \, dw
\end{aligned}$$

hence

$$\begin{aligned}
\overline{\mathcal{C}}(1,1) &= \frac{|S^{d-2}|}{\sqrt{4\pi}^d} \int_{\mathbb{R}^d} \int_0^{\pi/2} \| w \|^2 \, |\cos\theta|^2 \, B(\sqrt{T} \, \| w \| \, , |\cos\theta|) \cdot \\
&\qquad \cdot e^{-\frac{\| w \|^2}{4}} \, |\sin\theta|^{d-2} \, d\theta \, dw \\
&= \frac{|S^{d-2}| \, |S^{d-1}|}{\sqrt{4\pi}^d} \int_0^{\infty} \int_0^{\pi/2} |\cos\theta|^2 \, B(\sqrt{T} \, r, |\cos\theta|) \cdot \\
&\qquad \cdot r^{d+1} \, e^{-\frac{r^2}{4}} \, |\sin\theta|^{d-2} \, d\theta \, dr
\end{aligned}$$

as was claimed, because $|S^{d-1}| = \frac{2\sqrt{\pi}^d}{\Gamma(d/2)}$. □

5.8 Hydrodynamic Limits II – Proof of Theorem 5.6.6

By introducing the slow time $\tau = \epsilon \, t$ one can study the limiting behavior of a singularly perturbed system in terms of a scaling limit. The main result of this procedure is Proposition 5.4.1. Applying this result to the Boltzmann equation in its singular perturbation form, Theorem 5.6.1, we immediately obtain the dissipative compressible Euler equations as stated in Theorem 5.6.2.

This scaling limit does produce the convective, but not the dissipative transport. This is due to the use of the hyperbolic scaling. Because of the lack of the dissipative terms, solutions to the Euler equations develop shocks. And as long as the solutions remain smooth, the Euler equations are reversible and have no entropy production term in them. This is in contrast to the Boltzmann equation and the Navier-Stokes equations, which are irreversible and do increase entropy. This shortcoming of the Euler equations is due to the fact that they are obtained through a scaling limit. Therefore, we seek for a method to derive hydrodynamic limits without using a scaling limit.

Note that as long as the invariant manifold $\mathcal{M}_\epsilon$ of Theorem 5.6.4 is normally hyperbolic, all solutions to the Boltzmann equation are shadowed by some solution on $\mathcal{M}_\epsilon$. Thus it suffices to study the Boltzmann equation on $\mathcal{M}_\epsilon$, and derive asymptotic expansions only for such solutions. The asymptotic expansion to first order in ϵ is precisely the content of equation (21). And since its derivation only assumes normal hyperbolicity and regularity of $\mathcal{M}_\epsilon$, we can apply this asymptotic expansion to the Boltzmann equation in its singular perturbation form to prove Theorem 5.6.6.

The actual proof will be presented as a corollary of a slightly more general result. Namely, so far we did not assume any special symmetry of the particle interactions. Therefore, we will first derive the general form of the dissipative compressible Navier-Stokes equations in Theorem 5.8.1. Then we specialize the general case to that of rotationally symmetric interactions, which is the setting of Theorem 5.6.6.

Theorem 5.8.1 (Dissipative Compressible Navier-Stokes Equations)**.** *The solutions of the Boltzmann equation restricted to the invariant manifold $\mathcal{M}_\epsilon$ shadow all solutions of the Boltzmann equation, and have the dissipative compressible Navier-Stokes*

equations

$$
\begin{aligned}
0 &= (\partial_t + \epsilon\, u \cdot \nabla_\xi) n + \epsilon\, n\, \operatorname{div}_\xi u \\
0 &= n\,(\partial_t + \epsilon\, u \cdot \nabla_\xi) u_i + \epsilon \sum_{j=1}^{d} \partial_{\xi_j} \widehat{\Pi}_{ji} \\
-\alpha\, \widehat{\mathcal{S}} &= n\, \frac{d}{2}\,(\partial_t + \epsilon\, u \cdot \nabla_\xi) T + \epsilon\, \operatorname{div}_\xi \widehat{q} + \epsilon \sum_{i,j=1}^{d} \widehat{\Pi}_{ij}\, \partial_{\xi_j} u_i
\end{aligned}
$$

with

$$
\begin{aligned}
\frac{\widehat{\Pi}_{kl}}{n\,T} - \delta_{kl} &= \epsilon \sum_{i=1}^{d} \frac{\partial_{\xi_i}\sqrt{T}}{n} \left\langle\, \mathcal{L}_\perp^{-1}\phi_i, \phi_{kl} \,\right\rangle_{\mathscr{H}^\perp} + \epsilon \sum_{i,j=1}^{d} \frac{\partial_{\xi_j} u_i}{n} \left\langle\, \mathcal{L}_\perp^{-1}\phi_{ij}, \phi_{kl} \,\right\rangle_{\mathscr{H}^\perp} \\
&\quad - \epsilon\, \partial_\epsilon\big|_{\epsilon=0} \left\langle\, \mathscr{P}\mathcal{Q}(1,1), \mathcal{L}_\perp^{-1}\phi_{kl} \,\right\rangle_{\mathscr{H}^\perp} \\
\frac{2\,\widehat{q}_k}{n\,\sqrt{T}^3} &= \epsilon \sum_{i=1}^{d} \frac{\partial_{\xi_i}\sqrt{T}}{n} \left\langle\, \mathcal{L}_\perp^{-1}\phi_i, \phi_k \,\right\rangle_{\mathscr{H}^\perp} + \epsilon \sum_{i,j=1}^{d} \frac{\partial_{\xi_j} u_i}{n} \left\langle\, \mathcal{L}_\perp^{-1}\phi_{ij}, \phi_k \,\right\rangle_{\mathscr{H}^\perp} \\
&\quad - \epsilon\, \partial_\epsilon\big|_{\epsilon=0} \left\langle\, \mathscr{P}\mathcal{Q}(1,1), \mathcal{L}_\perp^{-1}\phi_k \,\right\rangle_{\mathscr{H}^\perp} \\
\widehat{\mathcal{S}} &= \frac{1}{2}\, n^2\, T\, \overline{\mathcal{C}}(1+h, 1+h) \\
h &= -\epsilon\, \partial_\epsilon\big|_{\epsilon=0} \mathcal{L}_\perp^{-1} \mathscr{P}\mathcal{Q}(1,1) + \epsilon \sum_{i=1}^{d} \frac{\partial_{\xi_i}\sqrt{T}}{n}\, \mathcal{L}_\perp^{-1}\phi_i + \epsilon \sum_{i,j=1}^{d} \frac{\partial_{\xi_j} u_i}{n}\, \mathcal{L}_\perp^{-1}\phi_{ij}
\end{aligned}
$$

as their first order asymptotic expansion.

Proof. The general form of the first order asymptotic expansion of a singularly perturbed system is (21).

Recall that by equation (23c) of Theorem 5.6.1 we have that

$$
\begin{aligned}
\widehat{G}(n, u, T, h, 0) &= n\, \mathscr{P}\mathcal{Q}_0(1+h, 1+h) \\
\widehat{G}(n, u, T, 0, \epsilon) &= n\, \mathscr{P}\mathcal{Q}(1,1) - \epsilon \sum_{i=1}^{d} \phi_i\, \partial_{\xi_i}\sqrt{T} - \epsilon \sum_{i,j=1}^{d} \phi_{ij}\, \partial_{\xi_j} u_i
\end{aligned}
$$

and that

$$
\mathcal{Y}_0(n, u, T) = 0
$$

is the parametrization of the invariant manifold $\mathcal{M}_\epsilon$ for $\epsilon = 0$. Therefore the first order asymptotic expansion of h becomes

$$h = -\epsilon\, \partial_h\big|_{h=0} \widehat{G}(n,u,T,h,0)^{-1} \partial_\epsilon\big|_{\epsilon=0} \widehat{G}(n,u,T,0,\epsilon) + \mathcal{O}(\epsilon^2)$$

by using (21).

Notice that

$$\begin{aligned}
\partial_h\big|_{h=0} \widehat{G}(n,u,T,h,0) &= n\, \mathscr{P} \partial_h\big|_{h=0} \mathcal{Q}_0(1+h,1+h) \equiv n\, \mathcal{L}_\perp \\
\partial_\epsilon\big|_{\epsilon=0} \widehat{G}(n,u,T,0,\epsilon) &= n\, \partial_\epsilon\big|_{\epsilon=0} \mathscr{P}\mathcal{Q}(1,1) - \sum_{i=1}^d \phi_i\, \partial_{\xi_i} \sqrt{T} - \sum_{i,j=1}^d \phi_{ij}\, \partial_{\xi_j} u_i
\end{aligned}$$

hold. Hence

$$\begin{aligned}
h &= -\epsilon\, \frac{1}{n}\, \mathcal{L}_\perp^{-1} \Big[n\, \partial_\epsilon\big|_{\epsilon=0} \mathscr{P}\mathcal{Q}(1,1) - \sum_{i=1}^d \phi_i\, \partial_{\xi_i} \sqrt{T} - \sum_{i,j=1}^d \phi_{ij}\, \partial_{\xi_j} u_i \Big] + \mathcal{O}(\epsilon^2) \\
&= -\epsilon\, \partial_\epsilon\big|_{\epsilon=0} \mathcal{L}_\perp^{-1} \mathscr{P}\mathcal{Q}(1,1) + \epsilon \sum_{i=1}^d \frac{\partial_{\xi_i} \sqrt{T}}{n}\, \mathcal{L}_\perp^{-1} \phi_i + \epsilon \sum_{i,j=1}^d \frac{\partial_{\xi_j} u_i}{n}\, \mathcal{L}_\perp^{-1} \phi_{ij} + \mathcal{O}(\epsilon^2)
\end{aligned}$$

for the first order asymptotic expansion of h, i.e. the first order asymptotic expansion of the invariant manifold $\mathcal{M}_\epsilon$.

The equations for the slow variables n, u, T depend on h only through the hydrodynamic quantities $\widehat{\Pi}_{ij}$, $\widehat{q}_i$, $\widehat{\mathcal{S}}$. By Lemma 5.7.6 these depend on h only through certain projections, which we compute next. Substituting the above derived expression for h yields

$$\begin{aligned}
\big\langle\, \phi_{kl}, h \,\big\rangle_{\mathscr{H}^\perp} &= \epsilon \sum_{i=1}^d \frac{\partial_{\xi_i} \sqrt{T}}{n} \big\langle\, \mathcal{L}_\perp^{-1} \phi_i, \phi_{kl} \,\big\rangle_{\mathscr{H}^\perp} + \epsilon \sum_{i,j=1}^d \frac{\partial_{\xi_j} u_i}{n} \big\langle\, \mathcal{L}_\perp^{-1} \phi_{ij}, \phi_{kl} \,\big\rangle_{\mathscr{H}^\perp} \\
&\quad - \epsilon\, \partial_\epsilon\big|_{\epsilon=0} \big\langle\, \mathcal{L}_\perp^{-1} \mathscr{P}\mathcal{Q}(1,1), \phi_{kl} \,\big\rangle_{\mathscr{H}^\perp} \\
\big\langle\, \phi_{k}, h \,\big\rangle_{\mathscr{H}^\perp} &= \epsilon \sum_{i=1}^d \frac{\partial_{\xi_i} \sqrt{T}}{n} \big\langle\, \mathcal{L}_\perp^{-1} \phi_i, \phi_{k} \,\big\rangle_{\mathscr{H}^\perp} + \epsilon \sum_{i,j=1}^d \frac{\partial_{\xi_j} u_i}{n} \big\langle\, \mathcal{L}_\perp^{-1} \phi_{ij}, \phi_{k} \,\big\rangle_{\mathscr{H}^\perp} \\
&\quad - \epsilon\, \partial_\epsilon\big|_{\epsilon=0} \big\langle\, \mathcal{L}_\perp^{-1} \mathscr{P}\mathcal{Q}(1,1), \phi_{k} \,\big\rangle_{\mathscr{H}^\perp}
\end{aligned}$$

where we dropped the $\mathcal{O}(\epsilon^2)$ terms.

Furthermore, the linearized collision operator $\mathcal{L}_\perp$ is self-adjoint, e.g. [23], hence

$$\left\langle \mathcal{L}_\perp^{-1}\mathscr{P}\mathcal{Q}(1,1), \phi_{kl} \right\rangle_{\mathscr{H}^\perp} = \left\langle \mathscr{P}\mathcal{Q}(1,1), \mathcal{L}_\perp^{-1}\phi_{kl} \right\rangle_{\mathscr{H}^\perp}$$
$$\left\langle \mathcal{L}_\perp^{-1}\mathscr{P}\mathcal{Q}(1,1), \phi_{k} \right\rangle_{\mathscr{H}^\perp} = \left\langle \mathscr{P}\mathcal{Q}(1,1), \mathcal{L}_\perp^{-1}\phi_{k} \right\rangle_{\mathscr{H}^\perp}$$

follow. □

Because we consider only weak (proportional to ϵ) dissipations the quantities determining the Navier-Stokes equations in Theorem 5.8.1 are largely the same as in the non-dissipative case. In particular, we only need to know the usual terms $\mathcal{L}_\perp^{-1}\phi_k$ and $\mathcal{L}_\perp^{-1}\phi_{kl}$ from the non-dissipative theory to compute all hydrodynamic terms (including the expression for h), which has significant computational advantages, as known results from the non-dissipative theory can simply be reused to compute the dissipative corrections.

In applications, a large class of non-dissipative interactions are rotational invariant. The prime examples are interaction potentials, which depend only on the distance, and contact interactions as for hard spheres. This symmetry allows to simplify the expressions for the hydrodynamic quantities in the general Navier-Stokes equation, Theorem 5.8.1, to the ones given in Theorem 5.6.6.

The key observation is that for rotationally invariant interactions the linear collision operator preserves this symmetry. A more specific form of this property is given by the following Corollary 5.8.3 which will be the key ingredient to simplifying the Navier-Stokes equations of Theorem 5.8.1. Before we state Corollary 5.8.3 we prove a more general result, which is the next Proposition 5.8.2. This result implies Corollary 5.8.3, and the proof we will give is a generalized version of the results of [30].

Proposition 5.8.2 (Algebraic Identities)**.** *Let $a(\psi)$ be a linear functional and let $b(\psi_1, \psi_2)$ be a bilinear form, which satisfy $a(\psi \circ R) = a(\psi)$ and $b(\psi_1 \circ R, \psi_2 \circ R) =$*

$b(\phi_1, \psi_2)$ *for all* $R \in O(d)$. *Then*

$$\begin{aligned} a(\phi_i) &= 0 \,, \qquad a(\phi_{ij}) = 0 \,, \\ b(\phi_i, \phi_j) &= \delta_{ij}\, b(\phi_1, \phi_1) \,, \qquad b(\phi_i, \phi_{kl}) = 0 \,, \qquad b(\phi_{kl}, \phi_i) = 0 \,, \\ b(\phi_{ij}, \phi_{kl}) &= \big[\delta_{ik}\,\delta_{jl} + \delta_{il}\,\delta_{jk} - \frac{2}{d}\,\delta_{ij}\,\delta_{kl}\big]\,\frac{1}{2}\,\frac{d}{d-1}\,b(\phi_{11}, \phi_{11}) \end{aligned}$$

hold.

Proof. From the defintion of ϕ_i the equation

$$\phi_i \circ R = \sum_{k=1}^{d} R_{ik}\,\phi_k$$

follows. Hence

$$a(\phi_i) = a(\phi_i \circ R) = \sum_{k=1}^{d} R_{ik}\, a(\phi_k)$$

holds for all $R \in O(d)$, which can only be true if $a(\phi_i) = 0$ for all i.

Notice that

$$\phi_{ij} \circ R = \sum_{m,n=1}^{d} R_{im}\,\phi_{mn}\,R_{jn}$$

and therefore

$$a(\phi_{ij}) = a(\phi_{ij} \circ R) = \sum_{m,n=1}^{d} R_{im}\,R_{jn}\,a(\phi_{mn})$$

holds for all $R \in O(d)$. But this is only possible if the matrix with entries $a(\phi_{ij})$ is a multiple of the identity matrix, i.e. $a(\phi_{ij}) = \delta_{ij}\,a(\phi_{11})$. On the other hand we have that $\sum_{i=1}^{d} \phi_{ii} = 0$, hence $a(\phi_{ij}) = 0$ follows for all i and j.

Set $M_{ij}{:=}b(\phi_i, \phi_j)$, and let $R \in O(d)$ be arbitrary. The assumption on the bilinear form b yields

$$M_{ij} = b(\phi_i \circ R, \phi_j \circ R) = \sum_{k,l=1}^{d} R_{ik}\, b(\phi_k, \phi_l)\, R_{jl} \qquad \text{i.e.} \qquad M = R\,M\,R^T \,.$$

But this can only hold true for all $R \in O(d)$ if M is a multiple of the identity matrix. Thus $b(\phi_i, \phi_j) = \delta_{ij}\, b(\phi_1, \phi_1)$ must hold, which is the first of the claimed equations.

Set N_{ijk}:=$b(\phi_{ij}, \phi_k)$, then

$$N_{ijk} = b(\phi_{ij} \circ R, \phi_k \circ R) = \sum_{l,m,n=1}^{d} R_{im}\, R_{jn}\, R_{kl}\, N_{mnl}$$

holds for all $R \in O(d)$. By replacing R by $-R$ we see that $N_{ijk} = -N_{ijk}$ and hence $N_{ijk} = 0$ follows. This proves the first part of the second claimed equation. The other part, i.e. $b(\phi_k, \phi_{ij}) = 0$ follows from the same reasoning.

It remains to show the third equation. Let $L_{ijkl} = b(\phi_{ij}, \phi_{kl})$. As soon as one index in L_{ijkl} appears with multiplicity one, the orthogonal matrix R which flips the sign of that entry of w flips the overall sign of L_{ijkl}. Hence $L_{ijkl} = 0$ follows. Therefore, all indices must appear in pairs. And since there are only for indices in total there are only three possible ways of pairing up the indices, so that

$$L_{ijkl} = \delta_{ij}\, \delta_{kl}\, L_{iikk} + \delta_{ik}\, \delta_{jl}\, L_{ilil} + \delta_{il}\, \delta_{jk}\, L_{ikki} - 2\, \delta_{ij}\, \delta_{jk}\, \delta_{kl}\, L_{iiii}$$

must hold.

Consider the first term L_{iikk}. If $i \neq k$ the identity $\sum_{i=1}^{d} \phi_{ii} = 0$ implies

$$i \neq k \implies L_{iikk} = L_{11kk} = \frac{1}{d-1} \sum_{k=2}^{d} L_{11kk} = -\frac{1}{d-1}\, L_{1111}\ .$$

Furthermore, if $i \neq k$ we also have that $L_{ikki} = L_{1212} = L_{ikik}$, so that

$$L_{ijkl} = (1 - \delta_{ij})\, [\delta_{ik}\, \delta_{jl} + \delta_{il}\, \delta_{jk}]\, L_{1212} + \left[d\, \delta_{jk} - 1\right] \delta_{ij}\, \delta_{kl}\, \frac{L_{1111}}{d-1}$$

follows.

The symmetry property of ϕ_{ij} yields

$$L_{ijkl} = b(\phi_{ij} \circ R, \phi_{kl} \circ R) = \sum_{o,p,q,r=1}^{d} R_{io}\, R_{jp}\, R_{kq}\, R_{lr}\, L_{opqr}$$

for L. In particular

$$\begin{aligned}
L_{1212} &= \sum_{o,p,q,r=1}^{d} R_{1o}\, R_{2p}\, R_{1r}\, R_{2q}\, L_{opqr} \\
&= \sum_{o,p,q,r=1}^{d} R_{1o}\, R_{2p}\, R_{1r}\, R_{2q}\, (1-\delta_{op})\, [\delta_{oq}\, \delta_{pr} + \delta_{or}\, \delta_{pq}]\, L_{1212} \\
&\quad + \sum_{o,p,q,r=1}^{d} R_{1o}\, R_{2p}\, R_{1r}\, R_{2q}\, \big[d\, \delta_{pq} - 1\big]\, \delta_{op}\, \delta_{qr}\, \frac{L_{1111}}{d-1} \\
&= L_{1212} \sum_{p,q=1}^{d} R_{1q}\, R_{2p}\, R_{1p}\, R_{2q} + L_{1212} \sum_{p,q=1}^{d} R_{1q}^2\, R_{2p}^2 - 2\, L_{1212} \sum_{p=1}^{d} R_{1p}^2\, R_{2p}^2 \\
&\quad + \frac{d\, L_{1111}}{d-1} \sum_{p=1}^{d} R_{1p}^2\, R_{2p}^2 - \frac{L_{1111}}{d-1} \sum_{p,q=1}^{d} R_{1p}\, R_{2p}\, R_{1q}\, R_{2q}
\end{aligned}$$

for L_{1212}. Since R is an orthogonal matrix we have that

$$\sum_{p,q=1}^{d} R_{1q}\, R_{2p}\, R_{1p}\, R_{2q} = 0 \qquad \text{and} \qquad \sum_{p,q=1}^{d} R_{1q}^2\, R_{2p}^2 = 1$$

hence

$$L_{1212} = L_{1212} - 2\, L_{1212} \sum_{p=1}^{d} R_{1p}^2\, R_{2p}^2 + \frac{d\, L_{1111}}{d-1} \sum_{p=1}^{d} R_{1p}^2\, R_{2p}^2$$

must hold for any $R \in O(d)$. This is true if and only if

$$L_{1212} = \frac{1}{2}\, \frac{d}{d-1}\, L_{1111}$$

which completes the proof of the third equation after some elementary simplifications.

□

Corollary 5.8.3. *For rotationally invariant interactions (in the non-dissipative setting) the identities*

$$\begin{aligned}
\big\langle\, \mathcal{L}_\perp^{-1}\phi_i, \phi_k \,\big\rangle &= \delta_{ik} \big\langle\, \mathcal{L}_\perp^{-1}\phi_1, \phi_1 \,\big\rangle\,, & \big\langle\, \mathcal{L}_\perp^{-1}\phi_i, \phi_{kl} \,\big\rangle &= 0 \\
\big\langle\, \mathcal{L}_\perp^{-1}\phi_{ij}, \phi_{kl} \,\big\rangle &= \big[\delta_{ik}\, \delta_{jl} + \delta_{il}\, \delta_{jk} - \frac{2}{d}\, \delta_{ij}\, \delta_{kl}\big]\, \frac{1}{2}\, \frac{d}{d-1} \big\langle\, \mathcal{L}_\perp^{-1}\phi_{11}, \phi_{11} \,\big\rangle \\
\big\langle\, \mathcal{Q}(1,1), \mathcal{L}_\perp^{-1}\phi_i \,\big\rangle &= 0\,, & \big\langle\, \mathcal{Q}(1,1), \mathcal{L}_\perp^{-1}\phi_{ij} \,\big\rangle &= 0
\end{aligned}$$

hold.

Proof. The rotational invariance of the kernel of the collision operator implies

$$(\mathcal{L}_\perp^{-1}\psi)\circ R = \mathcal{L}_\perp^{-1}(\psi\circ R) \quad \text{and} \quad \mathcal{Q}(1,1)\circ R = \mathcal{Q}(1,1) \quad \text{for all} \quad R\in O(d)$$

for any function ψ. Thus the claims follow directly from Proposition 5.8.2. □

Corollary 5.8.4. *Let*

$$g = g_* + \sum_{i=1}^d \alpha_i\, \mathcal{L}_\perp^{-1}\phi_i + \sum_{i,j=1}^d \beta_{ij}\, \mathcal{L}_\perp^{-1}\phi_{ij}$$

for some constants α_i and β_{ij} and some rotationally invariant function g_*. For rotationally invariant interactions (in the non-dissipative setting) the equation

$$\begin{aligned}\overline{\mathcal{C}}(g,g) = \overline{\mathcal{C}}(g_*,g_*) + \overline{\mathcal{C}}(\mathcal{L}_\perp^{-1}\phi_1,\mathcal{L}_\perp^{-1}\phi_1)\sum_{i=1}^d \alpha_i^2 \\ + \frac{1}{2}\,\frac{d}{d-1}\,\overline{\mathcal{C}}(\mathcal{L}_\perp^{-1}\phi_{11},\mathcal{L}_\perp^{-1}\phi_{11})\sum_{k,n=1}^d \Big[\beta_{kn}\,\beta_{kn} + \beta_{kn}\,\beta_{nk} - \frac{2}{d}\,\beta_{kk}\,\beta_{nn}\Big]\end{aligned}$$

holds.

Proof. The bilinearity of $\overline{\mathcal{C}}$ yields

$$\begin{aligned}\overline{\mathcal{C}}(g,g) = \overline{\mathcal{C}}(g_*,g_*) + \sum_{i=1}^d \alpha_i\,\overline{\mathcal{C}}(\mathcal{L}_\perp^{-1}\phi_i,g_*) + \sum_{k,l=1}^d \beta_{kl}\,\overline{\mathcal{C}}(\mathcal{L}_\perp^{-1}\phi_{kl},g_*) \\ + \sum_{n,r=1}^d \beta_{nr}\,\overline{\mathcal{C}}(g_*,\mathcal{L}_\perp^{-1}\phi_{nr}) + \sum_{i,n,r=1}^d \alpha_i\,\beta_{nr}\,\overline{\mathcal{C}}(\mathcal{L}_\perp^{-1}\phi_i,\mathcal{L}_\perp^{-1}\phi_{nr}) \\ + \sum_{k,l,n,r=1}^d \beta_{kl}\,\beta_{nr}\,\overline{\mathcal{C}}(\mathcal{L}_\perp^{-1}\phi_{kl},\mathcal{L}_\perp^{-1}\phi_{nr}) + \sum_{m=1}^d \alpha_m\,\overline{\mathcal{C}}(g_*,\mathcal{L}_\perp^{-1}\phi_m) \\ + \sum_{i,m=1}^d \alpha_i\,\alpha_m\,\overline{\mathcal{C}}(\mathcal{L}_\perp^{-1}\phi_i,\mathcal{L}_\perp^{-1}\phi_m) + \sum_{k,l,m=1}^d \alpha_m\,\beta_{kl}\,\overline{\mathcal{C}}(\mathcal{L}_\perp^{-1}\phi_{kl},\mathcal{L}_\perp^{-1}\phi_m)\end{aligned}$$

Applying now Proposition 5.8.2 shows that

$$\overline{\mathcal{C}}(g_*,\mathcal{L}_\perp^{-1}\phi_m) = 0\,, \qquad \overline{\mathcal{C}}(g_*,\mathcal{L}_\perp^{-1}\phi_{nr}) = 0\,, \qquad \overline{\mathcal{C}}(\mathcal{L}_\perp^{-1}\phi_{kl},\mathcal{L}_\perp^{-1}\phi_m) = 0$$

$$\overline{\mathcal{C}}(\mathcal{L}_\perp^{-1}\phi_i,\mathcal{L}_\perp^{-1}\phi_m) = \delta_{im}\,\overline{\mathcal{C}}(\mathcal{L}_\perp^{-1}\phi_1,\mathcal{L}_\perp^{-1}\phi_1)$$

$$\overline{\mathcal{C}}(\mathcal{L}_\perp^{-1}\phi_{kl},\mathcal{L}_\perp^{-1}\phi_{nr}) = \big[\delta_{kn}\,\delta_{lr} + \delta_{kr}\,\delta_{ln} - \frac{2}{d}\,\delta_{kl}\,\delta_{nr}\big]\,\frac{1}{2}\,\frac{d}{d-1}\,\overline{\mathcal{C}}(\mathcal{L}_\perp^{-1}\phi_{11},\mathcal{L}_\perp^{-1}\phi_{11})$$

which yields

$$\overline{\mathcal{C}}(g,g) = \overline{\mathcal{C}}(g_*,g_*) + \sum_{i,m=1}^{d} \alpha_i\,\alpha_m\,\overline{\mathcal{C}}(\mathcal{L}_\perp^{-1}\phi_i, \mathcal{L}_\perp^{-1}\phi_m) + \sum_{k,l,n,r=1}^{d} \beta_{kl}\,\beta_{nr}\,\overline{\mathcal{C}}(\mathcal{L}_\perp^{-1}\phi_{kl}, \mathcal{L}_\perp^{-1}\phi_{nr})$$

and thus the claim after simplifying the sums. □

Now that we know how the symmetry affects the various geometric (in $\mathscr{H}$) expressions, which enter the hydrodynamic quantities we can prove Theorem 5.6.6.

Proof of Theorem 5.6.6. The symmetry properties derived in Corollary 5.8.3 simplify the the general results for the hydrodynamic variables of Theorem 5.8.1 to

$$\begin{aligned}
\frac{\widehat{\Pi}_{kl}}{n\,T} - \delta_{kl} &= \epsilon\left[\partial_{\xi_l} u_k + \partial_{\xi_k} u_l - \delta_{kl}\,\frac{2}{d}\,\mathrm{div}_\xi\, u\right]\frac{1}{2\,n}\,\frac{d}{d-1}\big\langle\, \mathcal{L}_\perp^{-1}\phi_{11}, \phi_{11}\,\big\rangle_{\mathscr{H}^\perp} \\
\frac{2\,\widehat{q}_k}{n\,\sqrt{T}^3} &= \epsilon\,\frac{\partial_{\xi_k}\sqrt{T}}{n}\,\big\langle\, \mathcal{L}_\perp^{-1}\phi_1, \phi_1\,\big\rangle_{\mathscr{H}^\perp} \\
\widehat{\mathcal{S}} &= \frac{1}{2}\,n^2\,T\,\overline{\mathcal{C}}(1+h, 1+h) \\
h &= -\epsilon\,\partial_\epsilon\big|_{\epsilon=0}\mathcal{L}_\perp^{-1}\mathscr{P}\mathcal{Q}(1,1) + \epsilon\sum_{i=1}^{d}\frac{\partial_{\xi_i}\sqrt{T}}{n}\,\mathcal{L}_\perp^{-1}\phi_i + \epsilon\sum_{i,j=1}^{d}\frac{\partial_{\xi_j} u_i}{n}\,\mathcal{L}_\perp^{-1}\phi_{ij}\ .
\end{aligned}$$

Comparing the form of $g \equiv 1+h$ with the one of Corollary 5.8.4 yields

$$g_* = 1 - \epsilon\,\partial_\epsilon\big|_{\epsilon=0}\mathcal{L}_\perp^{-1}\mathscr{P}\mathcal{Q}(1,1)\ , \quad \alpha_i = \epsilon\,\frac{\partial_{\xi_i}\sqrt{T}}{n}\ , \quad \beta_{ij} = \epsilon\,\frac{\partial_{\xi_j} u_i}{n}$$

and therefore

$$\begin{aligned}
\overline{\mathcal{C}}(1+h,1+h) = \overline{\mathcal{C}}&(1 - \epsilon\,\partial_\epsilon\big|_{\epsilon=0}\mathcal{L}_\perp^{-1}\mathscr{P}\mathcal{Q}(1,1), 1 - \epsilon\,\partial_\epsilon\big|_{\epsilon=0}\mathcal{L}_\perp^{-1}\mathscr{P}\mathcal{Q}(1,1)) \\
&+ \overline{\mathcal{C}}(\mathcal{L}_\perp^{-1}\phi_1, \mathcal{L}_\perp^{-1}\phi_1)\ \Big\|\ \frac{\epsilon}{n}\,\nabla_\xi\sqrt{T}\ \Big\|^2 \\
&+ \frac{1}{2}\,\frac{d}{d-1}\,\overline{\mathcal{C}}(\mathcal{L}_\perp^{-1}\phi_{11}, \mathcal{L}_\perp^{-1}\phi_{11})\sum_{k,n=1}^{d}\frac{\epsilon^2}{n^2}\,\big[\partial_{\xi_n} u_k\,\partial_{\xi_n} u_k + \partial_{\xi_n} u_k\,\partial_{\xi_k} u_n \\
&\qquad - \frac{2}{d}\,\partial_{\xi_k} u_k\,\partial_{\xi_n} u_n\big]
\end{aligned}$$

as a consequence of Corollary 5.8.4. This completes the proof. □

5.9 The Dissipative Hard Sphere Gas

In this section we consider the dissipative hard sphere gas. As was explained in Section 5.2, this model is the key motivation behind the kinetic model.

In addition of being a motivating example, the hard sphere gas is among the most popular models for molecular dynamics simulations. Because hard spheres interact only upon collisions, there is no need to numerically integrate a large systems of differential equations describing the dynamics of all the particles. Rather one computes the next time of a collision, and then repeatedly proceeds from one collision to the next. The spherical shape of the particles is computationally advantageous over other shapes in determining the point of collision.

Such simulations were carried out to understand experiments on fluidized granular media, e.g. [57, 58, 5, 6, 64]. In particular the aspect of pattern formation and their stability played a central theme in these works.

And since molecular dynamics simulations can handle systems with about a million particles, one can compare the kinetic model with physical experiments and direct simulations. In [61] such a comparison was carried out. It was shown that there is a good agreement between the kinetic model and molecular dynamics in a vertically oscillated thin layer of dissipative hard spheres.

Because our approach to derive a hydrodynamic description of the dissipative hard sphere gas differs from the standard methods, we compared our predictions against direct simulations.

Let δ denote the diameter of the hard spheres. As is shown in [24, 45], if density fluctuations over distances of the order of δ are neglected, the kernel B of the collision operator $Q(f, f)$ reads

$$B = B(\| v_2 - v_1 \|, |\cos\theta|) = \frac{\delta^{d-1}}{2} |(v_2 - v_1) \cdot \omega| \equiv \frac{\delta^{d-1}}{2} \| v_2 - v_1 \| \, |\cos\theta| \qquad (27)$$

for $\omega \in S^{d-1}$.

Lemma 5.9.1. *For the hard sphere gas*

$$\overline{\mathcal{C}}(1,1) = \delta^{d-1}\sqrt{T}\,\frac{4\sqrt{\pi}^{d-1}}{\Gamma\left(\frac{d}{2}\right)}$$

holds.

Proof. The general result of Proposition 5.7.7 combined with the actual form of the collision kernel B for hard spheres (27) yields

$$\begin{aligned}
\overline{\mathcal{C}}(1,1) &= \frac{16\sqrt{\pi}^{d-1}}{\Gamma\left(\frac{d}{2}\right)\Gamma\left(\frac{d-1}{2}\right)}\int_0^\infty\int_0^1 \frac{\delta^{d-1}}{2}\,2\sqrt{T}\,x\,z\,x^{d+1}\,e^{-x^2}\,z^2\,\sqrt{1-z^2}^{d-3}\,dz\,dx \\
&= \delta^{d-1}\sqrt{T}\,\frac{16\sqrt{\pi}^{d-1}}{\Gamma\left(\frac{d}{2}\right)\Gamma\left(\frac{d-1}{2}\right)}\int_0^\infty x^{d+2}\,e^{-x^2}\,dx\int_0^1 z^3\,\sqrt{1-z^2}^{d-3}\,dz \\
&= \delta^{d-1}\sqrt{T}\,\frac{8\sqrt{\pi}^{d-1}\,\Gamma\left(\frac{d+3}{2}\right)}{\Gamma\left(\frac{d}{2}\right)\Gamma\left(\frac{d-1}{2}\right)}\int_0^1 z^3\,\sqrt{1-z^2}^{d-3}\,dz \\
&= \delta^{d-1}\sqrt{T}\,(d^2-1)\,\frac{2\sqrt{\pi}^{d-1}}{\Gamma\left(\frac{d}{2}\right)}\int_0^1 z^3\,\sqrt{1-z^2}^{d-3}\,dz\,.
\end{aligned}$$

Using

$$\begin{aligned}
\int_0^1 z^3\,\sqrt{1-z^2}^{d-3}\,dz &= \frac{1}{2}\int_0^1 t\,\sqrt{1-t}^{d-3}\,dt = \frac{1}{2}\int_0^1 (1-t)\,\sqrt{t}^{d-3}\,dt \\
&= \frac{1}{2}\int_0^1 \sqrt{t}^{d-3}\,dt - \frac{1}{2}\int_0^1 \sqrt{t}^{d-1}\,dt = \frac{2}{d^2-1}
\end{aligned}$$

we obtain the claim. □

With this result we immediately obtain the following prediction for the cooling, which is Haff's law as in Corollary 5.6.8.

Theorem 5.9.2 (Haff's Law for the Hard Sphere Gas)**.** *For a gas of hard spheres of diameter δ the homogeneous cooling state evolves asymptotically as*

$$\partial_t n = 0\,,\quad \partial_t u = 0\,,\quad \frac{1}{\sqrt{T(t)}} - \frac{1}{\sqrt{T(0)}} = \alpha\,\frac{2\sqrt{\pi}^{d-1}}{\Gamma\left(\frac{d}{2}\right)d}\,n\,\delta^{d-1}\,t$$

as $\epsilon \to 0$.

For comparison we carried out a direct numerical simulation of a spatially homogeneous hard sphere gas in dimension $d = 2$. The domain was chosen as a rectangular box of length and width of size 1, with all other lengths measured in the same units. We imposed periodic boundary conditions to reduce finite size effects. The diameter δ of the $N = 1000$ spheres was set 0.002. The parameter η was set to 0.2, which implies $\alpha = 0.18$ for the dissipation coefficient. For these numbers Theorem 5.9.2 predicts

$$\frac{1}{\sqrt{T(t)}} - \frac{1}{\sqrt{T(0)}} = \alpha \sqrt{\pi}\, n\, \delta\, t \approx 0.638083 \cdot t \tag{28}$$

for the temperature evolution.

Initially the spheres were placed uniformly at random, non-overlapping positions with velocity vectors drawn from a Maxwellian with $T = T(0) = 1$. If we denote the velocity of the i-th particle by $v^{(i)}$, then the velocity and temperature of the system was estimated by

$$u \approx \hat{u} = \frac{1}{N} \sum_{i=1}^{N} v^{(i)} \quad \text{and} \quad T \approx \hat{T} = \frac{1}{N-1} \sum_{i=1}^{N} \frac{1}{d} \parallel v^{(i)} - \hat{u} \parallel^2 ,$$

which are the usual estimators for the mean and variance, respectively.

The resulting graph of $1/\sqrt{T(t)}$ as a function of time, together with the theoretically obtained slope 0.638083 is shown in Fig. 23. As can be seen, there is an almost perfect agreement of the data and the prediction.

Of course, this only shows that the cooling rate of a homogeneous systems is obtained quite satisfactorily using our methods. The real difference between our and the standard methods is in the dependence of the cooling on spatial gradients, and how the transport coefficients are affected by the dissipation (compared to the non-dissipative case).

As pointed out in [61] such details a very difficult to measure using molecular dynamics simulations, and we have not investigated this in detail.

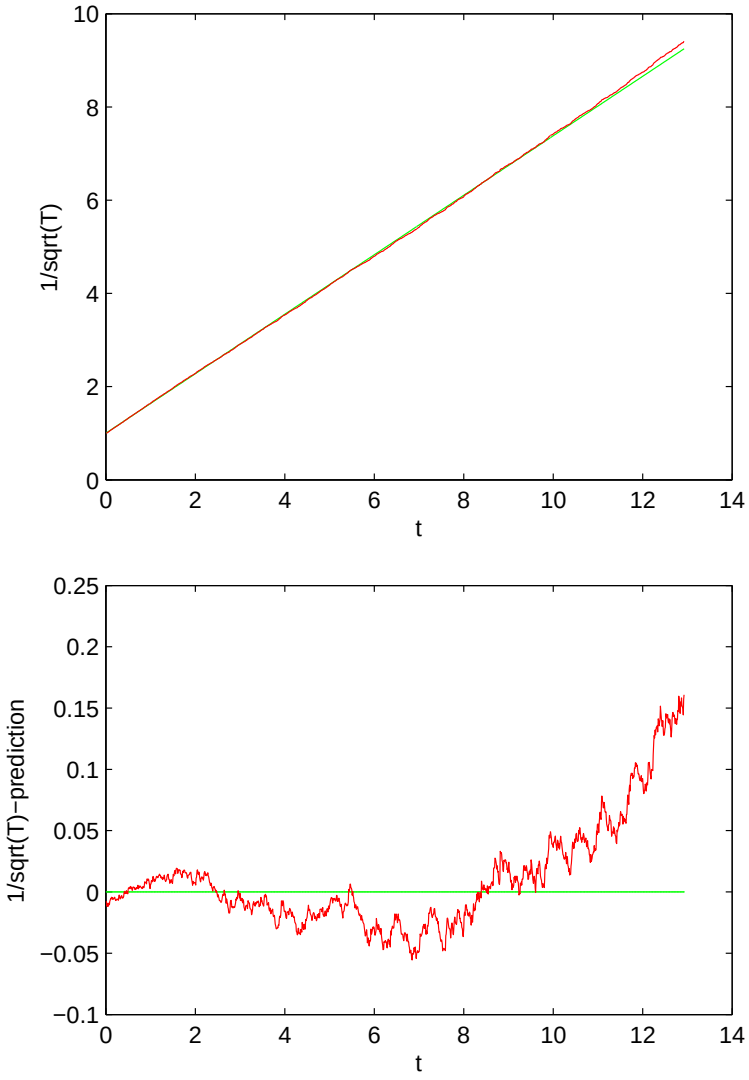

Figure 23: Numerical simulation of the cooling of a spatially homogeneous hard sphere gas of $N = 1000$ particles, compared to the theoretical prediction $1/\sqrt{T(t)} = 1 + 0.638083 \cdot t$. The upper plot shows the graph of the prediction (in green) for $1/\sqrt{T(t)}$ and the simulation data (in red). The lower plot shows the graph of the difference of the simulation data and the prediction.

5.10 Remarks on the Main Results and Comparison to Existing Results

Kinetic models of granular media differ from classical kinetic theory, because the interactions dissipate energy. The derivation of hydrodynamic equations from the kinetic model was done in [43] using Grad's moment method.

Since the appearance of [43] also the Chapman-Enskog method has been used to derive hydrodynamic equations for granular media. There is a large body of literature on the Chapman-Enskog method for the dissipative Boltzmann equations, e.g. [35] and references therein. However, due to the presence of two parameters (ϵ and α) the standard Chapman-Enskog method has to be modified in order to apply it to the dissipative setting. It is argued often, e.g. [35], that instead of a Maxwellian (as is done in the non-dissipative setting) a time-dependent cooling state should be used as the reference solution. About this reference state a formal power-series expansion is constructed, which follows the lines of the non-dissipative methods. But there are no explicit formulas available for the cooling state (unlike for the Maxwellian). Therefore, in order to get concrete expressions for the various hydrodynamic quantities (like transport coefficients and the cooling rate) the distribution function is expanded into Laguerre-polynomials.

Within this modified Chapman-Enskog framework the cooling rate does not contain terms involving gradients of the hydrodynamic fields at the Navier-Stokes level. It has been argued, e.g. [11, 39, 35], that this requires an expansion to an even higher (Burnett) order. For example, on page 9 of [39] it is stated that "In principle, the Navier-Stokes order hydrodynamics for inelastic collisions requires going one order further in the Chapman-Enskog expansion (Burnett order) to obtain the cooling rate to second order." However, even in standard kinetic theory not much is known about the Burnett equations; not even the boundary conditions, as is pointed out in [23] on pages 116 and 121.

Theorem 5.6.6 indicates that our expansion method does capture the gradient terms in the cooling rate already at the Navier-Stokes level. Furthermore, since we set up the series expansion about the usual Maxwellian, the cooling rate can be explicitly computed without an additional expansion. The resulting expression was

computed for a homogeneous hard sphere gas. The comparison with a direct numerical simulation in Section 5.9 demonstrated that at least in this case the prediction of our expansion methods matches very well the numerical data.

To the best of our knowledge, previous works on hydrodynamic limits of the (dissipative) Boltzmann equation do not make use of dynamical systems ideas the way that we propose. However, our approach has a lot in common the micro-macro decomposition of [55], which was used in [55, 54, 53] to study hydrodynamical limits of the non-dissipative Boltzmann equation. In particular, non-linear stability of global Maxwellians was shown. Without dissipation one can compute how the limiting global Maxwellian must look like just based on the initial data. But as soon as dissipation, or external forcing is allowed, this can no longer be done by considering the initial data only. And since our starting motivation was to model and study pattern formation in the (time-dependent) driven dissipative Boltzmann equation, we did not have a candidate for a possible limiting distribution. In order to study hydrodynamical limits we introduced special coordinates, and applied methods from dynamical systems theory as is done in geometric singular perturbation theory. These coordinates are quite similar to the representation of the distribution function in the micro-macro decomposition, but not the same.

The difference is quite important, because the separation of fast and slow variables in the micro-macro decomposition is not directly applicable to a dynamical systems setup. At least because the norms still depend on the macroscopic variables, and hence change in time. In our approach we first implement a complete separation of fast and slow variables. In particular, this allows for a construction of a state space and makes the dynamical systems framework appear in a natural way.

As we demonstrated, this setup allows one to use concepts of invariant manifold theory to study the hydrodynamic limit of the dissipative Boltzmann equation without ad hoc series expansions. In fact, we have explained that the invariant manifold

dictates the form of the perturbation expansion.

From the point of view of invariant manifold theory the difference of the dissipative and non-dissipative Boltzmann equation appears as follows. In Fig. 24 we illustrate

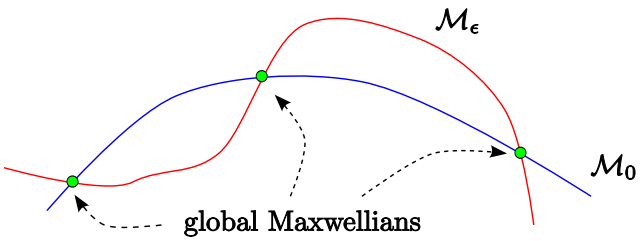

Figure 24: Illustration of the structure of the invariant manifolds $\mathcal{M}_0$ and $\mathcal{M}_\epsilon$ in the non-dissipative setting without fully separating fast and slow variables. In particular, the global Maxwellians are on $\mathcal{M}_\epsilon \cap \mathcal{M}_0$ and are equilibrium points for all ϵ.

how the invariant manifolds are organized in the non-dissipative Boltzmann equation without using specialized coordinates. Since the global Maxwellians are fixed points of the Boltzmann equation for all $\epsilon \geq 0$, one can use these common "landmarks" to study the limiting dynamics as $\epsilon \to 0$, without using a complete fast-slow separation, which is used in the micro-macro decomposition of [55].

In the dissipative Boltzmann equation (eventually with external forcing) these landmarks disappear, which is why we need to introduce a complete separation of fast and slow variables. The result is a straightened-out slow manifold $\mathcal{M}_0$, which is illustrated in Fig. 25. The persistence of this manifold for small enough values

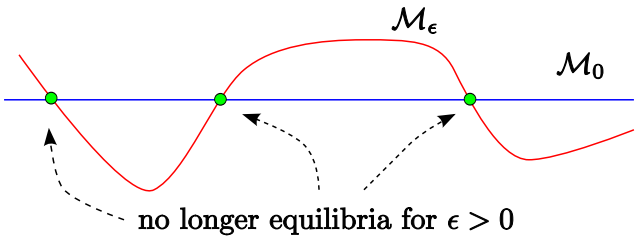

Figure 25: Illustration of the structure of the invariant manifolds $\mathcal{M}_0$ and $\mathcal{M}_\epsilon$ after separating fast and slow variables for the dissipative Boltzmann equation.

of ϵ follows formally from the spectral gap of the linearized collision operator. A rigorous proof and the investigation of the possibility of fold points is currently under

investigation.

5.11 Conclusion

Formal series expansion do not always give the right form of the asymptotic expansion of solutions to differential equations with a parameter. For singularly perturbed ordinary differential equations the study of invariant manifolds provides a geometric frame for the dynamics. In particular, this geometric approach provides the correct form of the expansion.

Hydrodynamic limits in kinetic theory are singular limits. However, to the best of our knowledge there have not been works using geometric perturbation theory to analyze this problem.

Motivated by experiments on pattern formation in driven granular media we introduced specialized coordinates to separate slow and fast variables of the Boltzmann equation, and apply methods from geometric singular perturbation theory to obtain a hydrodynamic description of the dissipative kinetic model.

The results we presented are new from several points of view. It was shown that, unlike in previous works, in our method the compressible Navier-Stokes equations are not obtained as a correction to the Euler equation. Rather are they obtained as the first correction to time-independent Maxwellians. Thus this expansion captures the convective and the diffusive terms of the compressible Navier-Stokes equations simultaneously.

Furthermore, in the context of the dissipative Boltzmann equation it is argued in the literature that in order to obtain the cooling term to second order one needs to go to higher than Navier-Stokes order. Our expansion gives these terms already at the Navier-Stokes level.

In addition, since we expand about Maxwellians, as is done in the non-dissipative case, the resulting expressions can be computed explicitly without further expansions.

This was demonstrated with the example of the cooling rate for dissipative hard spheres.

Studying the normal fibration of $\mathcal{M}_\epsilon$ allows for rigorous matched expansions. However, this and the rigorous proof of the existence of $\mathcal{M}_\epsilon$ is not part of this thesis, and is ongoing research.

Also, the dissipative Navier-Stokes equations derived by our methods differ from the ones obtained by other methods. In corresponding equations 6.15-6.17 of [35] there are three effects due to the dissipation: the cooling term and two new transport terms. In our methods the transport terms are no different than the ones of the non-dissipative case. Only their dependence on the temperature makes them change their numerical values in time due to the dissipation. This needs to be further investigated.

In light of the success of the micro-macro decomposition [55], which is quite similar to our expansion, we hope that the methods we presented will provide new interpretations and insight to hydrodynamic limits in the non-dissipative as well as the dissipative case.

REFERENCES

[1] Arnol′d, V. I., *Mathematical methods of classical mechanics*, vol. 60 of *Graduate Texts in Mathematics*. New York: Springer-Verlag, second ed., 1989.

[2] Bates, P. W., Lu, K., and Zeng, C., "Approximate normally hyperbolic invariant manifolds for semiflows," in *Differential equations and computational simulations (Chengdu, 1999)*, pp. 27–31, World Sci. Publ., River Edge, NJ, 2000.

[3] Bates, P. W., Lu, K., and Zeng, C., "Invariant foliations near normally hyperbolic invariant manifolds for semiflows," *Trans. Amer. Math. Soc.*, vol. 352, no. 10, pp. 4641–4676, 2000.

[4] Bates, P. W., Lu, K., and Zeng, C., "Persistence of C^k normally hyperbolic invariant manifolds for infinite dimensional dynamical systems," in *First International Congress of Chinese Mathematicians (Beijing, 1998)*, vol. 20 of *AMS/IP Stud. Adv. Math.*, pp. 403–410, Providence, RI: Amer. Math. Soc., 2001.

[5] Bizon, C., Shattuck, M. D., Swift, J. B., McCormick, W. D., and Swinney, H. L., "Patterns in 3d vertically oscillated granular layers: Simulation and experiment," *Phys. Rev. Lett.*, vol. 80, pp. 57–60, Jan 1998.

[6] Bizon, C., Shattuck, M., de Bruyn, J., Swift, J., McCormick, W., and Swinney, H., "Convection and diffusion in patterns in oscillated granular media," *Journal of Statistical Physics*, vol. 93, no. 3-4, pp. 449 – 65, 1998.

[7] Bobylev, A. V., Carrillo, J. A., and Gamba, I. M., "On some properties of kinetic and hydrodynamic equations for inelastic interactions," *J. Statist. Phys.*, vol. 98, no. 3-4, pp. 743–773, 2000.

[8] Bobylev, A. V., Carrillo, J. A., and Gamba, I. M., "Erratum on: "On some properties of kinetic and hydrodynamic equations for inelastic interactions" [J. Statist. Phys. **98** (2000), no. 3-4, 743–773; MR1749231 (2001c:82063)]," *J. Statist. Phys.*, vol. 103, no. 5-6, pp. 1137–1138, 2001.

[9] Boldrighini, C., Keane, M., and Marchetti, F., "Billiards in polygons," *Ann. Probab.*, vol. 6, no. 4, pp. 532–540, 1978.

[10] Bouchut, F., Golse, F., and Pulvirenti, M., *Kinetic equations and asymptotic theory*, vol. 4 of *Series in Applied Mathematics (Paris)*. Éditions Scientifiques et Médicales Elsevier, Paris: Gauthier-Villars, 2000.

[11] Brey, J., Dufty, J., Kim, C. S., and Santos, A., "Hydrodynamics for granular flow at low density," *Physical Review E (Statistical Physics, Plasmas, Fluids, and Related Interdisciplinary Topics)*, vol. 58, no. 4, pp. 4638 – 53, 1998.

[12] Brunovský, P., Chow, S.-N., and Mallet-Paret, J., "Theorems of Hartman-Grobman type for singularly perturbed vector fields," *Lefschetz Center for Dynamical Systems, Brown University*, 2002.

[13] Bunimovich, L. A., "Billiards that are close to scattering billiards," *Mat. Sb. (N.S.)*, vol. 94(136), pp. 49–73, 159, 1974.

[14] Bunimovich, L. A., "On ergodic properties of certain billiards," *Funkcional. Anal. i Priložen.*, vol. 8, no. 3, pp. 73–74, 1974.

[15] Bunimovich, L. A., "On the ergodic properties of nowhere dispersing billiards," *Comm. Math. Phys.*, vol. 65, no. 3, pp. 295–312, 1979.

[16] Bunimovich, L. A., "Many-dimensional nowhere dispersing billiards with chaotic behavior," *Phys. D*, vol. 33, no. 1-3, pp. 58–64, 1988. Progress in chaotic dynamics.

[17] Bunimovich, L. A., "Conditions of stochasticity of two-dimensional billiards," *Chaos*, vol. 1, no. 2, pp. 187 – 83, 1991.

[18] Bunimovich, L. A., "On absolutely focusing mirrors," in *Ergodic theory and related topics, III (Güstrow, 1990)*, vol. 1514 of *Lecture Notes in Math.*, pp. 62–82, Berlin: Springer, 1992.

[19] Bunimovich, L. A., "Absolute focusing and ergodicity of billiards," *Regul. Chaotic Dyn.*, vol. 8, no. 1, pp. 15–28, 2003.

[20] Bunimovich, L. A. and Del Magno, G., "Track billiards," *To appear in Comm. Math. Phys.*, 2008.

[21] Bunimovich, L. A. and Grigo, A., "Focusing components in typical chaotic billiards should be absolutely focusing," *To appear in Comm. Math. Phys.*, 2009.

[22] Bussolari, L. and Lenci, M., "Hyperbolic billiards with nearly flat focusing boundaries, I," *Physica D*, vol. 237, no. 18, pp. 2272 – 81, Sept. 2008.

[23] Cercignani, C., *Mathematical methods in kinetic theory*. New York: Plenum Press, second ed., 1990.

[24] Cercignani, C., *Rarefied gas dynamics*. Cambridge Texts in Applied Mathematics, Cambridge: Cambridge University Press, 2000. From basic concepts to actual calculations.

[25] Chernov, N. and Markarian, R., *Chaotic billiards*, vol. 127 of *Mathematical Surveys and Monographs*. Providence, RI: American Mathematical Society, 2006.

[26] Chow, S.-N., Liu, W., and Yi, Y., "Center manifolds for invariant sets," *J. Differential Equations*, vol. 168, no. 2, pp. 355–385, 2000. Special issue in celebration of Jack K. Hale's 70th birthday, Part 2 (Atlanta, GA/Lisbon, 1998).

[27] Chow, S.-N., Liu, W., and Yi, Y., "Center manifolds for smooth invariant manifolds," *Trans. Amer. Math. Soc.*, vol. 352, no. 11, pp. 5179–5211, 2000.

[28] De Masi, A., Esposito, R., and Lebowitz, J. L., "Incompressible Navier-Stokes and Euler limits of the Boltzmann equation," *Comm. Pure Appl. Math.*, vol. 42, no. 8, pp. 1189–1214, 1989.

[29] Del Magno, G. and Markarian, R., "On the Bernoulli property of planar hyperbolic billiards," 2006.

[30] Desvillettes, L. and Golse, F., "A remark concerning the Chapman-Enskog asymptotics," in *Advances in kinetic theory and computing*, vol. 22 of *Ser. Adv. Math. Appl. Sci.*, pp. 191–203, World Sci. Publ., River Edge, NJ, 1994.

[31] Dias Carneiro, M. J., Oliffson Kamphorst, S., and Pinto de Carvalho, S., "Elliptic islands in strictly convex billiards," *Ergodic Theory Dynam. Systems*, vol. 23, no. 3, pp. 799–812, 2003.

[32] Donnay, V. J., "Using integrability to produce chaos: billiards with positive entropy," *Comm. Math. Phys.*, vol. 141, no. 2, pp. 225–257, 1991.

[33] Douady, R., *Applications du théorème des tores invariants. Thèse de 3 e cycle.* PhD thesis, Université Paris VII, 1982.

[34] Du, Y., Li, H., and Kadanoff, L. P., "Breakdown of hydrodynamics in a one-dimensional system of inelastic particles," *Phys. Rev. Lett.*, vol. 74, pp. 1268–1271, Feb 1995.

[35] Dufty, J. W., "Nonequilibrium statistical mechanics and hydrodynamics for a granular fluid," 2007.

[36] Esposito, R., Lebowitz, J. L., and Marra, R., "The Navier-Stokes limit of stationary solutions of the nonlinear Boltzmann equation," *J. Statist. Phys.*, vol. 78, no. 1-2, pp. 389–412, 1995.

[37] Fenichel, N., "Geometric singular perturbation theory for ordinary differential equations," *J. Differential Equations*, vol. 31, no. 1, pp. 53–98, 1979.

[38] Gamba, I. M., Panferov, V., and Villani, C., "On the Boltzmann equation for diffusively excited granular media," *Comm. Math. Phys.*, vol. 246, no. 3, pp. 503–541, 2004.

[39] Garzo, V. and Dufty, J., "Dense fluid transport for inelastic hard spheres," *Physical Review E*, vol. 59, no. 5, pp. 5895 – 911, 1999.

[40] Guckenheimer, J. and Holmes, P., *Nonlinear oscillations, dynamical systems, and bifurcations of vector fields*, vol. 42 of *Applied Mathematical Sciences*. New York: Springer-Verlag, 1990. Revised and corrected reprint of the 1983 original.

[41] Haff, P., "Grain flow as a fluid-mechanical phenomenon," *Journal of Fluid Mechanics*, vol. 134, pp. 401 – 30, Sept. 1983.

[42] Hirsch, M. W., Pugh, C. C., and Shub, M., *Invariant manifolds*. Lecture Notes in Mathematics, Vol. 583, Berlin: Springer-Verlag, 1977.

[43] Jenkins, J. T. and Richman, M. W., "Grad's 13-moment system for a dense gas of inelastic spheres," *Arch. Rational Mech. Anal.*, vol. 87, no. 4, pp. 355–377, 1985.

[44] Kamphorst, S. O. and Pinto-de Carvalho, S., "The first Birkhoff coefficient and the stability of 2-periodic orbits on billiards," *Experiment. Math.*, vol. 14, no. 3, pp. 299–306, 2005.

[45] Klimontovich, Y. L., *Statistical physics*. Chur: Harwood Academic Publishers, 1986. Translated from the Russian by G. Pontecorvo.

[46] Krupa, M. and Szmolyan, P., "Relaxation oscillation and canard explosion," *J. Differential Equations*, vol. 174, no. 2, pp. 312–368, 2001.

[47] Lanford, III, O. E., "Time-evolution of infinite classical systems," in *Mathematical aspects of statistical mechanics (Proc. Sympos. Appl. Math., New York, 1971)*, pp. 65–75. SIAM–AMS Proceedings, Vol. V, Providence, R. I.: Amer. Math. Soc., 1972.

[48] Lanford, III, O. E., "Time evolution of infinite classical systems," in *Proceedings of the International Congress of Mathematicians (Vancouver, B. C., 1974), Vol. 2*, pp. 377–381, Canad. Math. Congress, Montreal, Que., 1975.

[49] Lanford, III, O. E., "Time evolution of large classical systems," in *Dynamical systems, theory and applications (Recontres, Battelle Res. Inst., Seattle, Wash., 1974)*, pp. 1–111. Lecture Notes in Phys., Vol. 38, Berlin: Springer, 1975.

[50] Lanford, III, O. E., "On a derivation of the Boltzmann equation," in *International Conference on Dynamical Systems in Mathematical Physics (Rennes, 1975)*, pp. 117–137. Astérisque, No. 40, Paris: Soc. Math. France, 1976.

[51] Lazutkin, V. F., "Existence of a continuum of closed invariant curves for a convex billiard," *Uspehi Mat. Nauk*, vol. 27, no. 3(165), pp. 201–202, 1972.

[52] Lazutkin, V. F., "Existence of caustics for the billiard problem in a convex domain," *Izv. Akad. Nauk SSSR Ser. Mat.*, vol. 37, pp. 186–216, 1973.

[53] Lee, M.-Y., Liu, T.-P., and Yu, S.-H., "Large-time behavior of solutions for the Boltzmann equation with hard potentials," *Comm. Math. Phys.*, vol. 269, no. 1, pp. 17–37, 2007.

[54] Liu, T.-P., Yang, T., Yu, S.-H., and Zhao, H.-J., "Nonlinear stability of rarefaction waves for the Boltzmann equation," *Arch. Ration. Mech. Anal.*, vol. 181, no. 2, pp. 333–371, 2006.

[55] Liu, T.-P. and Yu, S.-H., "Boltzmann equation: micro-macro decompositions and positivity of shock profiles," *Comm. Math. Phys.*, vol. 246, no. 1, pp. 133–179, 2004.

[56] Markarian, R., "Billiards with Pesin region of measure one," *Comm. Math. Phys.*, vol. 118, no. 1, pp. 87–97, 1988.

[57] Melo, F., Umbanhowar, P., and Swinney, H. L., "Transition to parametric wave patterns in a vertically oscillated granular layer," *Phys. Rev. Lett.*, vol. 72, pp. 172–175, Jan 1994.

[58] Melo, F., Umbanhowar, P. B., and Swinney, H. L., "Hexagons, kinks, and disorder in oscillated granular layers," *Phys. Rev. Lett.*, vol. 75, pp. 3838–3841, Nov 1995.

[59] Moser, J., *Stable and random motions in dynamical systems*. Princeton Landmarks in Mathematics, Princeton, NJ: Princeton University Press, 2001. With special emphasis on celestial mechanics, Reprint of the 1973 original.

[60] Mouhot, C., "Rate of convergence to equilibrium for the spatially homogeneous Boltzmann equation with hard potentials," *Comm. Math. Phys.*, vol. 261, no. 3, pp. 629–672, 2006.

[61] Shattuck, M., Bizon, C., Swift, J., and Swinney, H., "Computational test of kinetic theory of granular media," vol. 274, (Budapest, Hungary), pp. 158 – 170, Dec. 1999.

[62] Sinaĭ, Y. G., "Dynamical systems with elastic reflections. Ergodic properties of dispersing billiards," *Uspehi Mat. Nauk*, vol. 25, no. 2 (152), pp. 141–192, 1970.

[63] Toscani, G., "Hydrodynamics from the dissipative Boltzmann equation," in *Mathematical Models of Granular Matter*, vol. 1937 of *Springer LMS*, pp. 59–75, New York: Springer-Verlag, 2008.

[64] Umbanhowar, P. B., Melo, F., and Swinney, H. L., "Periodic, aperiodic, and transient patterns in vibrated granular layers," *Physica A: Statistical and Theoretical Physics*, vol. 249, pp. 1–9, Feb 1998.

[65] van der Pol, B., J., "Forced oscillations in a circuit with non-linear resistance," *Philosophical Magazine*, vol. 3, pp. 65 – 80, Jan. 1927.

[66] Wojtkowski, M., "Principles for the design of billiards with nonvanishing Lyapunov exponents," *Comm. Math. Phys.*, vol. 105, no. 3, pp. 391–414, 1986.